JOURNAL OF APPLIED PHYSICS

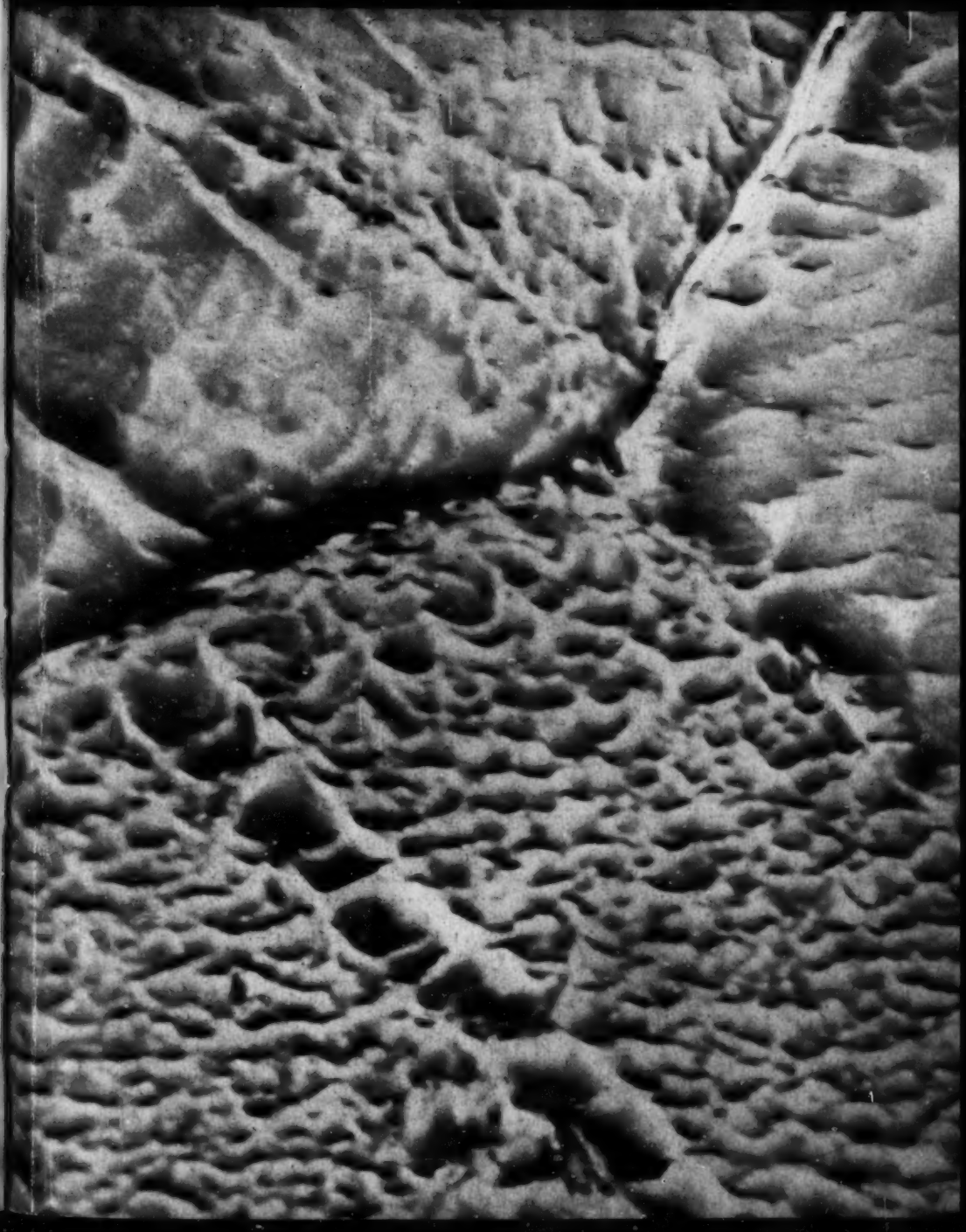

JOURNAL
OF
APPLIED PHYSICS

Vol. 14, No. 7 JULY, 1943

In This Issue

Contributed Original Research

	Page
Mobilization of Scientific Resources, II	311
Interpretation of Electron Micrographs of Silica Surface Replicas — Robert D. Heidenreich	312
Time Lag of Impulse Breakdown at High Pressures — J. D. Cobine and E. C. Easton	321
Some Applications of the High Resolving Power of the Electron Microscope — Henry Green and Ernest F. Fullam	332
Surge-Generator Circuits — Edward Fisher	341
Breakdown of Thixotropic Structure as Function of Time — Ruth N. Weltmann	343
Concerning the Roots of $J_n'(x)N_n'(kx) - J_n'(kx)N_n'(x) = 0$ — Rohn Truell	350
Electrical Circuit Analysis of Torsional Oscillations — Louis A. Pipes	352
Résumés of Recent Research	363

In Every Issue

New Instrument Booklets	364
New Books	365
Here and There	370
Calendar of Meetings	372
Recent Applications of Physics	viii
Innovations in Instruments	x
Index to Advertisers	xviii

BOARD OF EDITORS

Elmer Hutchisson, *Editor*

Associate Editors

Francis Bitter
W. F. Busse
S. H. Caldwell
Robley D. Evans
Selig Hecht
W. J. Lyons
Morris Muskat
Thomas H. Osgood
Paul E. Sabine
Frederick Seitz
J. R. Townsend
B. E. Warren
J. B. Whitehead

Publication of the American Institute of Physics

ADMINISTRATIVE STAFF

Henry A. Barton, *Director*

Madeline M. Mitchell, *Publications Manager*

John T. Tate, *Adviser on Publications*

GOVERNING BOARD

Paul E. Klopsteg, *Chairman*

George B. Pegram, *Secretary*

T. D. Cope
R. B. Dow
L. A. DuBridge
Floyd A. Firestone
Harvey Fletcher
R. C. Gibbs
K. S. Gibson
Arthur C. Hardy
Hermann Mark
A. G. Worthing
John T. Tate
N. W. Taylor
Wallace Waterfall

The Journal of Applied Physics, published monthly at Prince and Lemon Sts., Lancaster, Pa., is devoted to physics in its role as the science basic to other natural sciences and to the arts and industries. Previous to 1937 this publication was known as Physics. The Journal of Applied Physics publishes editorials, news of physicists and reviews, as well as technical papers of applied physics.

Manuscripts should be submitted to Elmer Hutchisson, Editor, 172 Fulton Street, Eleventh Floor, New York, New York.

Subscriptions and orders for back numbers should be addressed to Prince and Lemon Streets, Lancaster, Pa. or to the American Institute of Physics, 175 Fifth Avenue, New York, N. Y.

Subscription Price

	U. S. and Canada	Elsewhere
To members of scientific societies	$5.00	$5.70
To all others	7.00	7.70

Back Number Prices

Complete set: Vol. 1, July, 1931–Vol. 13, 1942—**$80.50**
Yearly back number rate: **$7.70**
Single copies: **$0.70** each.

Changes of address and proofs should be addressed to the Publications Manager.

Advertising rates supplied on request. Orders, advertising copy and cuts should be sent to the American Institute of Physics.

Entered as second class matter January 22, 1937, at the Post Office at Lancaster, Pennsylvania, under the Act of March 3, 1879. Accepted for mailing at the special rate of postage provided for in the Act of February 28, 1925, authorized May 2, 1932.

Copyright 1943, by the American Institute of Physics.

Journal
of
Applied Physics

Volume 14, Number 7 July, 1943

Mobilization of Scientific Resources, II

IN a previous issue of this Journal it was pointed out that the Science Mobilization bill now before Congress would profoundly influence the future of many scientists and the development of science in this country. During the last few weeks an avalanche of criticism has fallen upon this bill from scientists, scientific and technical societies, and from industrialists.

On May 8, 1943 the War Policy Committee of the American Institute of Physics passed the following resolution:

WHEREAS, the American Institute of Physics, representing the physicists engaged in all branches of activity in their profession, has made studies and surveys to determine the extent to which physicists are engaged in and contributing to the war effort; and

WHEREAS, the facts thus found show that practically all physicists are now applying themselves to the advancement of war research, war industry, and training personnel for the war effort; therefore

BE IT RESOLVED that the War Policy Committee of the American Institute of Physics, while conceding that there is room for improvement, nevertheless maintains that physics is well mobilized and is effectively working on the problems arising out of the war through such agencies as the Office of Scientific Research and Development; the laboratories of industry and of the various branches of the armed services and other government agencies; and in the laboratories and classrooms of our educational institutions where large numbers of personnel are being trained for war service; and

BE IT FURTHER RESOLVED that the War Policy Committee of the American Institute of Physics regards the proposals now before Congress in the forms of Senate bill No. S. 702 and House bill No. H.R. 2100 as not well conceived to increase the productivity of physics in the war, but rather tending to disorganize and retard the effective work now being done.

The impact upon Congress of this resolution along with similar ones from almost every other scientific and engineering group will be such that there is very little likelihood of these bills being enacted into law. Yet the urge upon the part of some to set up a broad governmental agency such as the one proposed will still exist and will soon rise again to the surface.

It behooves physicists and other true intellectuals to give this matter more thought. The intense conviction so often expressed by Professor Bridgman and more recently by President Hutchins that a stable and orderly society is possible and can be achieved by man through his intellectual processes will stand us in good stead in the post war period. Let us examine our present organizations for the mobilization of science and if deficiencies exist let us by all means correct them ourselves and not wait for others to attempt to do it in a manner as ill-conceived for the purpose as in the present science mobilization bill.

Contributed Original Research

Interpretation of Electron Micrographs of Silica Surface Replicas

ROBERT D. HEIDENREICH
The Dow Chemical Company, Midland, Michigan
(Received April 6, 1943)

Experiments are described for investigating the interpretation of polystyrene-silica surface replicas. It is demonstrated on a polished and etched stainless steel 18–8 specimen that the light microscope and electron microscope pictures are strikingly similar with corresponding regions easily recognized. The great value of stereo-pictures in determining relative surface elevations is demonstrated with a comparison of the topography as shown by the light microscope using oblique illumination. The question of resolution is discussed and a method of quantitatively determining the practical limiting resolution of replicas is described. A shape limitation factor, α, is defined and evaluated for both silica and Formvar replicas. With $\alpha=1$ being perfect reproduction, the values obtained were $\alpha\sim1.3$ for silica and $\alpha\sim3.8$ for Formvar. The value $\alpha\sim3.8$ is valid only for the surface employed in its determination while the value of $\alpha\sim1.3$ is realized on any surface to which the polystyrene-silica method can be applied.

INTRODUCTION

THE investigations to be described are the logical extension of the first results obtained with the polystyrene-silica surface replicas reported previously.[1,2] A technique for reproducing the surface structure of bulk materials was introduced which made use of a thermoplastic (polystyrene) and an evaporated silica film which served as the object in the electron microscope. Several pictures were included as examples, but no evidence as to the interpretation or reliable limit of the replicas was presented. This situation is also the case for the Formvar replica method[3,4] with the result that the electron microscope pictures produced by either method are of limited value due to the uncertainties involved in working back from the intensity distribution of the image to the topography of the original surface. It is obvious that these questions must be investigated if results of any value are to be obtained on the microstructure of metals and surface structure in general.

It has been found that stereomicrographs are of great value in interpreting silica replicas when considered along with the intensities. Silica replicas are well adapted to stereo-work and yield striking results on surfaces presenting abrupt changes in elevation. A stereo-pair is shown in Fig. 1 as an example.* The total angle between the pictures is 8°. The region shown is from a polished and etched magnesium alloy and, solely upon the basis of intensity, the interpretation is quite inconclusive. Viewing the pair with a stereoscope, however, indicates that this region consists of a large hole in the surface with fine structure on its interior walls. This pit is the result of the removal of a manganese particle during polishing.

Figure 1 illustrates the effectiveness of stereo-pictures in determining the actual topography of the replica film.

COMPARISON OF LIGHT AND ELECTRON MICROSCOPE

The problem of observing the same identical area of a surface in both the light and electron microscopes presents itself as the first step in reaching an understanding of the surface replica since in nearly all such work the electron microscope serves as an extrapolation of the light

[1] R. D. Heidenreich and V. G. Peck, Phys. Rev. **62**, 292 (1942).
[2] R. D. Heidenreich and V. G. Peck, J. App. Phys. **14**, 23 (1943).
[3] V. J. Schaefer and D. Harker, J. App. Phys. **13**, 427 (1942).
[4] V. J. Schaefer, Phys. Rev. **62**, 495 (1942).

* All pictures taken with an RCA electron microscope, type B.

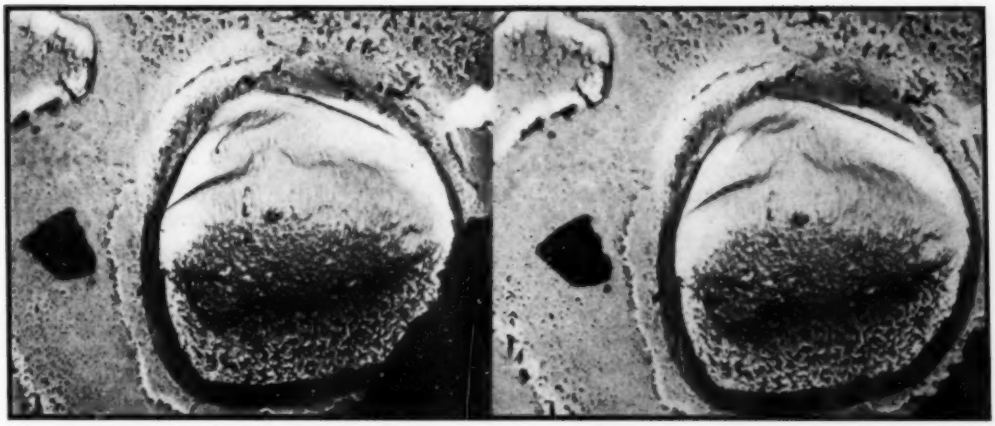

FIG. 1. Stereo electron micrographs of a silica replica of polished and etched magnesium-manganese alloy.

microscope. It is evident that for this purpose a surface presenting a relatively simple structure is desirable to facilitate recognition of the chosen region in both microscopes. Furthermore, it is important that the surface in question be free from corrosion and etching films since such films may greatly alter the topography, although they may not greatly effect the appearance of the specimen in the light microscope. An example of the difficulties due to corrosion of the metal surface is found in reference 3, Fig. 2. Similar results were obtained in this laboratory and it was found that the needle-like structure consisted of FeOOH crystals removed from the surface when the replica was stripped.

Some experimentation indicated that stainless steel (18–8) was suitable for the comparison due to its corrosion resistance, geometric microstructure, and relative hardness. The specimen was prepared by taking it down through 0000 metallographic paper and then electrolytically polishing in a sulfuric acid-phosphoric acid bath.[5] Etching was accomplished by reducing the current density in this bath with frequent examination in the light microscope to obtain a light-to-medium etch. The surface was then swabbed in a 3 percent nitric acid-ethanol solution, washed in distilled water followed by methanol, and then dried in a stream of air. This procedure gave a relatively clean surface, free from polishing scratches and any distortions of the surface layers that might have resulted from mechanical polishing.

A region about $\frac{1}{8}$ in.^{2} in the central portion was outlined by scribing and polystyrene molded against the surface at about 1500 lb./in.^{2} and at a temperature of 160°C. The metal was removed mechanically with ease and apparently gave no distortion of the replica. The silica was then evaporated onto the polystyrene surface in the vacuum chamber as described in reference 2. Before removal, however, the same square was scribed on the surface as on the metal, while the remainder of the surface was scribed into irregularly shaped areas so that the desired square was recognized when released from the polystyrene. The silica replica was mounted on the regular specimen screen and examined in the electron microscope at a magnification of 3400×. A region possessing more or less distinctive structure was chosen in the electron microscope and then recourse taken to the original metal specimen to locate that same structure in the light microscope. A short search of the scribed region resulted in locating the same region as chosen in the electron microscope.

Figure 2 is a sequence of photomicrographs showing the original metal surface, the polystyrene molding, and the silica replica. The polystyrene is somewhat difficult to photograph due to its transparency, as is the silica film. There is a tendency for the thin film to wrinkle near the wires of the screen so that the entire field is not in focus in the light microscope. The

[5] R. I. Imboden and R. S. Sibley, Metal Finishing, p. 592 (Nov. 1942).

difficulties in taking photomicrographs of electron microscope specimens have been described by Burton.[6] The chosen structure is easily visible in all three photomicrographs.

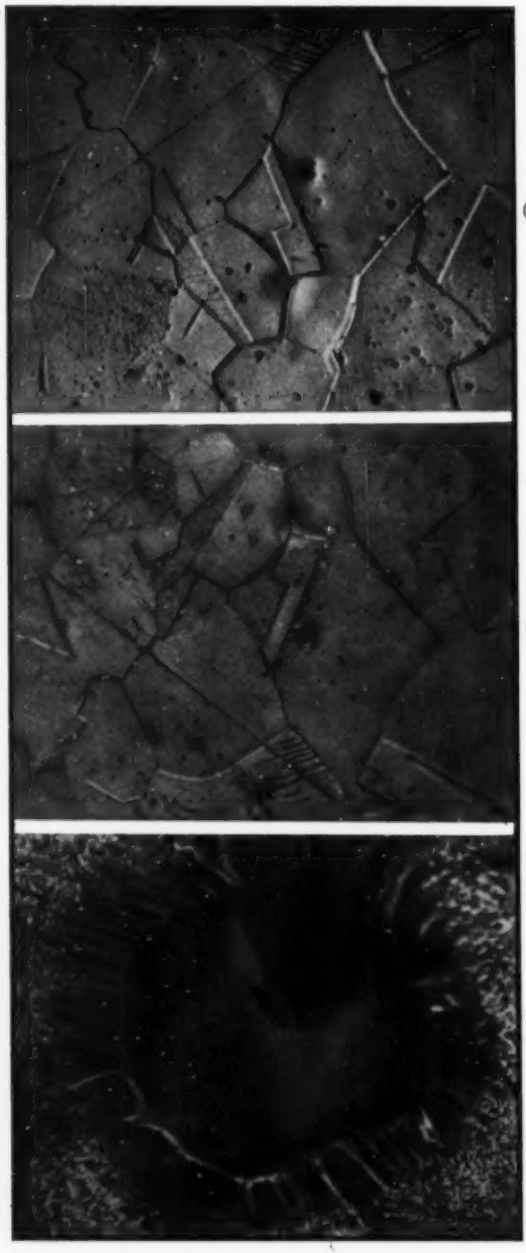

FIG. 2. Sequence of photomicrographs illustrating the replica process. a. Original metal 500×. b. Polystyrene replica 500×. c. Silica replica 500×.

[6] C. J. Burton, R. B. Barnes, and T. G. Rochow, Ind. Eng. Chem. **34**, 1429 (1942).

Figure 3 is a photomicrograph of the original metal taken at 2000× and enlarged to 4800×. Oblique illumination was employed in order that the high regions would stand out in relief. Figure 4 is the electron micrograph of the silica replica showing the identical region of Fig. 3 and at the same magnification so that Fig. 3 and Fig. 4 are directly comparable.

The similarity between Fig. 3 and Fig. 4 at first glance is quite striking and makes it very easy to recognize corresponding portions. Examination of these pictures indicates that the greatest difference between them is one of resolution. It is

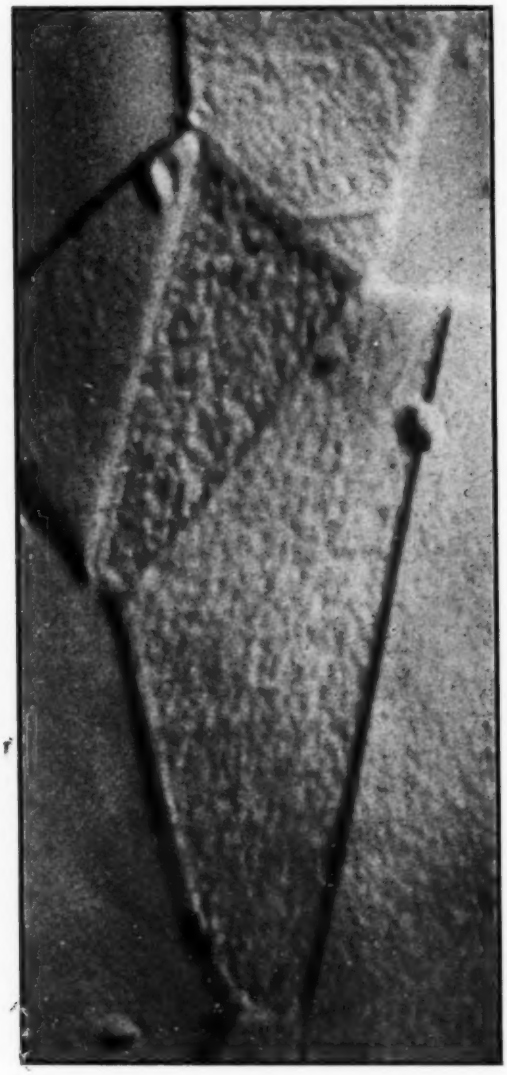

FIG. 3. Photomicrograph of stainless steel 18–8, 4800×.

noted that the finer internal structure of the grains is indicated in Fig. 3 as an indistinct roughness, while it appears sharp and clear in the electron micrograph. The light microscope is here at its limit of resolution, while the electron microscope is very far from its limit. Any desired region of Fig. 4 can be enlarged to bring out the fine structure. Figure 5 is a 4× enlargement, while Fig. 6 is an 8× enlargement of another region.

FIG. 4. Electron micrograph of the same region as Fig. 3, 4800×.

Distances approaching 100A can be seen in Fig. 6. The variations in orientation of the fine structure within the grains upon crossing a boundary eliminate doubt as to whether or not this structure is "real."

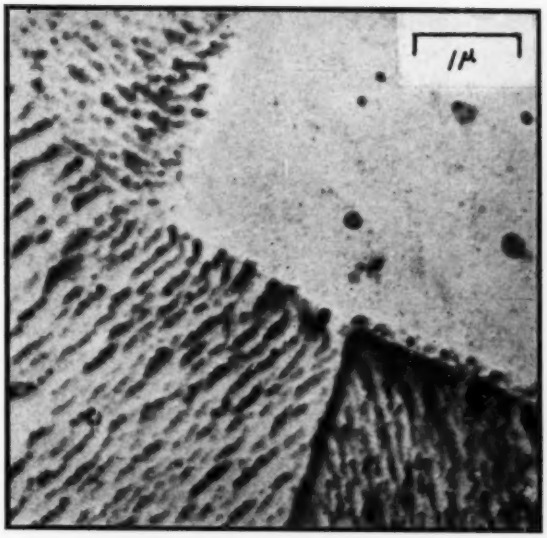

FIG. 5. Region of Fig. 4 enlarged 4×.

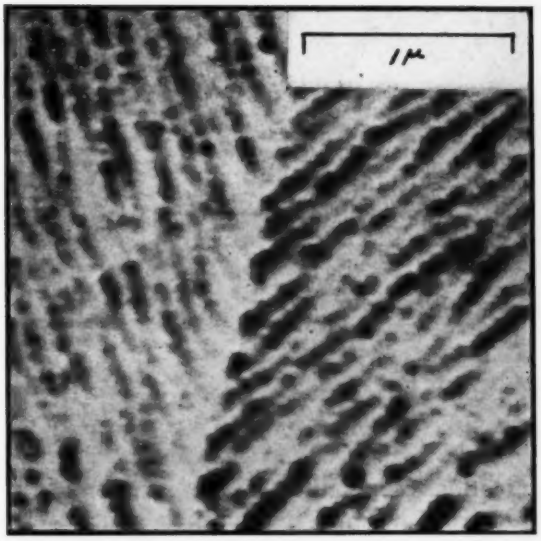

FIG. 6. Region of Fig. 4 enlarged 8×.

The relative elevations of the various grains on the original surface can be seen in Fig. 3, while the corresponding topography in the replica is apparent in the stereo-pair of Fig. 7.

It is seen that Fig. 3 and Fig. 7 are in agreement as to the relative elevations, demonstrating again the importance of the stereo-pictures.

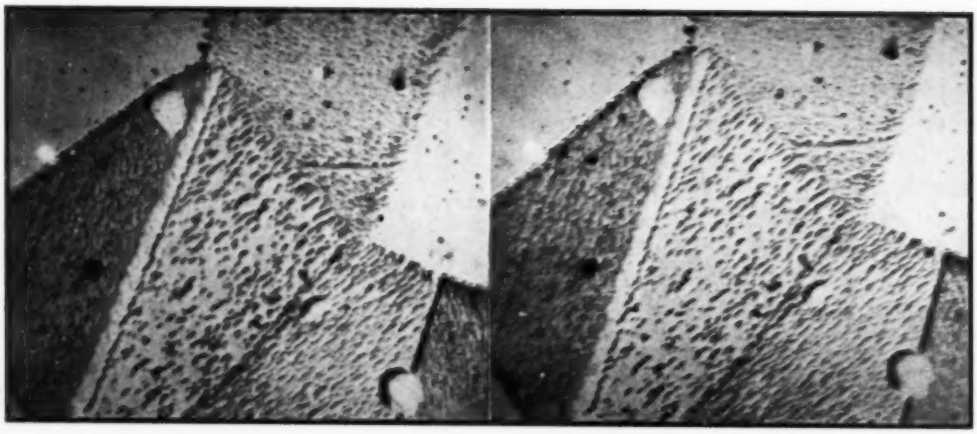

FIG. 7. Stereo electron micrographs for comparison with the photomicrograph of Fig. 3, ×4800.

INTENSITY DISTRIBUTION

It was stated in references 2 and 3 that an interpretation of electron micrographs of the surface replicas could be obtained from the intensity distribution in the image. In the case of the Formvar, a level upper surface was demonstrated for the replica film which gave thickness variations proportional to the topography of the original surface when the changes in elevation were of the order of the average film thickness or perhaps somewhat greater. A somewhat similar view was held for the silica replica and apparently is partially correct even though cases have arisen where this is not true. One of these will be pointed out presently.

Examination of enlargements of stereomicrographs of a region of Fig. 4 indicates that the small, dark spots within the grains are actually projections rising about 200A above the immediate surrounding surface which is in accordance with what might be expected from the intensities.

In Fig. 8 are compared the plate transmission, topography from the stereomicrograph, the profile of the actual metal surface from Fig. 3, and the cross section of the silica film as concluded from these observations. The vertical dimension is not quantitative but serves to demonstrate the intensity variations as compared with the topography. Since the intensity recorded on the photographic plate is dependent upon thickness variations in the film, it follows that the orientation of various parts of the surface will determine the effective film thickness even though the actual thickness may not vary. Such an explanation may partially account for the results of Fig. 8.

A detailed interpretation of the intensity variations observed in silica replicas cannot be made without further experimentation concerning the surface motion of the condensing molecules. This is a problem in itself, the solution for which will certainly aid in the understanding of the replicas, but which is not a serious disadvantage in applying the technique. The characteristics of the condensing silica are such as to give the impression that the replica films possess a cross section somewhat similar to that exhibited by drifting snow with a tendency to accumulate in surface irregularities. This very property is responsible for high contrast in the replicas with the projections and depressions more or less outlined by accumulation of silica along sharp variations in elevation. It is probable that surface irregularities possessing differences in elevation as small as 20A are made visible in the final pictures through the intensity difference.

RESOLUTION

The question of resolution has been of prime importance in the use of the electron microscope for general work and so it is in the case of the surface replicas. The actual determination of resolution in an electron micrograph is, more often than not, very difficult since frequently two points which are just separated by the instrument do not happen to lie in the field.

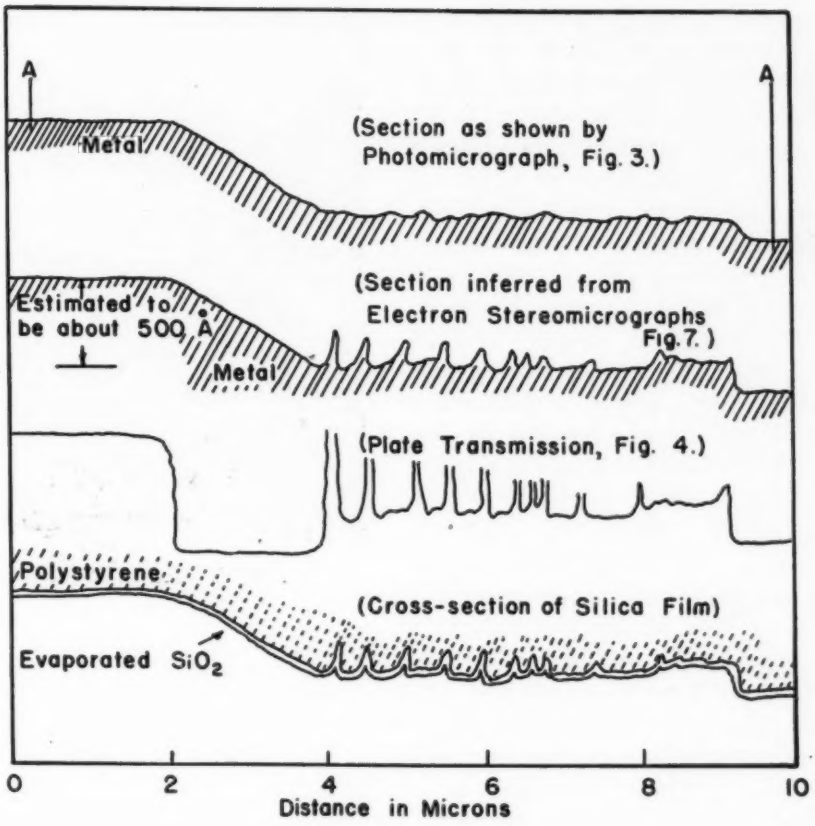

FIG. 8. Profiles along A–A (Fig. 4) as estimated from Figs. 3, 4, and 7. The vertical dimension is qualitative and the small irregularities are not to scale but merely demonstrate the roughness.

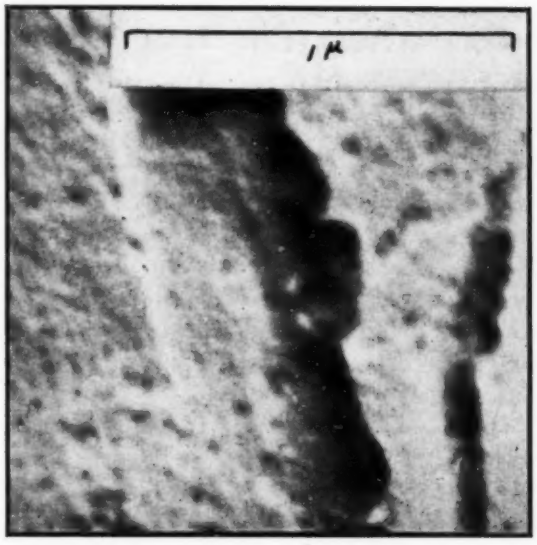

FIG. 9. Silica replica of calcite showing very small surface irregularities.

Perhaps one of the best criteria of resolution is the sharpness with which corners of crystals can be recorded in the image, since one can be reasonably certain that the edge of a crystal such as MgO approaches atomic dimensions. Such edges are actually rounded by the electron microscope with the result that the radius of curvature should be a direct measure of resolving power.

This rounding of sharp corners has been considered by Borries[7] and discussed by Marton[8] with the idea that in electron microscope images the resolving power manifests itself not only as a size limitation but as a shape limitation as well. Thus, an MgO crystal having a size of 50–60A may be detected in the image, but its shape

[7] B. v. Borries and G. A. Kausche, Kolloid Zeits. **90**, 132 (1940).
[8] L. Marton, J. Phys. Chem. **46**, 1023 (1942).

cannot be ascertained and it appears as a diffuse circle or dot. These two limitations are conveniently extended to replicas so that some idea as to the practical limit of usefulness of the replica can be gained. Figure 9 is an electron micrograph of a silica replica of a calcite crystal showing small surface irregularities.* Numerous blanks have failed to show any structure at magnifications of 100,000×, so that this structure must be taken as due to the original surface. Spots of the order of 100A are visible although they appear shapeless. Spots separated by less than 75A are visible in the original enlargement so that it is concluded that as far as size limitation is concerned, the silica replicas are quite good.

The actual geometric shapes of the structures that a surface may possess are of importance in metallographic work as in the case of precipitation in alloys giving rise to age hardening or precipitation hardening. The detection of such particles is of course desired, but it is also important to know whether or not the replica is capable of reproducing their shape. A method of determining the smallest geometric shape that can be recognized as such rests on comparing the replica of such a figure with the figure itself. Taking as a basis the diameter of the circle, D, having the same areas as an n-sided regular polygon, it is possible to compute this diameter[7, 8] from the relation

$$D=2d\left(1+\cos\frac{\pi}{n}\right)\left(\frac{n}{\pi}\cot\frac{\pi}{n}\right)^{\frac{1}{2}} \qquad (1)$$

where d is the resolution of the instrument.† If the viewpoint is adopted that the replica is the limiting factor in the reproduction of surface structure, rather than the microscope, then this shape limitation approach may be extended to the replicas as follows: A replica is produced by some means of a series of regular polygons, all of which are identical except for size. The smallest polygon that can still be recognized as such is determined and the diameter of the inscribed circle denoted by L. The "shape limitation factor," α, of that replica is now defined as the ratio of L to the value of D determined by Eq. (1), that is

$$\alpha\equiv L/D. \qquad (2)$$

If $\alpha=1$, the reproduction is perfect as far as the microscope is concerned and hence the value of α determined for a replica will measure the ability of that replica to reproduce small shapes compared to the ability of the microscope to form an image of the same shape. If it comes about that α is unity for a given replica, then it can only be said that the resolution obtained by the replica is at least as good as that obtainable by the microscope.

The shape limitation factor as defined is an over-all limitation imposed, not only by the actual reproduction itself, but by the ability of the microscope to produce high quality images of the replica film. Irrespective of which one of these factors actually limits the smallest shape recognizable in the image, this limitation is included in Eq. (2) and hence the practical limitation of the replica in any application is determined.

The value of L can be determined quite readily by employing as a test surface a rocksalt cleavage plane upon which has been deposited MgO smoke. The smoke is applied while the surface is wet with distilled water so that upon drying the crystals will be anchored to the surface.

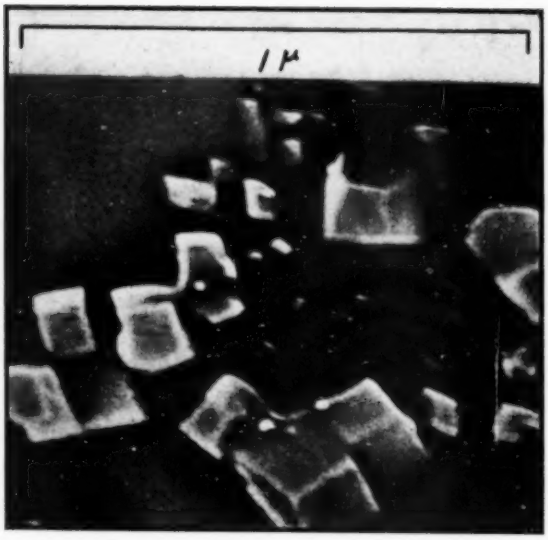

FIG. 10. Silica replica of MgO crystals.

* From the same crystal as described in reference 1.

† See also *Advances in Colloid Sciences* (Interscience Publishers, 1942), Vol. 1, pp. 360–361.

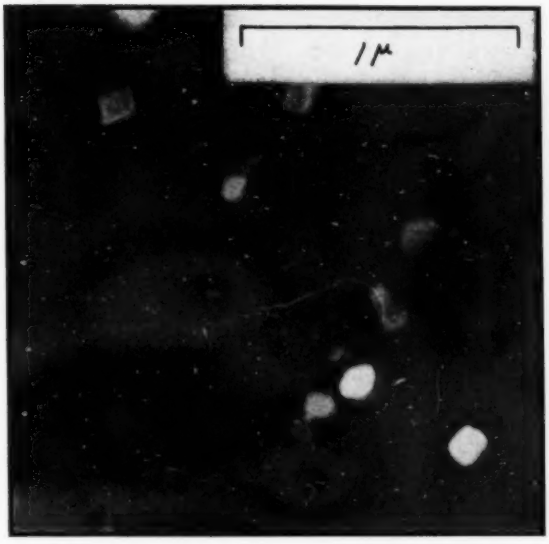

FIG. 11. Formvar replica of MgO crystals.

The polystyrene molding is freed from the rocksalt by means of acidified, warm distilled water and a silica replica evaporated as described.

An electron micrograph of such a replica is shown in Fig. 10. Several replicas were prepared and numerous pictures were taken of each replica so that Fig. 10 is considered to be representative. The smallest recognizable cube has a side $L \sim 180$A so that for this replica, on the basis of $D = 140$A, the shape limitation factor is $\alpha \sim 1.3$. A deposit of MgO crystals on a glass surface gave results in agreement with this value so that it is concluded that a silica replica having an average thickness of 200–300A will consistently yield a shape limitation factor of about 1.3 for any surface. α seems to be independent of molding pressures in the range of 2000–4000 lb. when a temperature of 160°C is maintained for 5 min. or more. Obviously, α will increase with film thickness due to increasing inelastic scattering and adverse electrical effects such as accumulation of surface charges on the film.

It is of interest to apply this criterion to other replicas. A surface identical with the ones prepared for the silica replicas was employed and Formvar replicas applied from a 0.75 percent solution of Formvar in 1,4 dioxane. The Formvar replica was removed in acidified water where no actual stripping was necessary since the rocksalt quickly dissolved from beneath the replica film. A representative electron micrograph of a thin Formvar film (200–300A) is shown in Fig. 11. Evidently the resolution is not as good as for the silica since here $L \sim 520$A and hence $\alpha \sim 3.8$. Similar results were obtained using an ethyl cellulose lacquer and it appears that this value is not out of line with the pictures obtained by Mahl[9] using a polystyrene lacquer so that the result is more dependent upon the solvent than the plastic as would be expected. Unfortunately this value of α is probably not applicable to any other surface nor to other solvents due to variations in wetting properties. A new α must be determined for each surface and for each solvent. The results obtained in this laboratory have indicated that, for several metals (including stainless steels), the value of α is 2 or 3 times greater than that obtained on the rocksalt when the solvents ethylene dichloride, dioxane, or chloroform are employed.

GENERAL REMARKS

The replicas used to demonstrate resolution, such as Fig. 10, also bring to attention a disadvantage of the silica replica for surfaces presenting a structure similar to MgO crystals on rocksalt. The random orientation of the MgO crystals in this case resulted in what might be termed "reentrant structure," whereby the polystyrene molding has impressed into its surface depressions in which the actual surface opening is considerably smaller in cross section than is the remainder of the depression. This reduced cross section at the surface opening results in reducing the amount of silica incident onto the interior walls of the depression so that the film thickness is here less than for the surrounding surface. Furthermore, when the silica film is removed from the molding in the solvent, the film is freed from the surface before the original surface opening in the polystyrene has been sufficiently enlarged by solution to accommodate the silica film from the interior walls. As a result, the replica of such a depression is pulled through this small opening and deformed or torn. From this point of view, the surface of the MgO crystals on the rocksalt was not a good standard since only those crystals that were suitably oriented

[9] H. Mahl, Zeits. f. tech. Physik **22**, 33 (1941). (See Fig. 8.)

gave a replica film that was not damaged upon removal. It is the suitably oriented crystals that were singled out to determine the resolution. This, however, is probably not too serious a disadvantage since in general surfaces adapted to electron microscope examination do not possess such a degree of reentrant structure and are not as rough as was this one.

The question of wetting of surfaces by liquids also reveals some indication as to the behavior of the replicas. It is well known that the radius of curvature of a liquid surface is dependent upon the pressure across the surface and for the spherical case can be computed from the relation $\Delta P = 2\gamma/R$, where γ is the surface tension and R, the radius of curvature. For a pressure difference of about one atmosphere and a surface tension of 25 dynes/cm, the radius of curvature is 5000A. Thus, if a local region of a surface were not completely wetted by the liquid, the film would follow the surface only where it presented a radius of curvature in the neighborhood of $\frac{1}{2}\mu$ with smaller structures simply rounded over. A great loss in resolution of plastic lacquer replicas would result in any area where wetting was not realized. Such a possibility should not be overlooked in interpreting these replicas.

In the case of the polystyrene molding where pressures of perhaps 1500 lb./in.^{2} are applied externally, the radius of curvature would be approximately 40A, where a surface tension of 30 dynes/cm is assigned to polystyrene at 160°C. This value seems to be consistent with the observed resolution. If insufficient molding time is allowed or if the temperature is too low, this value may never be attained, due to the viscosity of the polystyrene. These can be easily controlled, however, whereas the wetting properties are somewhat difficult to predict.

CONCLUSION

It has been the aim of these experiments to investigate the silica surface replicas somewhat critically and thereby gain a better understanding as to how they may be employed most effectively. The work of Burton, Barnes, and Rochow[6] served to illustrate how the electron microscope could be made of greater value by employing it in conjunction with and as an extrapolation of the light microscope. It is evident that in working in a size range of matter where 100A becomes a definite, measurable distance, it is difficult to establish a perspective and orientation with regard to ordinary microscopic and macroscopic dimensions. It is hoped that this paper will aid in firmly tieing the electron microscope in with the light microscope in the examination of the surface structure of opaque bodies.

As stated in the discussion of intensity, the relative elevations on a surface are usually more easily determined from the intensities with the Formvar or silver-collodion replica[10] than with the silica. This difficulty is easily overcome by the use of stereo-pictures. The resolution obtained with a silica replica is generally 3–5 times better than that for the Formvar and 50 times better than with the light microscope.

There are many problems involving surface structure which can be attacked very successfully with a combination of the light microscope, electron microscope, and x-ray and electron diffraction. Among these are metallography, corrosion, surface finish and catalysis, to mention a few.

In the field of surface finishing, it should be mentioned that, by using stereo-pictures of silica replicas and a contour finder as employed in aerial mapping,* it is possible quantitatively to determine profiles and contours of structures and imperfections of a size not satisfactorily detected by profilometers. This type of work should find a place in friction and lubrication studies.

The surface replica, however, will perhaps not suffice when microscopes of greater resolution are constructed. Examination of surface structure of dimensions below 75–100A will require such an instrument as the scanning microscope, but until that time, there are sufficient problems in the range of 100–3000A to justify a large amount of replica work.

---

[10] V. K. Zworykin and E. G. Ramberg, J. App. Phys. **12**, 642 (1941).

* Information regarding stereoscopes and contour finders may be obtained from Abrams Instrument Company, Lansing, Michigan.

Time Lag of Impulse Breakdown at High Pressures

J. D. Cobine and E. C. Easton
Graduate School of Engineering, Harvard University, Cambridge, Massachusetts

Experiments were conducted to determine the variation of time lag of spark breakdown as a function of gas pressure. All tests were made in pre-purified nitrogen using 1.250-inch diameter spheres of copper, aluminum and nickel with a gap spacing of 0.0125 inch. The voltage applied to the gap was in the form of a surge which reached its maximum value in one quarter of a microsecond and which decayed slowly to 97 percent of its maximum value in 5000 microseconds. Most of the recorded lags lay in the range from 5 to 5000 microseconds. The maximum value of the applied voltage was varied from 14 to 128 percent above the static breakdown value, while the gas pressure was varied from 7 to 100 pounds per square inch absolute. The most probable time lag was found to vary greatly with pressure, changing rather abruptly from a large value (10^{-2} sec.) to a small value (10^{-5}–10^{-6} sec.) at certain critical conditions of pressure and overvoltage. The change appears to occur under conditions at which the ions normally present in the gas begin to produce free electrons by negative-ion disintegration, or by positive-ion bombardment of the cathode. The distribution of time lags was found to vary with cathode material and condition of cathode surface. The nickel spheres quickly developed a heavy coating when sparked in nitrogen. The copper and aluminum spheres became only slightly discolored. The time lag distribution curves for copper and aluminum were of the same type, but different from that for nickel. The observations suggest methods for speeding the action of spark plugs and protective gaps, as well as for increasing the reliability of gas-insulated apparatus. Apparatus operated below the critical conditions can withstand surges which on the average are one thousand times as long as those which would cause the apparatus to fail when operated in the short time lag region. Similarly, a protective gap or spark plug which is to operate on very short surges can be made to break down more consistently by operating at an overvoltage and a gas pressure in the short time lag region.

INTRODUCTION

THIS paper describes a series of experiments which were conducted to determine the effect of gas pressure on the time lag of spark breakdown. As here used, the term "time lag" refers to the time which elapses between the application of an overvoltage and the subsequent breakdown of the gap. By overvoltage is meant a voltage greater than the static breakdown value for the gap. Breakdown of the gap is understood to have occurred when the gap voltage drops below the static breakdown value. The voltage applied to the gap was in the form of a surge which reached its maximum value in one quarter of a microsecond and which decayed slowly to 97 percent of its maximum value in 5000 microseconds. This was not a standard test surge[1] but served as an approximation to a rectangular wave since most of the observed lags lay in the range from 5 to 5000 microseconds, that is along the tail of the surge. If V_b (Fig. 1) is the static breakdown voltage of the gap, and V_a is the peak value of the surge, the overvoltage ratio Q is found by the formula $Q=(V_a-V_b)/V_b$.

The equipment necessary for this study consisted of four parts: the power supply, the switching mechanism, the gas chamber, and the timer. The power supply, switching mechanism, and timer have been described in a previous paper.[2] One of the most important features of this measuring apparatus is the device used to apply the nearly rectangular wave of voltage to the test gap. If a source of constant voltage be connected to a gap by an ordinary switch, the gap voltage rises in a saw-tooth manner. This

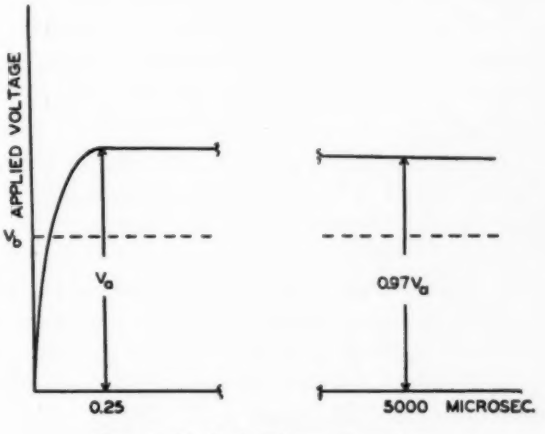

FIG. 1. Applied voltage wave form.

[1] EEI–NEMA Subcommittee Report, Trans. A.I.E.E. 59, 598 (1940).

[2] J. D. Cobine and E. C. Easton, Rev. Sci. Inst. 14, 301 (1941).

saw-tooth wave is caused by a spark which jumps the gap between the switch contacts before the switch is mechanically closed. This spark charges the stray capacitance of the switch to a voltage nearly equal to that of the source, whereupon the spark is extinguished. The charge on the switch then leaks off until the potential difference between contacts is sufficient to start another spark. Thus intermittent sparking with accompanying rise and fall of gap voltage occurs from the time of the first spark until the switch is mechanically closed.[2] In these experiments, a condenser and resistor were arranged so as to maintain the first spark and keep the switch closed electrically until the contacts could meet. The timer for measuring the length of the applied voltage wave consisted of a vacuum tube circuit designed to pass a constant current output as long as the bias to the first tube exceeds a predetermined value. The output current is passed through a ballistic galvanometer whose reading is a measure of the time during which the gap voltage remains above the datum level. A thyratron circuit was arranged to supply the timer with rectangular waves for the purpose of calibration. Checks by means of the cathode-ray oscillograph showed maximum timing errors of about 10 percent, with errors of less than 5 percent over most of the range. The chamber in which the gap was enclosed consisted of a cylindrical steel tank about 19 inches long and 8 inches in diameter. The negative electrode was fixed through an insulating bushing at one end of the tank, while the positive sphere was mounted on a steel rod threaded through the other end. The gap spacing could be adjusted by turning the threaded rod. The electrodes in all experiments were spheres, 1.250 inches in diameter, with a gap spacing of 0.0125 inch. The shafts on which the spheres were mounted were four inches long and $\frac{3}{8}$ inch in diameter. The field in the gap region was practically uniform. The tank could be evacuated by means of a Cenco Megavac pump, or filled with any desired gas from commercial tanks. In all the experiments herein described, the tank contained pre-purified nitrogen obtained from a 200 cubic foot tank as supplied for commercial lamp manufacture.[3] A bowl of calcium chloride was placed in the test chamber to absorb moisture.

[3] Air Reduction Sales Company.

EXPERIMENTAL PROCEDURE

In order to make measurements on the time lag of spark breakdown, a pair of spheres of the desired metal was selected and carefully polished. The spheres were then inserted in the test chamber and wiped off with paper towels dipped in petroleum ether and carbon tetrachloride. Great care was taken not to touch the spheres with the fingers, or to allow the metal to become soiled in any way before the tank was closed. Next, the tank was closed and thoroughly evacuated by the Cenco Megavac pump. The tank was then filled with nitrogen, evacuated again, and finally filled with gas to the desired pressure. The electrode spacing was then set, and the equipment was ready for use. The first measurements at each pressure were those to determine the static breakdown voltage of the gap. To make these measurements, a low voltage was applied to the gap and slowly raised until breakdown occurred. The breakdown voltage varied in an erratic manner during the first few sparks, but afterward remained fairly constant. (Howell[4] reported similar conditioning of the electrodes during his breakdown studies.) At each setting, several sparks were struck before the readings were recorded. Then the average of at least ten closely grouped values was taken as the static breakdown voltage for the existing conditions. A typical group of ten such readings taken with nickel spheres is: 3780, 3820, 3820, 3820, 3800, 3840, 3780, 3840, 3820, 3820 (average 3814). After the static breakdown voltage was determined, the timer was adjusted so that the galvanometer would carry current whenever the test gap voltage exceeded a value 10 percent less than that of static breakdown. In order to vary the galvanometer current from zero to full value or vice versa it was never necessary to vary the gap voltage more than 5 percent. Thus, since both the rise and fall of the test gap voltage are very rapid, this setting causes the galvanometer reading to represent very closely the time during which an overvoltage exists across the test gap.

[4] A. H. Howell, Elec. Eng. **58**, 193–204 (1939).

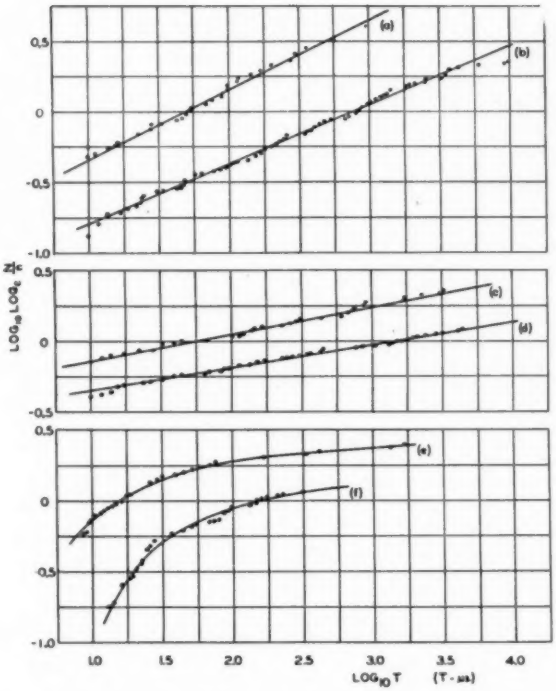

FIG. 2. Time lag distribution. (a) copper 37.0 percent overvoltage 64.7 lb./sq.in. absolute; (b) copper 82.6 percent overvoltage 24.7 lb./sq.in. absolute; (c) aluminum 37.0 percent overvoltage 49.7 lb./sq.in. absolute; (d) aluminum 82.6 percent overvoltage 19.7 lb./sq.in. absolute; (e) nickel 37.0 percent overvoltage 24.7 lb./sq.in. absolute; (f) nickel 14.1 percent overvoltage 29.7 lb./sq.in. absolute.

From 25 to 50 time lag observations were made under each set of conditions, after which the pressure or overvoltage would be changed. In every case the original conditions would be restored later and tested anew. Consider for example the tests with copper spheres at a gauge pressure of 10 pounds per square inch and 82.6 percent overvoltage. After the first set of 30 readings was taken, 32 other tests at different pressures and overvoltages were made before the 10 lb. per sq. in. run was repeated. Between the two 10 lb. per sq.in. tests the spheres were polished and the timer calibrated. Next came 32 more tests before the third trial at 10 lb. per sq. in., and 14 more before the fourth trial. All the observations made under the same conditions of pressure and overvoltage were then grouped together.

In order better to analyze the data, the time lags were arranged in order of increasing magnitude. Beside each lag was placed a number indicating what portion of the total number of lags had a length equal to or greater than the given lag. Thus if N is the total number of lags, and n is the number having a length equal to or greater than a given lag, then n/N would appear beside each lag. An attempt was then made to determine what relation existed between the length of the total time lag (T) and the ratio n/N. This relation appeared to be of the type $n/N = \exp[-bT^c]$ where b and c are constants. To determine b and c, if this relation should hold, it was necessary to plot a graph of $\log_{10} T$ against $\log_{10} \log_e (N/n)$, for $N/n = \exp[bT^c]$

hence

$$\log_e (N/n) = bT^c$$

and

$$\log_{10} \log_e (N/n) = c \log_{10} T + \log_{10} b.$$

Thus if a graph of $\log_{10} T$ *versus* $\log_{10} \log_e (N/n)$ were a straight line, c would be the slope of the line, and $\log_{10} b$ its intercept on the $\log_{10} \log_e (N/n)$ axis.

When such graphs were plotted from data taken with copper spheres and with aluminum spheres, it was found that the points were better fitted by straight lines than by any elementary curve. Hence, over this particular range of time lags, these distribution curves may be assumed straight. Of course, over the entire range from zero to infinity it may be necessary to represent a distribution curve by a multiplicity of elementary functions.[5] Two typical graphs for copper spheres are shown in Fig. 2(a) and (b), while two similar plots for aluminum spheres appear in Fig. 2(c) and (d). The graphs drawn from data taken with nickel spheres were not straight lines. Two typical curves for nickel are presented in Fig. 2(e) and (f).

DISCUSSION

The total time lag T used in plotting these graphs is composed of two parts, the "formative" lag f and the "statistical" lag t. The statistical lag is the time required for the appearance in the gap of an electron which leads to breakdown. The formative lag is the time required for this electron to complete the breakdown. In the gap

[5] T. B. Crumpler and J. H. Yoe, *Chemical Computations and Errors* (Wiley, 1940), pp. 202–226.

used, the formative lag should be considerably less than one microsecond, while the statistical lag may be several thousands of microseconds.[6] Thus the total lag is almost entirely accounted for by the statistical lag.

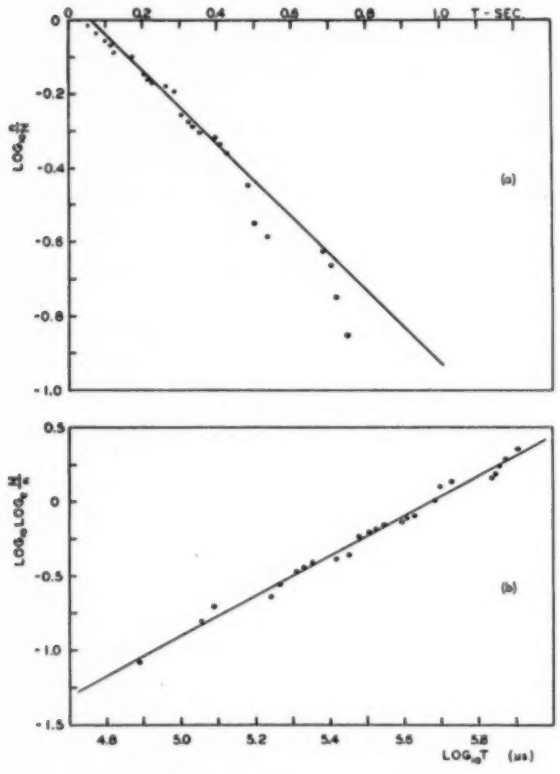

FIG. 3. Time lag distribution. Data from Tilles. Weakly irradiated gap. 1.8 percent overvoltage 14.7 lb./sq.in. absolute. Copper spheres in air. (a) $\log_{10}(n/N)$ *vs.* T; (b) $\log_{10}\log_e(N/n)$ *vs.* $\log_{10} T$.

Most of the investigators who have reported heretofore on time lag studies have assumed with von Laue and Zuber[7,8] that the distribution of lags follows the law $n/N=e^{-KT}$. Thus if $\log_{10}\log_e(N/n)$ were plotted against $\log_{10} T$ the graph would be a straight line with slope of unity. The data of this investigation do not follow such a distribution. For example, the graph for copper in Fig. 2(a) has a slope of 0.496, in Fig. 2(b) a slope of 0.422, while that for aluminum in Fig. 2(c) has a slope of 0.200, and in Fig. 2(d) a slope of 0.162. The graphs for nickel do not follow the exponential law even approximately.

A mathematical analysis of the time lag distribution can be carried out as follows. Let P_1 be the probability that an electron in a given field will lead to a spark. Let P_2 be the probability that an electron will be formed in a region of the field where it can lead to a spark. Let dn be the number of sparks which occur in the interval between t and $t+dt$. The probability of a spark occurring in a certain interval will depend on the independent factors, length of interval, P_1, P_2, and n (the number of lags whose length is equal to or greater than t). Thus,

$$dn=-kn_0P_1P_2ndt$$

where n_0 is the rate of production of electrons in the gap, and k is a constant. Solving,

$$\int_N^n \frac{dn}{n}=-\int_0^t kn_0P_1P_2dt,$$

$$\log_e\left(\frac{n}{N}\right)=-\int_0^t kn_0P_1P_2dt,$$

$$\frac{n}{N}=\exp\left[-\int_0^t kn_0P_1P_2dt\right].$$

If n_0, P_1 and P_2 are constant with respect to time, then n/N is a simple exponential function of t. This is the condition hypothesized by von Laue and Zuber. In most experimental apparatus, however, it is almost impossible to provide absolutely constant gap voltage over the entire interval t. Thus, in general, the field strength will vary with time, and n_0, P_1 and P_2 will vary with it. The gap voltage in this study varied in the form of a surge as already explained. All of the observed lags lay in a time range corresponding to the tail of this wave. With such a voltage applied to a copper gap or to an aluminum gap, the exponent in the equation above appears to vary as some power of T. Thus,

$$n/N=\exp\left[-bT^c\right].$$

To yield this exponent, the integral must take the form

$$\int_0^t kn_0P_1P_2dt=\int_0^t bc(t+f)^{c-1}\,dt$$
$$=b(t+f)^c-bf^c\approx bT^c,$$

[6] J. D. Cobine, *Gaseous Conductors* (McGraw-Hill, 1941), p. 190.
[7] K. Zuber, Ann. d. Physik **76**, 231–260 (1925).
[8] M. von Laue, Ann. d. Physik **76**, 261–265 (1925).

where t is the statistical lag, f the formative lag, and $T=t+f$, the total lag. The lag f may be assumed roughly constant and negligible in comparison with t. With the gap voltage which falls slowly over the range of measured values of t (5–5000 μsec.) the exponent c appears to be less than one. The reason for such a value of c can easily be seen in a qualitative way. The longer the statistical lag while waiting for the appearance of an electron in the effective gap space, the lower the gap voltage when the electron does arrive. The lower the gap voltage, the lower the probability that the electron will lead to breakdown. Thus an electron arriving late in the surge is less likely to cause breakdown than is one which arrives early. As a result, a greater portion of the lags fall in the long time range than would be the case with a constant gap voltage. This moves the long lag end of the $\log_{10} \log_e (N/n)$ *versus* $\log_{10} T$ graph toward the right and makes its slope less than that with constant applied voltage.

Tilles has reported[9] the results of some studies made on time lag with copper spheres of 0.750-inch diameter and a gap length of 0.0269 inch in dry air at atmospheric pressure. Tilles assumed that his data followed the simple exponential distribution $n/N=e^{-KT}$ and plotted his results on a graph of $\log_{10} (n/N)$ *versus* T. Such a graph of his data for weakly irradiated spheres at 1.8 percent overvoltage is shown in Fig. 3(a). Points from this graph have been re-plotted in Fig. 3(b) in the form $\log_{10} \log_e (N/n)$ *versus* $\log_{10} T$. This second graph is much nearer a straight line than the one assumed by Tilles, and has a slope of 1.34, indicating that Tilles' data may be better represented by the distribution

$$n/N=\exp\left[-2.52(10^{-8})T^{1.34}\right]$$

than by the simple exponential which he assumed. A study of Tilles' testing circuit, also described in the above reference, indicates that the gap voltage should have been in the form of a surge constantly increasing so as to approach its maximum value asymptotically. The gap voltage was obtained from the output condenser of a rectifier through a high resistance. The voltage across the capacitance of the gap must have risen to its maximum value at a relatively slow rate set by the high resistance.

Apparently, then, in a copper gap with little or no external radiation, the time lags follow a distribution of the form $n/N=\exp\left[-bT^c\right]$ where c is less than one for a falling gap voltage, equal to one for constant gap voltage, and greater than one for a rising gap voltage.

Tilles also presented data taken with a gap strongly irradiated with ultraviolet light. From such data with copper spheres he plotted a graph of $\log_{10} (n/N)$ *versus* T which he divided into two portions, one represented by a straight line and the other by a curve. Such a graph has been reproduced in Fig. 4(a). In Fig. 4(b) these same data have been plotted as graph of $\log_{10} \log_e (N/n)$ *versus* $\log_{10} T$. Apparently a single curve can include the complete range of variation. This single curve appears to be of the same nature as the curves obtained in our study with nickel

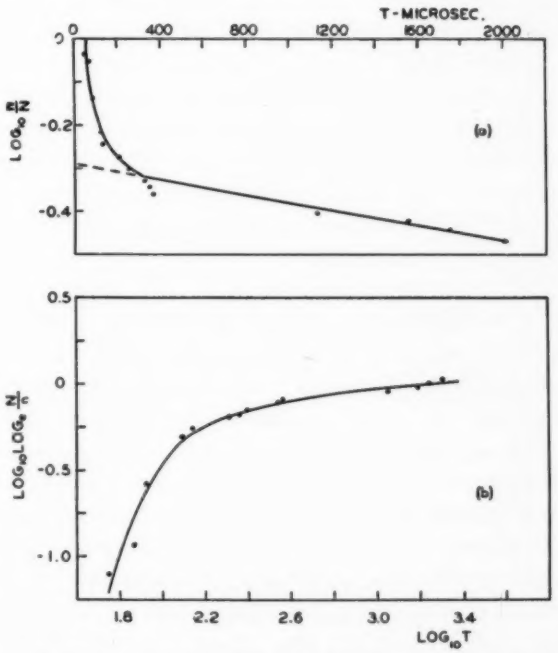

FIG. 4. Time lag distribution. Data from Tilles. Strongly irradiated gap. 1.7 percent overvoltage 14.7 lb./sq.in. absolute. Copper spheres in air. (a) $\log_{10} (n/N)$ *vs.* T; (b) $\log_{10} \log_e (N/n)$ *vs.* $\log_{10} T$.

spheres. Apparently Tilles obtained the same type of distribution with strongly irradiated copper spheres as was obtained here with unradiated nickel spheres, while the distribution obtained by Tilles with weakly irradiated copper

[9] A. Tilles, Elec. Eng. **54**, 868–876 (1935).

spheres corresponds to that obtained here with unradiated copper and aluminum spheres.

The electrode material should have little or no effect on P_1, the probability that an electron in the effective region of the gap will lead to breakdown. However, the electrode material and the condition of its surface must influence n_0, the rate of electron formation. After a number of sparks, the nickel cathode in this study was found to develop a rather thick coating, possibly of nickelic oxide.[10] It was further observed with nickel that sparking did not always occur at the same spot on the cathode, but varied so as to leave a group of cathode spots on the electrode. This suggests that tiny lumps of the coating may have acted as points to set up very high fields. These lumps of coating would extend farther into the gap than the microscopic points on a slightly discolored copper or aluminum surface, and would exert their effect on a greater portion of the gap volume. It is conceivable also that these points would be sharper than those on the surface of the copper or aluminum. The electrode surface conditions should also influence the value of P_2, the probability that an electron will arise in a region where it can lead to breakdown. With copper and aluminum electrodes, the original ions in the gas can form electrons by positive-ion bombardment of the cathode. These electrons, under the influence of the field, can form excited and metastable atoms in the gas. These atoms in turn produce electrons at random *in the body of the gas*. Hence the value of P_2 may vary widely among the electrons so formed. With nickel spheres, however, the coating on the electrode surface may become charged by positive-ion bombardment or by photons emitted in the gas. Subsequent neutralization of this charge causes the emission of electrons at the cathode (the Paetow effect). Thus if the coating on the nickel cathode should become charged by the initial positive ions and by photons emitted in the gas, the Paetow effect would account for the production of electrons at a reasonably high rate *at the cathode*. Electrons formed at the cathode are much more likely to produce breakdown than those formed in the gas. Thus with nickel spheres where many electrons are formed *at the cathode*

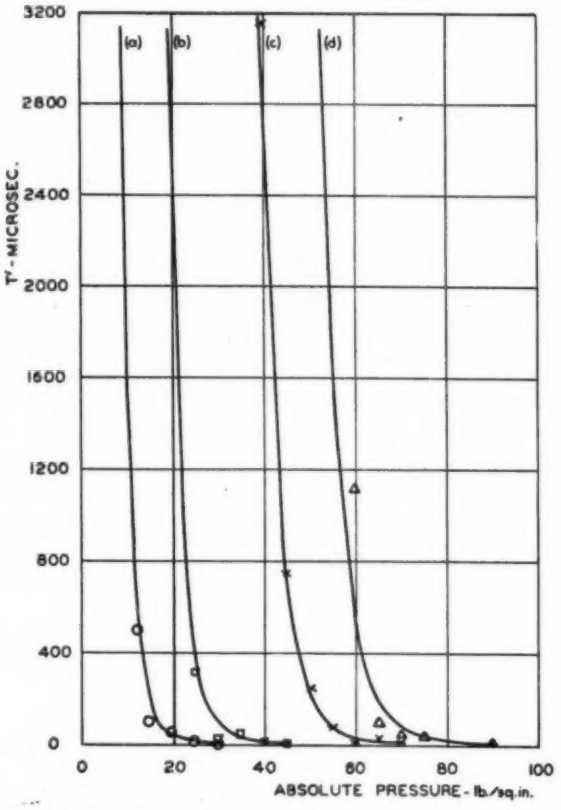

FIG. 5. Most probable time lag *vs.* pressure. Copper spheres in nitrogen. (a) 128 percent overvoltage; (b) 82.6 percent overvoltage; (c) 37.0 percent overvoltage; (d) 14.1 percent overvoltage. (Points for T' greater than 3200 microsec., determining the upper extremeties of curves (a), (b) and (d), have been omitted in order to permit a more convenient scale.)

we should expect a different lag distribution than that with copper or aluminum where most of the electrons are formed at random *in the gas*. This may explain the fact that the lag distribution observed here with nickel spheres is similar to that observed by Tilles with a strongly irradiated gap, while the lag distribution with copper and aluminum is similar to that observed by Tilles with a weakly irradiated gap. With Tilles' strongly irradiated gap and with our nickel electrodes, the majority of the electrons arise at the cathode. With Tilles' weakly irradiated gap and with our copper and aluminum spheres, most of the electrons are produced in the gas. For effective electrons produced at the cathode, P_2 is fairly constant. For those produced in the gas, P_2 varies widely with position.

Perhaps because of the variation in the condition of the electrode surfaces, the time lag

[10] G. Glockler and S. C. Lind, *The Electrochemistry of Gases and Other Dielectrics* (Wiley, 1939), p. 299.

measurements on nickel could not be reproduced reliably. However, with copper or aluminum spheres the results were as reproducible as is consistent with the theory of probability. On the basis of some 8000 observations with copper and aluminum, curves of $\log_{10}\log_e(N/n)$ *versus* $\log_{10} T$ were plotted for overvoltages of 14.1 percent, 37.0 percent, 82.6 percent, 128 percent, and at pressures ranging from 7 lb. per sq. in. absolute to 100 lb. per sq. in. absolute. For each condition of overvoltage and pressure, the most probable time lag T' was obtained from the graph. (T' is the value of T for which n/N is 0.50.) Curves showing the variation of the most probable time lag with pressure are shown for copper in Fig. 5 and for aluminum in Fig. 6. All these curves exhibit a rather abrupt transition from very long to very short lags. In the range from 5 to 5000 microseconds, these curves may be represented by the following equations, where T' is the most probable time lag in microseconds, p is the gas pressure in pounds per square inch absolute, V_a is the maximum value of the gap voltage, V_b is the static breakdown value, and $Q=(V_a-V_b)/V_b$. For copper spheres:

$$Q=0.141, \quad T'=3.00(10^{25})p^{-12.8},$$
$$Q=0.370, \quad T'=1.55(10^{21})p^{-11.1},$$
$$Q=0.826, \quad T'=1.41(10^{14})p^{-8.27},$$
$$Q=1.28, \quad T'=3.80(10^{8})p^{-5.28}.$$

Combining these formulas, we find

$$T'=6.60(10^{28})(1+Q)^{-56.6}p^{6.40(1+Q)-20.0},$$

which is a general formula valid for the particular conditions of these tests. For aluminum spheres:

$$Q=0.141, \quad T'=1.02(10^{42})p^{-20.5},$$
$$Q=0.370, \quad T'=3.16(10^{34})p^{-19.3},$$
$$Q=1.28\ , \quad T'=3.98(10^{16})p^{-13.6}.$$

In general,

$$T'=2.4(10^{46})(1+Q)^{-83.6}p^{6.11(1+Q)-27.5}.$$

(The dotted curve for 82.6 percent overvoltage in Fig. 6 is plotted from this general formula.)

When interpreting these formulas it must be remembered that the voltage applied to the test gap was a special form of surge as already mentioned. With the lowest overvoltage of 14.1 percent this surge remained greater than the static breakdown voltage for a period of 19,600 microseconds, which is longer than the longest lag recorded by the timer. At higher overvoltages the surge remained above the static breakdown value for even longer periods. The general formula for T' is significant only for those lags which are shorter than the time during which the surge voltage is greater than the static breakdown value.

The gas used in this investigation was prepurified nitrogen. In the tank as received from the manufacturer there was about 0.5 percent of impurities, mostly in the form of oxygen and water vapor. In the gas as actually used in the testing tank the percentage of impurities must have been higher. In such a gas at a pressure of six atmospheres there are about 40 ion pairs formed per cubic centimeter per second by radiation from the earth and atmosphere.[11] With a coefficient of recombination of 10^{-6} this would mean the permanent existence of approximately 6000 ion pairs in the gas. Most of the negative

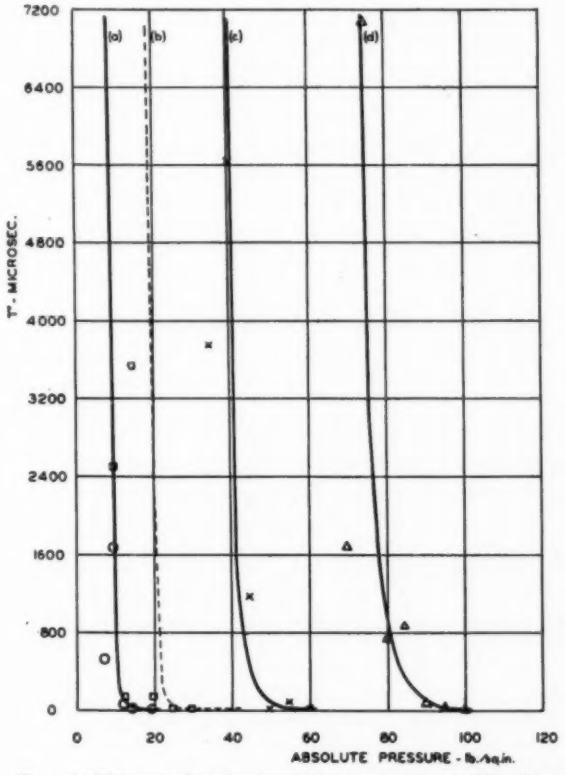

FIG. 6. Most probable time lag *vs.* pressure. Aluminum spheres in nitrogen. (a) 128 percent overvoltage; (b) 82.6 percent overvoltage; (c) 37.0 percent overvoltage; (d) 14.1 percent overvoltage.

[11] L. B. Loeb and J. M. Meek, *The Mechanism of the Electric Spark* (Stanford University Press, 1940), pp. 62, 63.

ions would exist in the form of neutral atoms to which an electron had become attached. Pure N_2 does not form such negative ions by attachment, but the impurities, such as O_2 or H_2O, would be very active in this regard. If the impurities amounted to 1 percent of the total gas, the average life of an electron might be approximately 10^{-5}–10^{-6} second.[12] Thus, on the average, from the 40 electrons which are formed each second, free electrons might be expected to exist for a period of $40(10^{-5})$ second. The average time between the disappearance of one free electron and the formation of another would thus be about $2.5(10^{-2})$ second. If the only free electrons in the gas were those produced by cosmic rays or radioactive emanations from the earth, the expected average statistical time lag of spark breakdown would be no less than $2.5(10^{-2})$ second. Since the average statistical lag under certain conditions is observed to be very much shorter than this, there must be some other source of electrons.

Some electrons may be expected to arise from field emission at the cathode. At minute irregularities on the surface of the electrode the field strength might rise to values 10 times as great as that of the average field across the gap.[13] This high gradient might pull electrons from the cold metal. A formula for the current density of such cold cathode emission has been derived by Stern, Gossling, and Fowler[14] and modified by Müller.[15] This formula, derived for highly purified and out-gassed surfaces, indicates that for the field strengths used in this study the cold cathode emission should yield approximately 10^{-13} electron per square centimeter per second. This number is negligible. However, since pure outgassed electrodes were not used here, it is possible that the current density due to cold cathode emission may have been higher.[16] Some ionization is produced thermally by collisions among the gas molecules themselves. The familiar Saha equation[17] indicates that at a pressure of six atmospheres and a temperature of 25°C, the fraction of the atoms which are ionized in this manner is 10^{-132}. Thus thermal ionization does not contribute enough additional electrons to account for the short statistical lag.

Under the action of an external electric field the negative and positive ions would be accelerated. If these ions could be brought to a *speed* as great as that of electrons which have fallen through the minimum ionizing potential, the ions would become effective ionizing agents.[18] Loeb has pointed out[19] that for molecular gases a positive ion must attain an energy greater than 500 volts in order to become an ionizer. However, because of the large energy exchanges upon impact between positive ions and gas molecules it is physically impossible for enough positive ions to gain the energy required to produce the observed effects in the range of X/p from 0–200 volts per cm per mm Hg. (Throughout these experiments, X/p varied from 60 to 190 volts per cm per mm Hg.)

Free electrons can be obtained by positive-ion bombardment of the cathode. It has been shown that all positive ions of energies over 50–100 volts can liberate electrons upon impact with a metal, the efficiency of the process increasing with the gas content of the surface and with the energy of the impacting ions.[20,21] Furthermore, if the work function of the surface is less than the ionization potential of the atoms, electron emission may take place with energies of less than 10 volts.

In the gas at a pressure of six atmospheres there may be some 6000 positive ions per cubic centimeter under equilibrium conditions. When the field is applied, the portion of these ions which are in the effective field region are swept to the cathode where they may release electrons upon impact. Those ions near the central axis of the sphere gap will arrive at the surface in approximately 10^{-6}–10^{-7} second, after which time a relatively small stream of ions will diffuse into the gap from the surrounding gas. At a pressure

[12] J. D. Cobine, *Gaseous Conductors*, p. 97.
[13] L. B. Loeb, *Fundamental Processes of Electrical Discharge in Gases* (Wiley, 1939), pp. 473, 474.
[14] T. E. Stern, B. S. Gossling, and R. H. Fowler, Proc. Roy. Soc. London **A124**, 699 (1929).
[15] E. W. Müller, Zeits. f. Physik **102**, 734 (1936).
[16] J. D. Cobine, *Gaseous Conductors*, p. 119.
[17] M. N. and N. K. Saha, *Treatise on Modern Physics* (India Press, 1934), vol. I, p. 632.
[18] J. D. Cobine, *Gaseous Conductors*, p. 84.
[19] L. B. Loeb, *Fundamental Processes of Electrical Discharge in Gases*, p. 377.
[20] L. B. Loeb, *Fundamental Processes of Electrical Discharge in Gases*, p. 382.
[21] L. B. Loeb, *Atomic Structure* (Wiley, 1938), pp. 287, 327.

of six atmospheres the mean free path of a positive ion is $2.22(10^{-6})$ cm. Thus with a voltage of 8800 volts (static breakdown value) across a gap of 0.03175 cm, or an average field strength of $2.78(10^5)$ volts per cm, an ion may pick up an energy of 0.615 electron volt while traversing one mean free path. However, the surface of the cathode is never smooth, and with microscopic irregularities of 10^{-5} to 10^{-6} cm radius the surface field strength at many points may be ten times the average for the gap.[13] Hence when an ion arrives to within one mean free path of the cathode surface it may be in a field of $27(10^5)$ volts per cm, and may thus strike the surface with an energy of 6 electron volts. Since the gas atom in this case has an ionizing potential which is greater than the work-function of the cathode material, it is quite possible for an ion with 6 electron volts energy to remove an electron from the cathode upon impact.[21]

If the effective cathode area has a diameter of 0.2 cm, the effective gap volume is 0.001 cubic cm. Thus, before the field is applied, the gap volume would contain about 6 positive ions at a pressure of six atmospheres, or one positive ion at one atmosphere. Hence for pressures above atmospheric, and with a value of γ (probability of electron emission by ion impact) of from 0.06 to 0.10,[22] the application of a certain minimum field may be expected to produce at least one electron as the original ions are swept out of the gap volume in 10 percent of the trials.

Loeb has shown that a negative ion may lose its electron upon impact with a gas molecule if conditions are favorable.[23] He estimates the energy of detachment of the electron from the negative O_2^- ion as lying between the limits of 0.136 and 0.68 electron volt.[24] We have just shown that at a pressure of six atmospheres in a field strength of $2.78(10^5)$ volts per cm an ion may attain an energy of 0.615 electron volt while traversing one mean free path. Hence we may expect the formation of some free electrons by disintegration of the negative ions.

When the field is applied to the gap, the ions in the gap region will be swept out in 10^{-6} to 10^{-7} second. If field and pressure conditions are suitable, some of the negative ions will disintegrate to form free electrons in the gas, while some of the positive ions will produce electrons by impact at the cathode. If there is a high probability that an electron arising in the effective gap volume will lead to breakdown (high P_1) then there is a high probability that breakdown will start in the interval during which the original ions are being swept out of the gap. If the electrons formed by the sweeping out of the original ions do not lead directly to breakdown, they will at least produce a number of excited and metastable atoms whose average life may be as long as 10^{-3} sec.[25] These excited and metastable atoms may produce electrons by collisions of the second kind for a period of 10^{-3} second after application of the field. Thus the original ions would set up a chain of events which would insure a relatively high rate of electron production almost immediately upon application of the field. Under these conditions, the most probable statistical lag would be very small.

If field and pressure conditions were not suitable for the formation of a reasonable number of electrons by the sweeping out of the original ions, breakdown would probably not start during the sweeping action but would await the formation of free electrons from some other source. Thus, below certain critical conditions the most probable statistical lag might be very long, but might change abruptly to a very short value when the critical conditions were reached.

These critical conditions must depend on the mean free path of the ions and on the field strength since the ion must attain a certain minimum energy before becoming effective either in negative-ion disintegration or positive-ion bombardment. The critical conditions must also depend on the cathode material and the condition of its surface. Electrons formed near the cathode are in a more favorable position for initiating breakdown than those formed elsewhere in the gas. Hence positive-ion bombardment of the cathode should be more effective for producing sparkover than negative-ion disintegration, and thus cathode material must influence the critical conditions.

The curves of most probable lag *versus* pres-

[22] J. D. Cobine, *Gaseous Conductors*, p. 159.
[23] L. B. Loeb, *Fundamental Processes of Electrical Discharge in Gases*, p. 291.
[24] L. B. Loeb, *Fundamental Processes of Electrical Discharge in Gases*, p. 293.
[25] J. D. Cobine, *Gaseous Conductors*, p. 77.

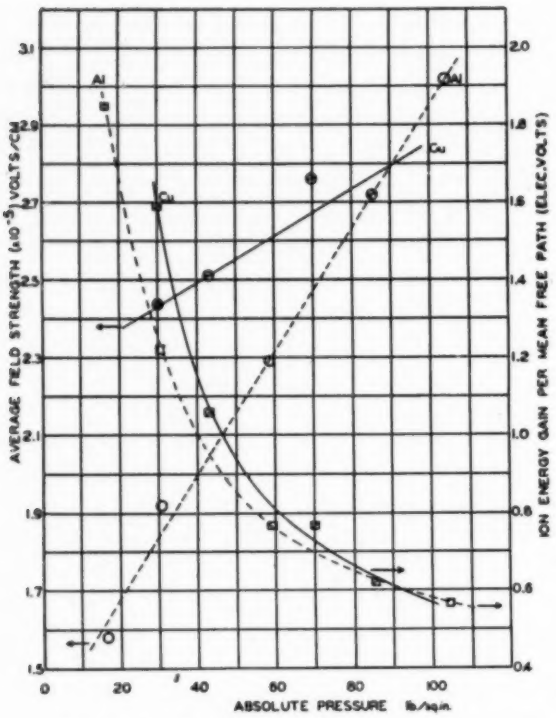

FIG. 7. Conditions at knee of T' *vs.* p curves.

sure (Figs. 5, 6) show rather abrupt changes from very long lags (10^{-2} sec.) to very short lags (10^{-5} to 10^{-6} sec.). The "knee" of each curve, or the point at which the curvature is greatest, occurs under conditions which are dependent on pressure, field strength, and electrode material. In Fig. 7 are plotted for copper and aluminum electrodes the applied field and the energy gained by an ion in one mean free path as a function of the absolute pressure at the knee of the curves of T' *versus* p. These curves show that the transition from very long to very short lags takes place when the energy gained by an ion during one mean free path is in the range 0.5 to 1.9 electron volts. The required energy varies inversely with the pressure as would be expected. At low pressures there are fewer original ions, and, to insure adequate electron production the fewer ions are given greater energy. The probability of electron appearance varies directly with ion energy. The curves of Fig. 7 show that the critical ion energy varies with electrode material. This would be expected since the type of cathode material influences the probability that an impacting ion will form an electron. Those factors, such as high field strength and low pressure, which favor high ion energy also produce high energies in the electrons, and therefore cause an increase in the probability of breakdown P_1. Thus we should expect that at the knee of the T' *vs.* p curves the value of T' should fall as p falls. This is definitely seen to be true for the aluminum data, although the trend is not pronounced for copper.

At low pressures the lags with aluminum were found to be shorter than those with copper. This is in agreement with the observations of Strigel at atmospheric pressure.[26] However, as the pressure increases, the lags with copper become shorter than those with aluminum. This phenomenon might be explained on the basis of a different rate of variation of γ with pressure. Measurements indicate that for certain ion energies γ is greater for aluminum than for copper.[22] This should result in shorter lags for aluminum at those energies. Now assume that γ for aluminum should increase more rapidly with increase in positive ion energy than does γ for copper. Also assume that at a certain positive ion energy the time lag is the same for both. Then a given increase in positive ion energy would produce a greater increase in γ for aluminum than for copper. Hence as the positive ion energy increases, the time lag for aluminum should become smaller than that for copper, while if the ion energy should decrease, the time lag might become greater for aluminum than for copper. Furthermore, the time lag for aluminum would vary over a greater range than that for copper. This is actually the case. Since the positive ion energy at static breakdown voltage increases with a decrease in pressure, this action might explain the observations. The writers have been unable to find in the literature any information regarding the variation of γ for aluminum and copper as just discussed, although such variation has been observed for Pt and NaH.[27,28]

The mechanism of spark breakdown in an unradiated gap can now be described as follows. For values of X and p below certain critical values, nearly all the free electrons which arise in the gap volume before breakdown are produced by cosmic rays and radioactive emanation

[26] R. Strigel, *Elektrische Stossfestigkeit* (Julius Springer, Berlin, 1939), p. 19.
[27] J. D. Cobine, *Gaseous Conductors*, p. 158.
[28] L. B. Loeb, *Fundamental Processes of Electrical Discharge in Gases*, pp. 394, 397.

from the earth, a very small number by field emission from the cathode, and thermal ionization, processes which are well known. Under these conditions the rate of electron formation is small, and the statistical time lag is large. When critical values of X and p have been reached, the ions in the gas may form free electrons either by negative ion disintegration (as Loeb has shown) or by the familiar process of positive ion impact at the cathode. The free electrons so formed can flood the gas with excited and metastable atoms whose neutralization leads to the formation of more electrons in the gap volume. Under these conditions, the rate of electron production may be high for a period of 10^{-3} second after the application of the field. As a result, the statistical time lag is small. In either case, the results of this investigation show that with electrons being formed principally in the body of the gas, the lag distribution in the range here studied can be described by the function $n/N=\exp[-bT^c]$. If the electrode surface should be covered with a certain type of coating such as that which formed on the nickel spheres during these tests, there may be copious production of electrons at the cathode by the Paetow effect. In this case, P_2 becomes nearly constant, and the lag distribution changes.

From Fig. 7 it is found that, for the gap and voltage wave form used in this study, the critical value of average field strength (X_c volts/cm) for a given pressure (p lb./sq.in. absolute) in the range from 10 to 90 pounds per square inch absolute can be found from the following formulas.

For copper, $X_c=602.4p+225{,}200.$
For aluminum, $X_c=1586p+136{,}200.$

From the curves of static breakdown voltage, the average field strength at the static breakdown value (X_b volts/cm) can be found approximately from the following equations. (The graphs of breakdown voltage *versus* pressure are slightly curved at very low and at very high pressures, but may be assumed to be approximately straight between 10 and 90 pounds per square inch absolute.)

For copper, $X_b=2396p+33{,}600.$
For aluminum, $X_b=2214p+35{,}300.$

The critical overvoltage ratio

$$[Q_c=(X_c-X_b)/X_b]$$

can be found from the following relations.

For copper, $$Q_c=\frac{191{,}600-1794p}{33{,}600+2396p}.$$

For aluminum, $$Q_c=\frac{100{,}900-628p}{35{,}300+2214p}.$$

CONCLUSIONS

To insure long lags, equipment should be operated so that for expected surges the value of Q is less than that of Q_c as given by the above formulas; for short lags, Q should be higher than Q_c. At 30 pounds per square inch absolute pressure, the critical overvoltage ratios are: for copper $Q_c=1.31$, for aluminum $Q_c=0.81$. At 90 pounds per square inch absolute pressure the critical values are: for copper $Q_c=0.12$, for aluminum $Q_c=0.19$. Thus while an increase in the gas pressure increases the static breakdown voltage, it also renders the apparatus more likely to break down under short impulses of small overvoltage.

This information should be of value to the designer of high voltage gas-insulated apparatus. There is a temptation to increase the operating voltage simply by increasing the gas pressure. For most *reliable* operation, the equipment should be designed so that expected short surges cannot produce sufficient field strength to permit ions to form electrons. If this precaution be taken, the equipment may safely withstand surges a thousand times as long as those which might produce breakdown by means of ions. It is further apparent that metallic parts of such equipment should be kept clean and smooth.

It is also important to note that where rapid spark breakdown is desired (as in the operation of lightning arresters, protective gaps, spark plugs, etc.) the gap should be operated in the region where the ions can form electrons under the conditions of the expected surge.

The authors wish to express their gratitude to Professor H. E. Clifford for his helpful suggestions and criticism during the preparation of this paper.

Some Applications of the High Resolving Power of the Electron Microscope

HENRY GREEN AND ERNEST F. FULLAM
Interchemical Corporation, New York, New York
(Received April 26, 1943)

The high resolving power attained with the electron microscope has extended the field of pigment microscopy to cover particles falling within the range of 0.20–0.004 micron. High resolving power also brings into view many particles that would otherwise be invisible, and shows definite shape in particles that with optical instruments appear simply as diffraction disks.

WHEN Köhler, in 1904, brought forth his ultraviolet microscope, resolving power was multiplied by a factor of 2. This startling advance in microscopy not only gave untold pleasure to those who were fortunate enough to own such an instrument—for the revelation of unsuspected detail more than met expectations—but it also broadened the field of microscopy itself and stirred the imagination with the hope that perhaps this was not all. Maybe a factor of 3 or of even 4 might be attained some day.

As is now well known, the electron microscope did not give a factor of 3 or 4. It went so far beyond that limit that the imagination itself becomes ineffective. The electron microscope gives a factor of approximately 50. It is the object of this paper to show graphically this increase in resolving power.

The development of the electron microscope does not mean that the optical microscope has become obsolete. Of the two instruments the latter will always be, perhaps, the more generally useful. It is certainly not the intention of the various manufacturers of electron microscopes to claim that their instruments will eventually replace ordinary microscopes. These manufacturers are fully aware of the irreparable damage such an advertising campaign would entail. As a matter of fact, they are so conscious of this point that they will not publish photographs showing a comparison of results obtained with both the optical and the electron instruments. Such comparisons should be made, of course, only by completely disinterested investigators.

A balance that can weigh a hundred pound sample is just as useful as a chemical balance that can detect a difference of 0.2 mg. It would be unwise to discard the former on the argument that the latter is more sensitive, for the latter can never measure a weight of 100 pounds. Both instruments are equally useful; they simply operate in different fields. So it is with the electron microscope. Its most useful field lies just beyond the resolving power of the optical instrument. In order to demonstrate this fact, comparisons must be made on samples using both types of instruments.

In making such comparisons the argument might be raised that the optical instrument is not shown to its best advantage. This is a difficult argument to meet for no matter how good a photomicrograph might be there will, nevertheless, always be room for improvement. Better results could be obtained, no doubt, by using absolutely monochromatic light; by mounting the microscope on a heavy concrete column; by applying devices for controlling the fine adjustment to a higher degree of exactness than can be done manually; and by using hand-picked objectives that for some reason or other happen to be a little better corrected than ordinary stock lenses. When all these things are accomplished, however, the net gain in resolving power is quite negligible when compared with the gain from the factor of 50 obtained with the electron microscope.

Another argument of a rather unusual nature has been raised at times. This argument claims that the absence of Brownian motion in the electron microscope indicates an unnatural state and that electron micrographs, are, therefore, in all probability nothing more than some form of illusion. Of course, the same argument could, on most occasions, be used against the optical instrument; but the optical microscopist is so accustomed to finding what he expects to find in both size and shape of image that he would

TABLE I. Various limits of resolution.

Type of microscope	d, limit of resolution	N.A. numerical aperture	Wave-length	Radiation	
Glass	0.25μ	1.40	0.58μ	Yellow light, strongest component of white light	C. Beck[1]
Glass	0.19	1.40	0.439	Blue line in magnesium spark	Calculated[2]
Glass, ultraviolet	0.16	1.40	0.365	Mercury arc line	Calculated[2]
Quartz, ultraviolet	0.134	1.25	0.275	Cadmium spark line	Calculated[2]
Quartz	0.125	1.25	0.257	Cadmium spark line	Calculated[2]
Quartz	0.11	1.25	0.275	Cadmium spark line. Oblique illumination	Trivelli[3]
Electron	0.0040	$\leqq$0.02	0.000005	Electron beam 60 kv	Practical limit[4]
Electron, theoretical	0.00058	1.00	0.000005	Electron beam 60 kv	R. Rebsch equation

[1] Conrad Beck, *The Microscope Part II* (1924), p. 82. Beck gives no definite wave-length. He simply states that the resolving power of white light is that of its strongest component, yellow.
[2] $d = 0.61\lambda/\text{N.A.}$
[3] A. P. H. Trivelli, Sci. Mo. **33**, 175–179 (1931).
[4] This is the limit attained by the authors of this paper.

disregard such an argument as absurd. It should be pointed out that the electron microscopist's experiences are similar. He also finds that subjects of known size and shape appear as he would expect them to be when examining them in the electron microscope. That is, spheres appear as spheres, elongated particles as elongated, and diatoms of known shape still have the same shape in their electron image. If these materials do not give artificial effects, it seems reasonable that illusions are not produced,—except below the resolving power of the instrument, which is also true of the optical instrument. Artificial effects can be produced also in materials that are altered by vacuum (dehydration, degasifying) and by the accumulated heat arising from electron bombardment. As a rule, such materials are not examined with the electron microscope. The absence of detectable Brownian motion arises from the fact that the materials being examined are fastened to the solid nitrocellulose membrane, being either incorporated in it or attached to its surface. Since the amplitude of vibration of Brownian motion is inversely proportional to the square root of the viscosity of the supporting medium, which is very high, the possibility of seeing Brownian motion under the circumstances is nil.

Another type of argument. untenable as the two preceding ones, is encountered in the statement that the relatively large depth of focus of the electron microscope is a disadvantage. The idea involved is that optical sectioning by means of focusing at different depths through a transparent material becomes impossible because the entire object is usually in focus from top to bottom. The depth of focus of the electron microscope as recorded in the literature varies from 1–10 microns. The authors' experience is that it is at least 5 microns and probably considerably more. This is an enormous amount when compared with 0.4 micron, the approximate depth of focus of the average oil immersion objective.

The large depth of focus of the electron microscope is an advantage in at least two ways: First, in photographing materials that vary considerably in "depth," like non-uniform pigments, which are composed of both large and small particles. In such a case it is not necessary to resort to a compromise focus (or to take more than one exposure in different planes) because the largest and smallest particles are invariably in focus at the same time. Second, the large depth of focus makes it possible to take stereoscopic pictures, which show the object in three dimensions. Valuable information can be obtained from these pictures. For instance, flat particles standing at an angle on edge can be seen to be thin plates or not, whereas viewed normally (non-stereoscopically) it would be impossible to determine whether they are thick or thin. See Fig. 6.

Compared with the optical microscope (N.A. 1.4) the numerical aperture of the electron

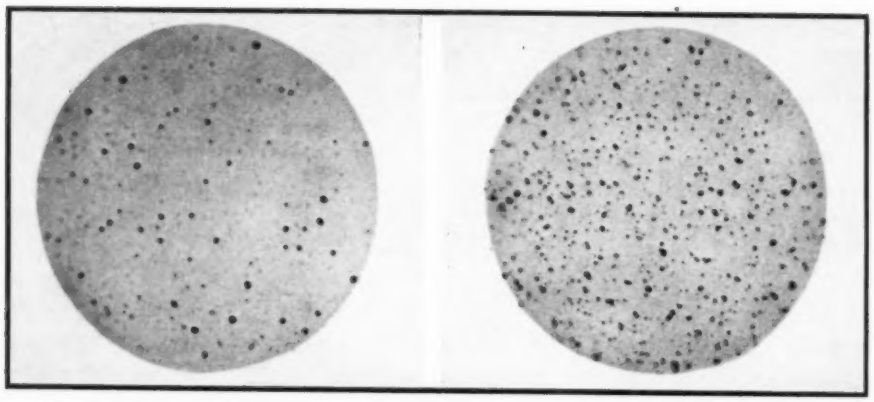

(a) 1575×. (b) 1575×.

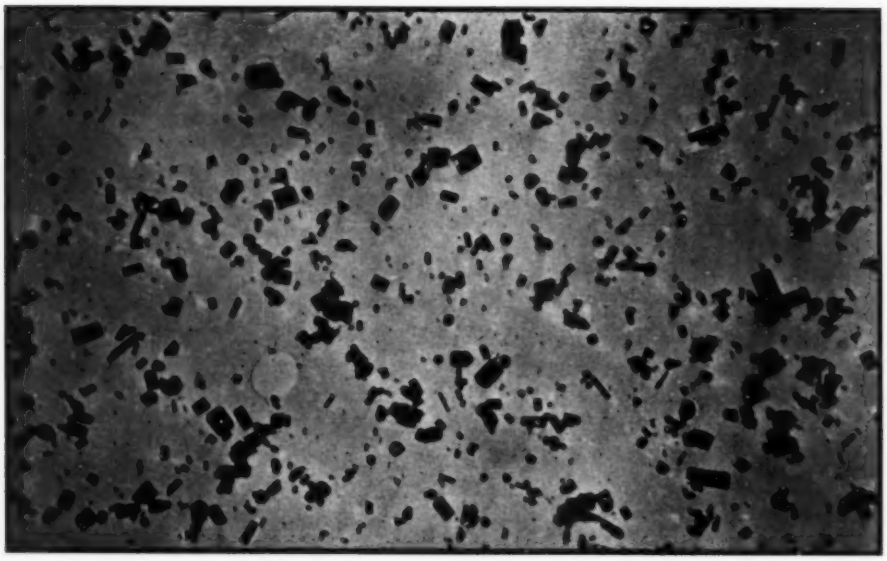

(c) 13,000×.

FIG. 1. Fine-grained zinc oxide.

microscope is relatively small (see Table I). This fact is sometimes erroneously used as an argument against any possible gain in the resolving power of the electron microscope. Borries and Ruska[1] give 0.02 as the largest practical N.A. for the electron microscope. Ardenne[2] states, from theoretical considerations, that to maintain a resolving power of the order of 10A, the N.A. can have values ranging from 0.006 to 0.015. These numerical apertures are from 70 to 230 times smaller than 1.4, the numerical aperture of the optical microscope. Because the limit of resolution in general varies inversely with N.A., it would appear offhand, from what has been said, that the resolving power of the electron microscope is negligibly small. This is not the case, however, for the associated wave-length of 60 kv electrons (used in the electron microscope) is 0.05A. Since this wave-length is approximately 100,000 times smaller than the average wave-length used in the optical instrument, there is actually a large net gain in resolving power. The equations for determining the limit of resolution follow:

For the optical microscope, the formula most frequently given is

$$d=0.61\lambda/\text{N.A.} \qquad (1)$$

[1] B. v. Borries and E. Ruska, Zeits. f. tech. Physik **8**, 225 (1939).
[2] M. v. Ardenne, *Electronen Uebermikroskopie* (Springer, Berlin, 1940).

where d is the limit of resolution and λ is the wave-length.

For the *theoretical* limit of resolution of the electron microscope Rebsch[3] gives,

$$d=0.7\lambda(f/\lambda)^{\frac{1}{4}} \qquad (2)$$

where f is the focal length. The numerical aperture does not appear in this equation because "theoretical limit" implies maximum conditions, i.e., N.A. is taken as unity.

Ardenne[4] gives 10A as the correct order for the theoretical limit of resolution of the electron microscope. The authors' instrument has a focal length of 3.9 mm at 60 kv. Substituting this value for f and 0.05A for λ in Eq. (2) gives a theoretical limit of 5.8A.

In actual practice the N.A. of the electron microscope is considerably less than unity. Unfortunately, there is no practical or convenient method for calculating it directly. However, a practical value for d can be obtained by measuring the smallest discernible particle on an electron micrograph of known magnification. The authors have carried out this procedure numerous times and have arrived at the conclusion that a fair practical limit of resolution for their instrument is 40A. Lower values have been claimed where ideal conditions of alignment, freedom from deposits in the objective pole piece diaphragm, etc. have been obtained. The reason that the actual practical limit of resolution does not reach the theoretical limit of 5.8A is because Eq. (2) gives the limit insofar as it is affected by diffraction and spherical aberration. There are other aberration effects not taken into account in Eq. (2), and these are sufficient to raise the limit of resolution to a value of approximately 40A. It seems likely, however, that improvement in the present limit will be attained in the none too distant future.

The four arguments (improper comparisons, artifacts, depth of focus, resolving power) against any possible gain obtained with the electron microscope seem superfluous to the electron microscopist; but to the microscopist who does

[3] R. Rebsch, Ann. der Physik **31**, 551 (1938).
[4] M. v. Ardenne, Zeits. f. Physik **108**, 338 (1938).

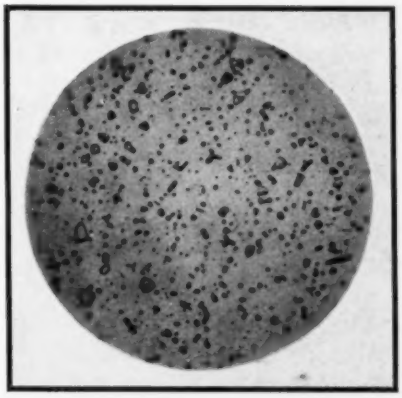

(a) 1250×.

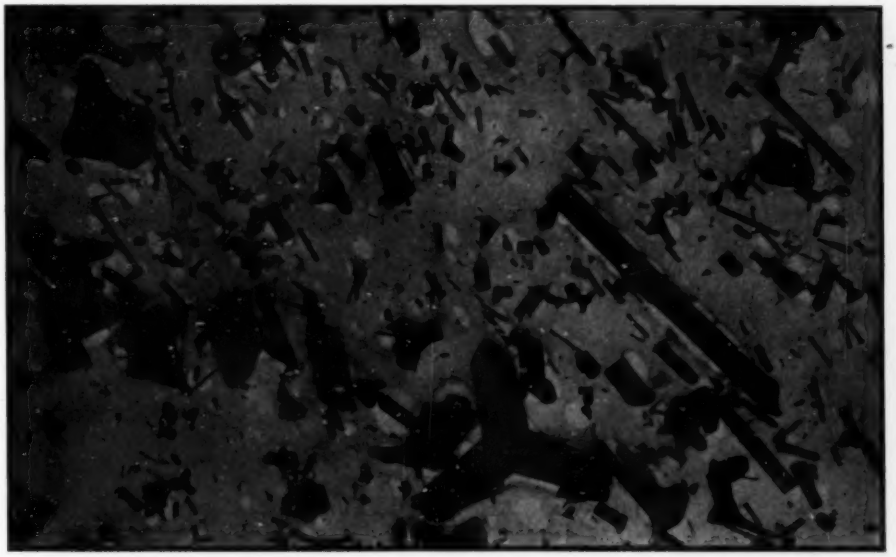

(b) 13,000×.

FIG. 2. Normal particle size zinc oxide.

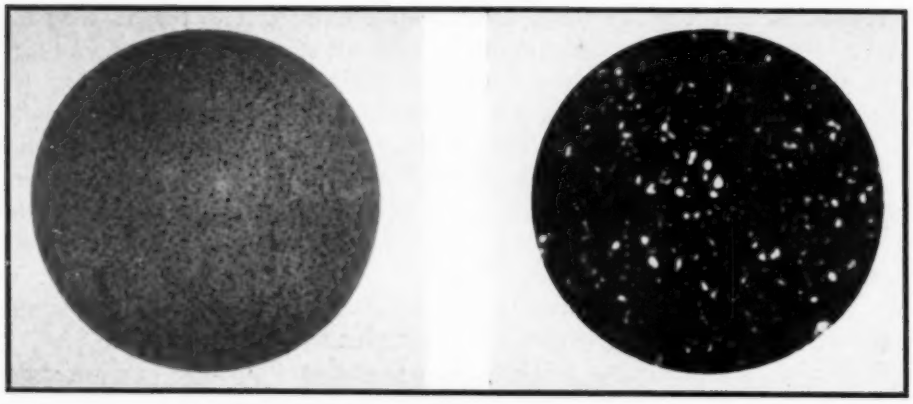

(a) 1250×. (b) 1250×.

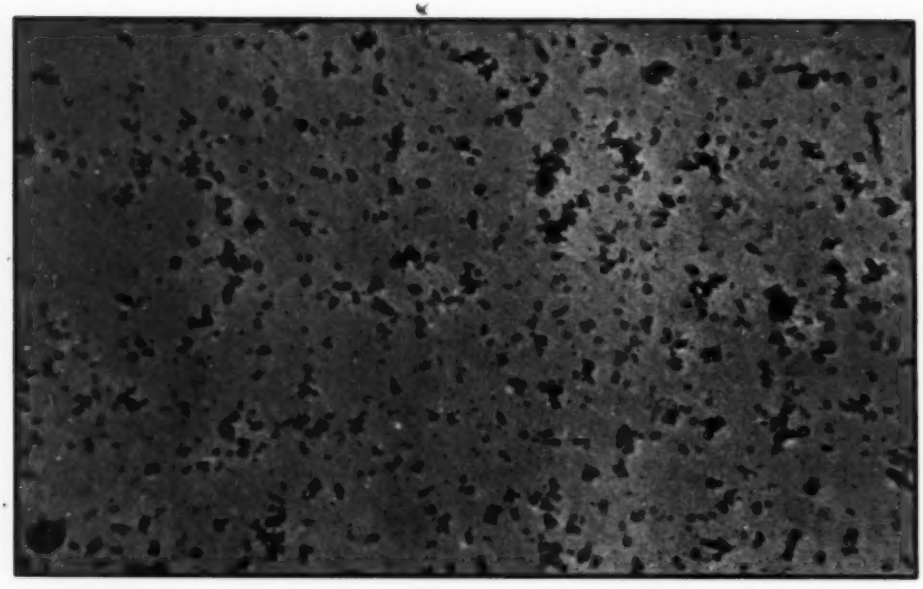

(c) 13,000×.

FIG. 3. Iron blue.

not work with an electron instrument these arguments sometimes appear to be of great importance. It is for this reason that they have been discussed in some detail here. In a few years, when knowledge of the electron microscope becomes more general, the above arguments will have been forgotten.

In the meantime, the actual advance in the limit of resolution has been approximately from 0.20μ to 0.004μ (40A). Just what does this amount to and how does it extend the field of microscopy? An electron micrograph of an unknown subject can give by itself no indication of the gain accomplished from the increased resolution. In order to demonstrate such improvement it is necessary to show comparative photographs, one taken with the optical and the other with the electron microscope. Furthermore, the investigator should restrict himself to a field in which he has had a sufficient number of years of experience. This is necessary so that full justice is done both to the instruments and to the subject.

Industrial pigments, of the kind used in paints and printing inks, constitute an important field in microscopy. Though many pigments have particle sizes large enough for detailed examination with the optical instrument, the majority of pigments fall just beyond this limit. In other words, they fall within the range that is now

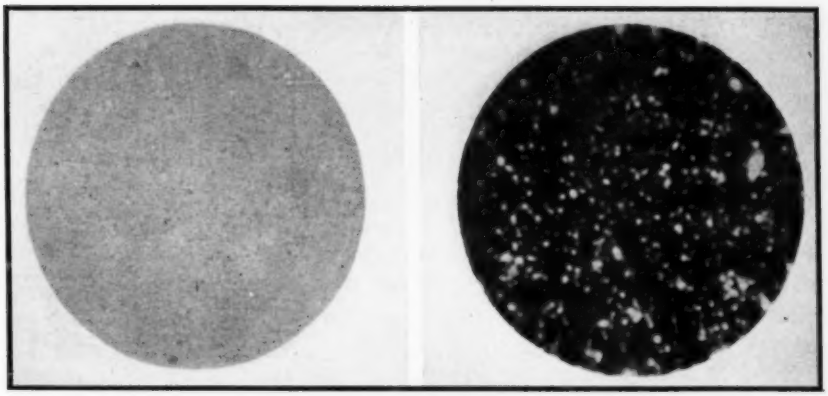

(a) 1250 ×. (b) 1250 ×.

(c) 25,000 ×.

FIG. 4. Hydrated ferric oxide.

substantially covered by the increase in resolution obtained with the electron microscope. The field of microscopy, then, has been extended; it now covers finely divided powders of colloidal size and also other materials of similar size such as bacteria and viruses.

A rectangular particle will appear as such only when its dimensions are large compared with the limit of resolution employed. When a rectangular particle is as small as a half-micron its angles will appear round and not sharp when viewed with an optical microscope. As the particle is further decreased in size the roundish appearing corners approach one another and the particle eventually appears to be a sphere. This type of image, of course, is a pure optical effect and arises solely from insufficient resolution. If such a particle is now examined with the electron microscope its true rectangular shape will be seen, provided its size is still large in comparison with the limit of resolution of the electron microscope.

Figure 1a is a photomicrograph of an exceedingly fine-grained zinc oxide. The dimensions of the particles are small in comparison with the limit of resolution, consequently the particles appear spherical. The objective was an exceptionally fine apochromat of 1.40 N.A. Strip photographs were taken above, at, and below the focus and examined for maximum definition. When the best position was found the fine adjustment was returned to that setting, taking care to do it in such a way that backlash did not

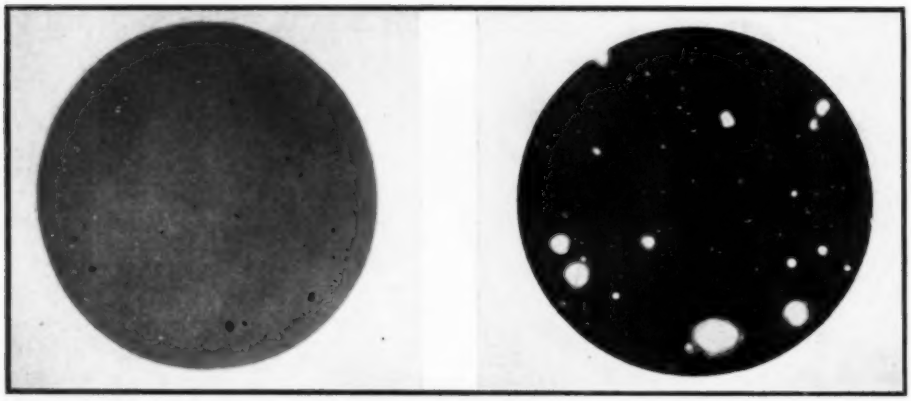

(a) 1250×. (b) 1250×.

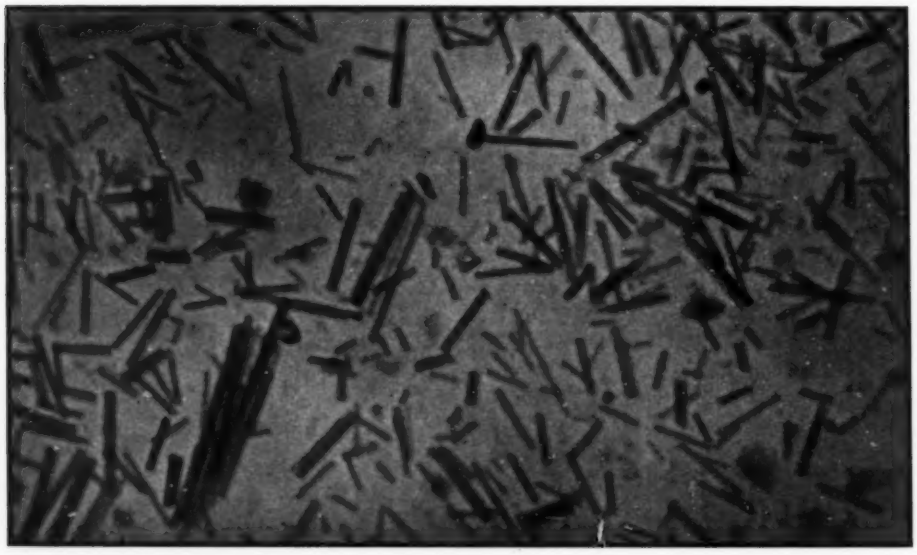

(c) 40,000×.

FIG. 5. Attapulgus clay.

interfere with the results. The condenser was adjusted at a position very slightly below critical illumination. The blue line (4390.6) in the magnesium spark spectrum was the illuminant. The magnification is 1575×. Any increase in the magnification would add nothing further in detail, i.e., the particles would still appear to be spheres.

Figure 1b is the same mount and spot; but this time ultraviolet light was used. The objective was an 1.7 mm quartz monochromat, glycerine immersed and the illuminant was the 0.275μ cadmium line. The magnification, 1575×, is possibly a little too low to produce the maximum detail obtainable with this lens; but the photograph shows approximately what a twofold increase in resolving power means. Compare Fig. 1a with Fig. 1b. Some of the larger particles no longer appear spherical but still their exact crystalline shape cannot be observed.

In passing from a twofold to a fiftyfold increase in resolving power one practically enters a new world. Figure 1c is the same type of zinc oxide as shown in the previous photographs, but in this case a different mount is used. On account of the high resolving power of the electron microscope higher magnification can be employed to advantage. The magnification in this case is 13,000×. The crystalline shape of the particle is now clearly defined and many particles are present which would be entirely invisible with an optical instrument.

In cases where a limit of resolution of 0.2μ is sufficient to show *all the detail*, the advantage of higher resolution is not so important. There is one exception, however, and that is where a measurement on a particle is to be made. The diffraction effect in the optical instrument always makes the particle image larger than it should be for the magnification employed. The percentage difference in this direction is substantial when the particle is smaller than 0.5μ. This diffraction effect is nearly absent in the electron microscope and so the particle can be measured with more accuracy provided the magnification is known. Unfortunately it is not so easy to determine magnification in the electron microscope as it is in the optical instrument. This is a condition, however, which is gradually being improved as new methods of calibration are developed.

Figure 2a is a zinc oxide of larger particle size than that shown in Fig. 1. An apochromatic objective, N.A. 1.4, was also employed here as well as in the other photomicrographs that follow. Figure 2a gives much of the detail that is to be found in this type of oxide; consequently there is not the same advantage gained in using the electron microscope here as in the previous case. Figure 2b is the electron micrograph of this pigment.

The pigment iron blue is shown in Fig. 3. Figure 3a is as it appears in the optical microscope. The particles are barely detectable. They are mounted in a very thin nitrocellulose membrane, an adjacent part of which was also used in making the corresponding electron micrograph, Fig. 3c. Figure 3b is the same spot on the membrane as shown in Fig. 3a; but in this latter case dark field illumination was employed. It should be noted that neither Fig. 3a nor 3b gives any indication as to the particle size or shape, except that the size is evidently very small. Figure 3c demonstrates the real value of the high resolving power gained with the electron microscope. From this electron micrograph the average particle size can be determined readily. It is found to be approximately 0.05μ. In addition, the shape of the particle is revealed, probably for the first time, and is seen to be cubical in appearance.

The material shown in Fig. 4 is a specially precipitated hydrated ferric oxide. Figure 4a was taken with the optical microscope and light field. Figure 4b is the same spot on the mount taken with dark field illumination. In these two photomicrographs the particles are discernible but the particle shape is not. The electron micrograph, Fig. 4c shows the particles to be acicular with a tendency to form shieves. This revelation

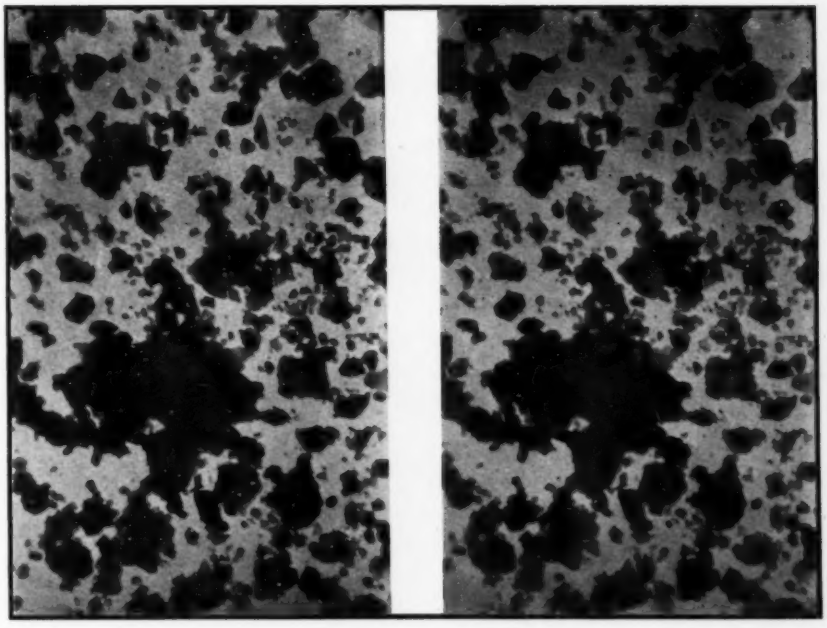

FIG. 6. China clay—3100×.

(a)

(b)

FIG. 7. (a) Lepra bacilli—30,000×. (b) Pleurosigma Obscurum—30,000×.

of detail is typical of the advantage gained by high resolution.

Figure 5 is attapulgus clay. It has exceptionally low contrast in the nitrocellulose film and is practically invisible in the optical microscope. See Fig. 5a. By using dark field, Fig. 5b, more particles are detected; but no conception of their size and shape is evident. The electron microscope again reveals the actual size and shape of the particle.

Figure 6 is a stereoscopic electron micrograph of a clay composed of hexagonal particles. This material has been mounted in such a manner that some of the particles are tilted, showing that they are exceedingly thin plates. This illustrates one advantage of the large depth of focus of the electron microscope.

Another great advantage of the high resolving power of the electron microscope is obtained in the examination of fine structural detail in objects such as bacteria and diatoms.

Figure 7a is an electron micrograph of Lepra bacilli and shows the structure including the capsule, in a way that can be obtained only with difficulty with the relatively low resolving power of the optical instrument. Figure 7b is the diatom Pleurosigma Obscurum, also taken with the electron microscope. The hexagonal pattern surrounding the puncta is a structure that has never been seen before.

ACKNOWLEDGMENT

The authors thank the Interchemical Corporation for permission to publish this paper. They also wish to express their indebtedness to Ruth N. Weltmann, Mary C. Schuster, and Vincent Salines for their assistance and advice.

Surge-Generator Circuits

EDWARD FISHER
Department of Physics, University of Maryland, College Park, Maryland
(Received February 26, 1943)

Formulas are developed for the free periods and damping factors of high voltage surge-generator circuits in discharge that contain a large number of meshes. The approximations used are based on an actual case, a generator in the High Voltage Laboratory of the National Bureau of Standards.

THE surge-voltage generator of n meshes in line is represented in discharge schematically as $n-1$ identical capacitors of capacitance C, discharged in series by spark-gaps through leads having identical resistances R and inductances L, a capacitance to ground of amount C_g being associated with each capacitor and its spark-gap terminals, and an nth mesh—where the high voltage developed is used—containing capacitance C_n, inductance L_n, and resistance R_n. See Fig. 1.

The theory of such a generator has been developed by Lewis.[1] The notation and equations of the present note come from his paper, in which also references to the literature will be found. Lewis reduced the problem of determining the harmonics of the voltage-wave—which are what one starts from in fitting the oscillogram taken of the discharge—to that of obtaining the roots, φ, of a secular equation, where $2\cosh\varphi = C_gL\Lambda^2 - C_gR\Lambda + (C_g/C) + 2$, $\Lambda = \mu + 2\pi i\nu$, and μ and ν are damping factor and frequency, respectively, of the harmonic.

An application of Lewis' theory by Dr. Silsbee and Dr. Harris in the High Voltage Laboratory of the Bureau of Standards led to the need for expressions for the roots, φ, under the conditions $L_n = L$, $R = O = C_g/C$. Although these simplifying conditions are used in developing the formulas below, the method itself is more general: for example, we could take $L_n/L = O(1)$; and R and C_g/C need not be negligible. Neglecting R and C_g/C yields $\Lambda_k = [\pm 2/(C_gL)^{\frac{1}{2}}] \sinh \frac{1}{2}\varphi_k$, where subscript k merely indicates the kth root. Then, taking $L_n = L$ and introducing $B = \mp R_n(C_g/L)^{\frac{1}{2}}$, $D = (C_g/C_n) - 1$, we can write Lewis' secular equation as

$$-e^{(2n-1)\varphi} = (2B \sinh \tfrac{1}{2}\varphi + D + e^{-\varphi})/(2B \sinh \tfrac{1}{2}\varphi + D + e^{\varphi}). \quad \text{(E)}$$

The rest of the experimental conditions kindly given me by Drs. Silsbee and Harris were: $C_n = 10^{-10}$ farad, $L = 5\times 10^{-6}$ henry, $R_n = 4000$ ohms, C_g somewhere between 10^{-11} and 10^{-10} farad, and $n = 20$. Substituting these values in B and D, we see that a useful formula might result from deriving the asymptotic form of the roots, φ_k, of (E) when $n \gg 1$, $B/n = O(1)$, $D = O(1)$. Because of the physical significance of φ we need consider only the following possibilities as n and $B \to \infty$: $|e^{\varphi}| \to \infty$, $|e^{-\varphi}| \to \infty$, $|e^{\varphi}| = O(1)$. The first two in (E) lead to contradiction. Hence, as n and $B \to \infty$, we have

$$e^{(2n-1)\varphi} \to -1, \quad \varphi_k \to \frac{2k-1}{2n-1}\pi i,$$

where k is any integer or zero. And so, we assume the expansion

$$\varphi_k = \frac{2k-1}{2n-1}\pi i + \frac{a_k}{n} + \frac{b_k}{n^2} + \frac{c_k}{n^3} + \cdots. \quad \text{(S)}$$

The voltage-wave is a sum of terms, each containing a factor of the form $\exp(-\Lambda_k t)$. And from (S)—if it can exist—we have

$$\Lambda_k = \frac{\pm 2i}{(C_gL)^{\frac{1}{2}}} \sin\left(\frac{2k-1}{2n-1}\frac{\pi}{2}\right) + \text{higher order terms.}$$

Hence the $\pm$ sign must be chosen so as to make the real part (as determined by the higher order terms) of $\Lambda_k \geqslant 0$. And the lowest harmonics correspond to the smallest values of $|2k-1|$.

Substituting (S) in (E) and equating coef-

[1] A. B. Lewis, Research paper (RP929), J. Res. Nat. Bur. Stand. **17** (1936).

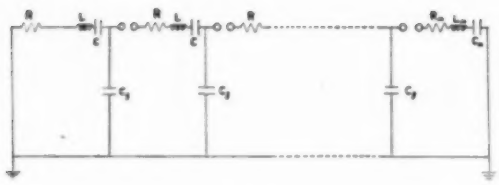

FIG. 1.

ficients of like-order terms, we are forced to consider two cases, $k=O(1)$ and $k=O(n)$. For $k=O(1)$:

$$\varphi_k=\pi(k-\tfrac{1}{2})\left[\frac{i}{n-\frac{1}{2}}-\frac{\sigma e^{i\theta}}{(n-\frac{1}{2})^2}-\frac{D+1}{(n-\frac{1}{2})^3}\sigma^2e^{3i\theta}\right]+O(n^{-4}), \quad (S_1)$$

where

$$\frac{e^{-i\theta}}{\sigma}=\pi B\frac{k-\frac{1}{2}}{n-\frac{1}{2}}-i(D+1).$$

And for $k=O(n)$:

$$\varphi_k=i\pi\frac{k-\frac{1}{2}}{n-\frac{1}{2}}-\frac{\cos\theta}{B(n-\frac{1}{2})}-i\cot\theta\frac{D+\cos 2\theta}{(2n-1)B^2}+O(n^{-4}), \quad (S_2)$$

where

$$\theta=\frac{2k-1}{2n-1}\frac{\pi}{2}.$$

Since there is no closed expression available for the terms represented by the $O(n^{-4})$ in (S_1) —and likewise in (S_2)—and since the convergence of the series-representation is uncertain, to put it mildly, we drop these terms from φ_k, calling the remaining closed expression $\bar{\varphi}_k$, and show that $\bar{\varphi}_k$ is in fact an approximation to φ_k.

To this end write (E) in the form $f=0$, where

$$f(\varphi)=\cosh(n+\tfrac{1}{2})\varphi+[2B\sinh(\varphi/2)+D]\cosh(n-\tfrac{1}{2})\varphi.$$

And write $\bar{f}\equiv f(\bar{\varphi})$, $df/d\varphi=F(\varphi)$, $F(\bar{\varphi})\equiv\bar{F}$. Then we have

$$\varphi=\bar{\varphi}+(f-\bar{f})(d\varphi/df)+\tfrac{1}{2}(f-\bar{f})^2(d^2\varphi/df^2)+\cdots,$$

a convergent series, where the derivatives are taken at $f=\bar{f}$. And if convergence is very rapid we have, approximately, $\varphi=\bar{\varphi}-(\bar{f}/\bar{F})$. Using $\bar{\varphi}$ from (S_1) we find $\bar{f}=O(n^{-3})$—where now the series-representation for $O(n^{-3})$ is convergent—$\bar{F}=O(n)$ and similarly $d^2\varphi/df^2=O(n^{-2})$, etc. And so, neglecting terms $O(n^{-4})$ in the series-representation of $\bar{f}$, and similarly using only the highest order terms in $\bar{F}$ and in $\bar{\varphi}$, we get, approximately:

$$\frac{\varphi_k-\bar{\varphi}_k}{\bar{\varphi}_k}(n-\tfrac{1}{2})^3=(D+1)\sigma^4e^{6i\theta}+\frac{\pi^2}{6}(k-\tfrac{1}{2})^2\sigma\times[(2\sigma^2+\tfrac{1}{8})ie^{3i\theta}+3\sigma e^{2i\theta}-\tfrac{7}{8}ie^{i\theta}].$$

In the same way we drop $O(n^{-4})$ from (S_2) to get $\bar{\varphi}_k$ for $k=O(n)$, and then find that, approximately,

$$\frac{\varphi_k-\bar{\varphi}_k}{\bar{\varphi}_k}=\frac{\cot\theta}{(2n-1)\theta B^3}\left[\frac{i}{3}\sin\theta\cos^2\theta-i\frac{(D+\cos 2\theta)^2}{4\sin\theta}+\frac{B\sin^2\theta}{2n-1}\right].$$

The above solutions can be grouped in fours. If $\varphi(k,B)\equiv\varphi_1+i\varphi_2$—where φ_1 and φ_2 are real—denote a solution for a certain k and B, then $\varphi(1-k,B)=\varphi_1-i\varphi_2$, $\varphi(k,-B)=-\varphi_1+i\varphi_2$, $\varphi(1-k,-B)=-\varphi_1-i\varphi_2$. Hence the computing need be done only for k and B positive. Corresponding to these four φ, incidentally, there are but two Λ, $\Lambda_1\pm i\Lambda_2$, because of the physical requirement, $\Lambda_1\geqslant 0$. Also, in connection with the computing, I might mention that in the case considered ($n=20$, etc.) solutions (S_1) and (S_2) —with their corrections—tended to fail rapidly when B fell below 6, and, surprisingly, (S_2) was as accurate as (S_1) for k as low as 3.

Obviously Λ_k can be found directly in terms of k, n, B, D; but the φ_k are the more fundamental, being needed, for example, to compute the charges on the capacitors in the generator. And, finally, it is understood that taking the correction terms in (S_1) and (S_2) to be $O(n^{-4})$—instead of $O(n^{-5})$ or $O(n^{-6})$—was no fault of the method: simplicity in the formulas was merely considered more desirable than additional accuracy.

Breakdown of Thixotropic Structure as Function of Time

RUTH N. WELTMANN
Interchemical Corporation, New York, New York

(Received April 20, 1943)

Measurements of the thixotropic breakdown of structure with time of agitation were performed at different rates of shear on a number of pigment suspensions and on various oils in a rotational viscometer. The product of rate of breakdown in thixotropic structure and time of agitation at any rate of shear was found to be a constant for each material. It is called "the time coefficient of thixotropic breakdown" and is independent of the rate of shear, which is applied to agitate the sample. The time coefficient of thixotropic breakdown is measured in absolute units, having the dimensions of viscosity (dynes sec./cm²). The equilibrium time—the time necessary to break the thixotropic structure down to its minimum at a specified rate of shear—was also found to be independent of the rate of shear applied while agitating.

A MATERIAL is called thixotropic if it undergoes an isothermal gel-sol-gel transformation upon agitation and subsequent rest. However, Freundlich[1] recognized that thixotropy does not require a change of a gel to a complete sol, hence any material is thixotropic if its structure will break down even partially upon agitation and will recover completely after a sufficient period of rest, while its temperature remains constant.

In the identification of thixotropy of a material, three different tests have been suggested in the literature. Each of these test methods in itself is sufficient to determine whether a material is thixotropic.

1. The presence of thixotropy in a material can be recognized by the continuously increasing breakdown of structure as a function of the increased rate of shear.

2. The existence of thixotropy in a material can be evidenced by rebuilding of the structure upon rest after a previous subjection to violent motion.

3. Thixotropy in a material can be identified by the continuously increasing breakdown of structure with the time during which the material is rapidly agitated.

To all of these three different methods reference has been made in the literature.

The first method for identifying thixotropy has been discussed in a recently published paper by Green and Weltmann.[2] In the determination of the thixotropic behavior of a material this method is very successful insofar as the experimental results are reproducible and thus quantitative information becomes available.

The second method which has been much more widely used in the past has suffered from the fact that reproducible experiments cannot be easily performed without a greater knowledge of the problem of thixotropic breakdown, which only recently is available. Fundamentally most of the investigators like Freundlich[1,3–10] and his co-workers, Schalek, and Szegvari,[11] Heller and Roeder,[12] McMillen,[13–15] Sheets,[16] and Pryce-Jones[17,18] subjected the material under investigation to some agitation and brought thereafter this material to rest and measured the solidification of the material by means of different methods, some primitive and some ingenious. The inherent difficulty is caused by the fact that the solidification as function of time depends upon the breakdown condition of the structure at the point of maximum agitation, that is just before the ma-

[1] Freundlich and others, Editors, *The Colloidal State I, Thixotropy* (Paris, 1935), p. 267.
[2] Green and Weltmann, Ind. Eng. Chem. Anal. Ed. **15**, 201 (1943).
[3] Freundlich, Protoplasma **2**, 278 (1927).
[4] Freundlich, Kolloid Zeits. **46**, 289 (1929).
[5] Freundlich, Kolloid Zeits. **45**, 348 (1928).
[6] Freundlich, Kolloid Zeits. **52**, 37 (1930).
[7] Freundlich and Bercumshaw, Kolloid Zeits. **40**, 19 (1926).
[8] Freundlich and Rawitzer, Kolloid Zeits. **41**, 102 (1927).
[9] Freundlich and Rawitzer, Kolloid Beih. **25**, 231 (1927).
[10] Freundlich and Schaleck, Zeits. f. physik. Chemie **108**, 153 (1923).
[11] Schaleck and Szegvari, Kolloid Zeits. **33**, 326 (1923).
[12] Heller and Roeder, Trans. Faraday Soc. **38**, 5, 191 (1942).
[13] McMillen, J. Rheology **3**, 75 (1932).
[14] McMillen, J. Rheology **3**, 163 (1932).
[15] McMillen, J. Rheology **3**, 179 (1932).
[16] Sheets, Paper Trade J. **16** (1943).
[17] Pryce-Jones, J. Oil Colour Chem. Assoc. **17**, 305 (1934).
[18] Pryce-Jones, J. Oil Colour Chem. Assoc. **19**, 295 (1936).

terial is brought to rest. To be able to judge the breakdown condition of the structure of a material, the maximum rate of shear to which the material has been subjected and how long it has been submitted to that rate of shear has to be known. Pryce-Jones[19] realized that the structure of a thixotropic material breaks down with time, while under a constant rate of shear. He speaks of an equilibrium value which can be obtained, but fails to see the important influence the previous history of the material has upon the results of the measurements made in accordance with the second method. To make the second method really effective, if one wants to use it at all, the third method has to be investigated more carefully and the relationship of the breakdown of thixotropic structure as a function of time for different rates of shear has to be established.

INSTRUMENT

A series of experiments have therefore been undertaken using the rotational viscometer for these measurements. The rotational viscometer is described in another paper[20] and also in more detail in a paper by Green.[21] The cup rotating at various speeds imparts—due to the material between cup and bob—a deflection to the bob counter-balanced by the torsion of a helical spring on which the bob is suspended. Regular flow curves are obtained by plotting increasing and decreasing speeds against deflections. The speeds are obtained in revolutions per minute (r.p.m.) and can be converted into rates of shear (sec.$^{-1}$) by multiplying the r.p.m. by a constant equal to 0.73. This constant is obtained according to an equation given in another paper,[20] where all instrumental dimensions are substituted in accordance with the viscometer used. The deflections obtained are in degrees and can be converted into torques (dynes/cm) by multiplying the degrees deflection by the torsion constant of the spring employed. Various springs are used to increase the range of materials measurable on the viscometer. The calibration of the springs is shown in a paper by Green.[21]

[19] Pryce-Jones, J. Sci. Inst. March (1941).
[20] Weltmann, to be published.
[21] Green, Ind. Eng. Chem. Anal. Ed. **14**, 576 (1942).

EXPERIMENTAL PROCEDURE

Figure 1, curve T_2AT_2 shows a flow curve of a thixotropic plastic material. The branch of the flow curve obtained during the period of speed increase is curved, while the branch obtained during speed decrease has a large linear portion. Attention may be called to the fact that these flow curves are obtained in a rapid measurement bringing the material under investigation up to the top rate of shear as fast as possible and thereafter reducing the speed immediately.

If the material under investigation is subjected for a certain length of time to the top rate of shear before the down curve is started, a flow curve BT_2, Fig. 1, is obtained. If the top rate of shear is sustained for a sufficiently long time, which may be called "the equilibrium time," a flow curve CT_2, Fig. 1, results. This flow curve CT_2 represents the limiting case since the structure of the material will not break down any further even if it is continuously submitted to this same rate of shear.

The linear branches of the flow curve, Fig. 1, which are obtained by decreasing the rate of shear are representative for the thixotropic condition of the material under investigation. These linear portions are indicative of the plastic viscosity and the yield value at a given breakdown condition of the material and have therefore been rightly called thixotropic levels.[2, 20, 21]

For the various thixotropic levels the plastic viscosities and the yield values can be obtained from Reiner's[22] equation as follows:

$$U=\frac{T-T_2}{\omega}S \tag{1}$$

and

$$f=T_2C \tag{2}$$

where U is the plastic viscosity in poises, f is the yield value in dynes per square centimeter, T is the torsion in dynes centimeter, T_2 is the torsion at the intercept of the straight line with the torque axis and is also measured in dynes centimeter, ω is the angular velocity in sec.$^{-1}$ and S and C are instrumental constants. S is equal to $(1/R_b^2-1/R_c^2)/4\pi h$ and C is equal to $S/1n(R_c/R_b)$, where R_c is the radius of the cup, R_b is the radius of the bob and h is the immersed height of the bob.

[22] Reiner and Riwlin, Kolloid Zeits. **43**, 1 (1927).

To obtain the relationship between the breakdown of thixotropic structure and the time during which the material is subjected to a constant rate of shear, the following procedure has been adopted. The drive mechanism of the rotational viscometer is adjusted to a speed that will produce the desired rate of shear. The instrument is started by connecting the drive mechanism to the power supply, thus obtaining the desired top rate of shear practically without any delay. The bob will be deflected because of the resulting torque and the time measurement is started as soon as the bob reaches its maximum deflection, that is, just before it starts to reverse. The time of maximum deflection is called t_0. Because of the inertia effects of the system t_0 is not very well defined; but the errors introduced are usually

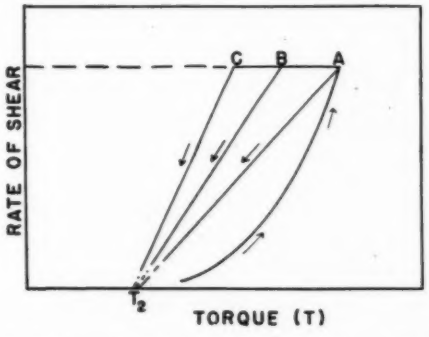

FIG. 1. Schematic flow curve. *A*, regular flow curve as obtained by first increasing and then immediately decreasing the rate of shear; *B*, *C*, two other thixotropic levels of the same material as obtained after different time intervals at the same constant top rate of shear.

insignificant inasmuch as materials have been used for experimental investigations where changes of breakdown have been observed over periods of minutes, thus making a few seconds error as regards to t_0 negligible.

For most materials a down curve is taken after a period of about 5 to 10 seconds at t_S, Fig. 2, subsequent to the time reading at t_0. After having obtained this down curve by decreasing the speed of the cup as fast as it is conveniently possible to do so while taking deflection readings of the bob, the speed of the cup is raised again to produce the original rate of shear. The deflection of the bob is found to be somewhat higher than it was at t_S before the first down curve was started, due to the necessary time consumption of the measurement which produced a slight

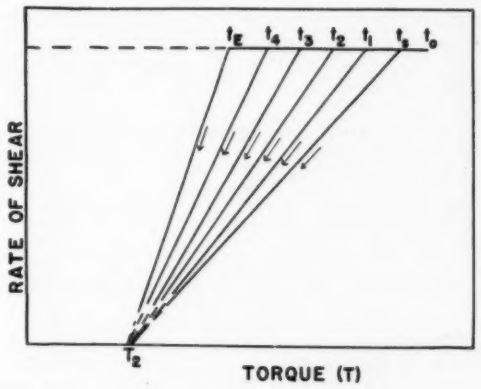

FIG. 2. Schematic drawing of the experimental procedure. Each straight line represents a different thixotropic level of the same material obtained after various time intervals at a constant rate of shear.

buildup in thixotropic structure. As soon as the thixotropic level of the first down curve is reached, the measurement of a new time interval is started, at the end of which at t_1 a second down curve is taken. The same process is repeated until the material does not show any further breakdown. The time interval between t_0 and the time necessary to obtain such an equilibrium condition is the equilibrium time t_E. The plastic viscosity obtained from this minimum thixotropic level is called the equilibrium plastic viscosity, U_E, for the designated top rate of shear. An approximate equal spacing of the thixotropic levels is obtained by measuring down curves after a constant loss in top torque. The time necessary for obtaining the down curves, consisting of about thirteen points each, was less than one minute.

The experiments show as is also indicated in Fig. 2, that the various thixotropic levels intersect the torque axis at about the same point, indicating that the yield value for each top rate of shear remains constant for all practical purposes independent of the breakdown with time of the material. Since the yield value and thus T_2 is essentially constant, Eq. (1) shows that the plastic viscosities of the various thixotropic levels are linearly related to their top torques at constant top rates of shear.

One may wonder why so much trouble has been taken in obtaining the different down curves, Fig. 2, for establishing thixotropic levels and measuring plastic viscosities. Offhand, it appears that sufficiently accurate information

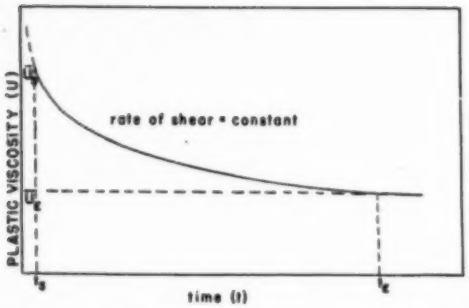

FIG. 3. Plastic viscosity—time curve of one material drawn schematically for one constant top rate of shear.

can be compiled by establishing the relationship of bob deflection (torque) as a function of time, which has been done in another paper[20] to prove the existence of thixotropic structure. However, the author felt that the experimental evidence may not be sufficiently reliable and therefore chose this more complicated but considerably more accurate procedure.

RESULTS

Plastic viscosities rather than torques have been plotted in all the following curves in order to make the results independent of the instrument used.

Figure 3 shows the relationship between plastic viscosity, U, and the time interval, t, over which the constant rate of shear was applied, as obtained from Fig. 2. This curve, Fig. 3, between the values t_S and t_E approaches a logarithmic curve. Below t_S, the plastic viscosity values are slightly too high due to the above-mentioned inertia effects, and above t_E the plastic viscosity remains constant, since it has reached its minimum at that point.

If the time axis is therefore plotted on a logarithmic scale a straight line is obtained between these limits. By plotting plastic viscosity-ln time curves, for different top rates of shear as parameters, parallel lines are obtained, Fig. 4.

The interesting fact is that by plotting $U-U_E$ as function of the logarithm of time only one straight line is obtained for each material, Fig. 5. This means that t_E has practically the same value for different top rates of shear and furthermore means that the rate of breakdown of thixotropic structure is independent of the top rates of shear.

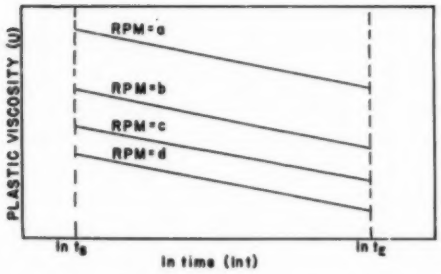

FIG. 4. Plastic viscosity-ln time curves of one material drawn schematically for various constant top rates of shear.

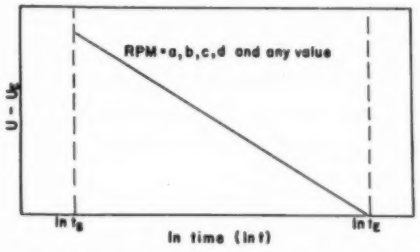

FIG. 5. Schematic curve showing the relationship between $U-U_E$ and ln t for one material obtained at various constant top rates of shear.

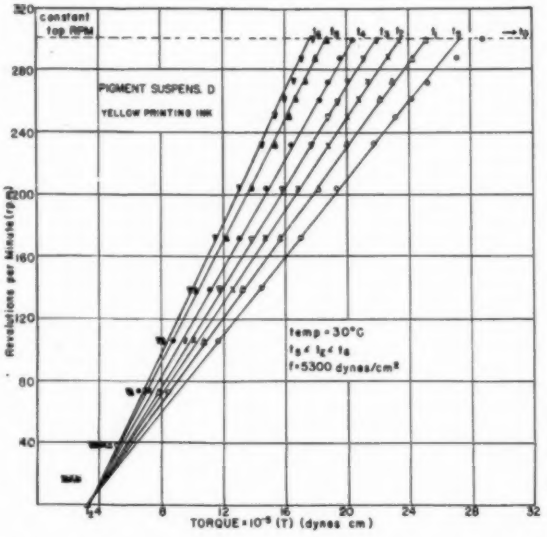

FIG. 6. Experimental curves showing various thixotropic levels of one pigment suspension obtained at a constant top r.p.m. after various time intervals.

The following empirical equation was easily deduced from these curves and is in accordance with the facts stated above.

$$\exp\left[-(U_1-U_2)/B\right]=t_1/t_2 \qquad (3)$$

where the plastic viscosities U_1 and U_2 are any

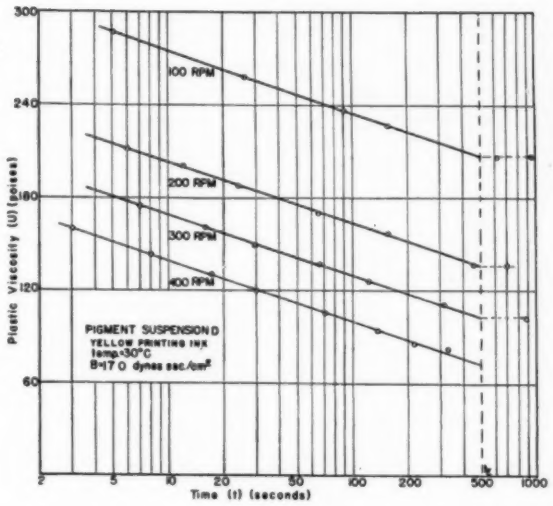

FIG. 7. Experimental curves showing the relationship between plastic viscosity and logarithm of time of agitation of one pigment suspension obtained at various constant top r.p.m.

TABLE I. Various thixotropic levels of a pigment suspension, D, obtained after various time intervals at a constant top r.p.m. (yellow printing ink, Fig. 6). Constants: Temp. = 30°C; $T_2 = 3.3 \times 10^5$ dynes cm; $f = 5300$ dynes/cm²; $t_E = 530$ sec.

		Torque $\times 10^{-5}$ (dynes cm)						
r.p.m.	t_0	$t_0=7$ sec.	$t_1=16$ sec.	$t_2=29$ sec.	$t_3=66$ sec.	$t_4=121/.5$ sec.	$t_5=315$ sec.	$t_6=880$ sec.
300	43.0	28.8	25.2	23.4	22.0	20.5	18.8	17.9
288		27.2	24.3	22.8	21.2	19.6	18.0	17.2
273		25.3	23.0	21.4	20.1	18.8	17.4	16.7
262		24.3	22.2	20.8	19.5	18.3	16.7	16.0
250		23.2		20.1	18.9		16.4	15.4
233		21.8	20.0	18.8	17.8	16.4	15.4	14.6
204		19.4	18.2	16.8	15.9	14.8	13.9	13.1
172		17.1	15.7	14.7	13.9	13.1	12.2	11.5
139		14.5	13.3	12.6	11.8	11.2	10.3	9.8
106		11.7	10.8	10.1	9.6	8.8	8.2	7.9
73		8.5	7.9	7.3	7.0	6.6	6.1	5.9
38		5.2	4.7	4.4	4.2	4.0	3.6	3.5
17		2.7	2.6	2.3	2.2	2.0	2.0	1.8

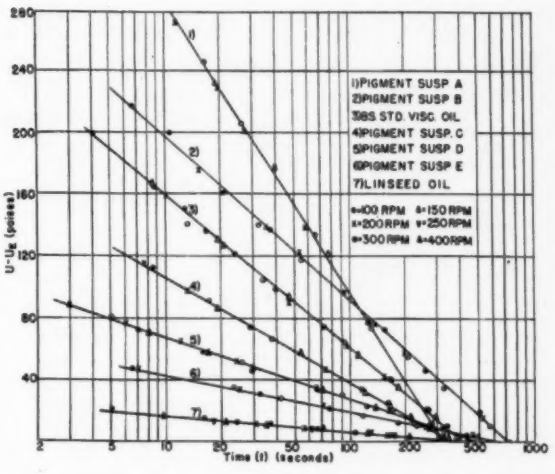

FIG. 8. Experimental curves showing the relationship between $U - U_E$ and $\ln t$ of five pigment suspensions and two oils obtained at various constant top r.p.m.

TABLE II. Decrease in plastic viscosity, U, with increase in time of agitation, t, of a pigment suspension, D, for different constant top r.p.m. (yellow printing ink, Fig. 7). Constants: Temp. = 30°C; $t_E = 530$ sec.

Time coefficient of thixotropic breakdown, $B = 17.0$ dynes sec./cm²					
U (poises)	$U - U_E$ (poises)	t (sec.)	U (poises)	$U - U_E$ (poises)	t (sec.)
100 R.P.M.			200 R.P.M.		
288	81	5	213	77	6
258	51	26	201	65	12
237.5	30.5	90	188	52	24
228	21	158.5	170	34	65.5
207	0	608.5	157	21	153.5
207	0	960	137	5	458
			136	0	700
300 R.P.M.			400 R.P.M.		
175	72	7	160	88	3
161	58	16	143	71	8
149	46	29	130	58	17
137	34	66	120	48	29.5
126	23	121.5	106	34	70.5
112	9	315	95	23	138.5
103	0	885	86	14	217
			82.5	10.5	333

viscosities between U_S and U_E, obtained at the respective times of application t_1 and t_2, which are between t_S and t_E, Fig. 3.

The proportionality constant B, is the tangent of the angle the straight lines form with the ln time axis, Figs. 4 and 5. By differentiating Eq. (3), the definition of B and its physical significance can be found.

$$B = -\frac{dU}{dt} \times t. \qquad (4)$$

According to Eq. (4), B can be defined as the product of rate in breakdown of plastic viscosity and time, that is the time during which the agitation at constant rate of shear has been applied. Since it has been shown above that the yield value is practically a constant for each rate of shear, if applied over various lengths of time, B, which shall be called "the time coefficient of thixotropic breakdown" is the product of rate in breakdown of *thixotropic structure* and time of agitation at constant rate of shear. The

TABLE III. Decrease in plastic viscosity, U, with increase in time of agitation, t, of four pigment suspensions and two oils for different constant top r.p.m. Constant Temp. = 30°C.

Pigment suspension, *A*. (black printing ink) $t_E = 320$ sec.
Time coefficient of thixotropic breakdown, $B = 82.7$ dynes sec./cm²

U (poises)	$U-U_E$ (poises)	t (sec.)	U (poises)	$U-U_E$ (poises)	t (sec.)	U (poises)	$U-U_E$ (poises)	t (sec.)
	100 R.P.M.			150 R.P.M.			200 R.P.M.	
975	245	16.5	740	232	18.5	590	272	11.5
936	206	26	686	178	39.5	546	228	19.5
864	134	62.5	629	121	75	518	200	26.5
804	74	127.5	586	78	128.5	456	138	56.5
744	14	276.5	508	0	348.5	394	76	133.5
			508	0	710	323	5	314
						318	0	470
						318	0	700

Pigment suspension, *B*. (blue printing ink) $t_E = 730$ sec.
Time coefficient of thixotropic breakdown, $B = 45.7$ dynes sec./cm²

	100 R.P.M.			200 R.P.M.			300 R.P.M.	
490	140	32	388	176	15	360	217	6.5
467	117	54	351	139	35	343	200	10.5
426	76	125	335	123	52.5	304	161	20.5
405	55	208	298	86	115.5	280	137	36.5
385	35	319	270	58	196.5	240	97	92.5
360	10	570	230	18	511	216	73	152.5
350	0	730	212	0	841	189	46	257.5
			212	0	870	162	19	500

Pigment suspension, *C*. (red printing ink) $t_E = 355$ sec.
Time coefficient of thixotropic breakdown, $B = 29.5$ dynes sec./cm²

U (poises)	$U-U_E$ (poises)	t (sec.)	U (poises)	$U-U_E$ (poises)	t (sec.)
	100 R.P.M.			150 R.P.M.	
340	91	17	286	86	19
316	67	37	258	58	53
272	23	159.5	232	32	119
249	0	460	216	16	211
249	0	610	202	2	334
	200 R.P.M.			300 R.P.M.	
265	115	7.5	222	112	8.5
248	98	13	184	74	28.5
197	47	73	134	24	158.5
184	34	114	112	2	313.5
158	8	268.5	110	0	432
151	1	335	110	0	600

Pigment suspension, *E*. (green printing ink) $t_E = 630$ sec.
Time coefficient of thixotropic breakdown, $B = 10.0$ dynes sec./cm²

U (poises)	$U-U_E$ (poises)	t (sec.)	U (poises)	$U-U_E$ (poises)	t (sec.)	U (poises)	$U-U_E$ (poises)	t (sec.)
	100 R.P.M.			200 R.P.M.			300 R.P.M.	
128	35	23	117	47	7	104	47	6.5
121	28	41.5	103	33	25	88	31	32
110	17	116.5	93	23	71	78	21	77
104	11	229.5	79	9	256	70	13	179.5
97	4	479.5	70	0	650	61	4	425
93	0	730				57	0	635

negative sign in Eq. (4) indicates that dU represents a decrease in plastic viscosity with time of agitation and not an increase. Then from Eq. (3)

$$B = \frac{U_1 - U_2}{\ln t_2/t_1} \tag{5}$$

where B is independent of the instrument and has the same dimensions as viscosity, (dynes sec./cm²).

For the torques T, a similar relationship can be established by substituting Eq. (1) for the plastic viscosities, U, keeping in mind that T_2 is essentially a constant.

TABLE III.—*Continued*

Bureau of Standard's standard viscosity oil (mineral oil) $t_E = 420$ sec.
Time coefficient of thixotropic breakdown, $B = 39.1$ dynes sec./cm²

U (poises)	$U - U_E$ (poises)	t (sec.)	U (poises)	$U - U_E$ (poises)	t (sec.)
	100 R.P.M.			150 R.P.M.	
690	140	13	576	166	8.5
655	105	33.5	540	130	19
615	65	91.5	504	94	46
590	40	165.5	465	55	108.5
571	21	271	446	36	182
550	0	477	426	16	290
			410	0	500
	200 R.P.M.			300 R.P.M.	
448	160	9.5	360	200	4
416	128	20.5	325	165	8.5
378	90	46.5	310	150	12.5
350	62	94.5	296	136	16.5
330	42	150.5	281	121	23.5
310	22	261	259	99	39.5
288	0	477	234	74	71.5
			201	41	161.5
			170	10	337

Linseed oil $t_E = 500$ sec.
Time coefficient of thixotropic breakdown, $B = 4.3$ dynes sec./cm²

	200 R.P.M.			250 R.P.M.	
102	11.0	30.5	106.5	20.3	5
100	9.0	56	100	13.8	18
97.1	6.1	128	94.8	8.6	61.5
96	5.0	159	90.8	4.6	170
93.2	2.2	300	87.8	1.6	306
92.5	1.5	370	86.2	0	520
91.0	0	570			
	300 R.P.M.			400 R.P.M.	
93.8	14.6	16	90.0	17	9.5
92	12.8	24.5	86	13	21
90.1	11.9	37	84.8	11.8	35.5
87.5	8.3	66.5	80.9	7.9	71
85.2	6.0	107	78.5	5.5	124
84	4.8	163.5	76.6	3.6	209
81.0	1.8	300	73.5	0.5	425
			73	0	645

EXPERIMENTAL CURVES

In all experimental curves and tables, r.p.m. are plotted and tabulated instead of rates of shear. The conversion factor for calculating revolutions per minute, r.p.m., into rates of shear for the viscometer used, is given earlier in this paper.

Figure 6, Table I, shows the various thixotropic levels obtained after various time intervals, during which the material has been agitated at a constant top r.p.m. (R.P.M.). It has been obtained following the above-described experimental procedure and is in accordance with the schematic Fig. 2. Figure 6 is obtained from a pigment suspension and is representative for all the curves obtained at various top rates of shear for the many pigment suspensions and oils, which have been investigated in this laboratory.

From the thixotropic levels of Fig. 6, the plastic viscosities are calculated and plotted against the logarithm of the time during which the constant rate of shear has been applied, Fig. 7, Table II. This is shown in Fig. 7 for various top rates of shear to demonstrate that the tangent of the angle the straight lines form with the ln time axis or the time coefficient of thixotropic breakdown, B, is independent of the top rate of shear or R.P.M.

Five pigment suspensions and two oils have been plotted in a convenient manner from experimental data obtained at various top r.p.m., Fig. 8, Tables II and III. From this plot it is

evident that not only B is independent of the top rate of shear but that also t_E, the equilibrium time, is the same for all top r.p.m.

The preceding analysis for pigment suspensions and oils may be extended to all thixotropic plastic materials. However, since only oils above a certain rate of shear which in another paper[20] has been called the "limiting rate of shear" behave like thixotropic plastics, above statements are only applicable for oils at higher rates of shear than their limiting rate of shear.

ACKNOWLEDGMENT

The author is indebted to Interchemical Corporation for permission to publish this paper, to Mr. H. Green for many valuable suggestions, and to Miss E. Berezin for assistance in carrying out the experiments.

Concerning the Roots of $J_n'(x)N_n'(kx)-J_n'(kx)N_n'(x)=0$

ROHN TRUELL
RCA Laboratories, Princeton, New Jersey

(Received April 8, 1943)

The relation $J_n'(x)N_n'(kx)-J_n'(kx)N_n'(x)=0$ arises in certain resonant cavity problems having cylindrical symmetry. The first roots of this relation are presented here as a function of k for $n=1, 2, 3, 4$. The M'Mahon relation does not allow calculation of the first roots despite statements to the contrary in several places. It is shown that the functions $J_n'(x)/N_n'(x)$ have relative maxima at $x=n$ except for $n=0$.

THE relation

$$J_n'(x)N_n'(kx)-J_n'(kx)N_n'(x)=0 \qquad (1)$$

arises in a certain class of boundary value problems. An expression for the solution of (1) is given for $k\to 1$ by J. M'Mahon in a paper, "On the Roots of the Bessel and Certain Related Functions."[1] The expression for the sth root, in order of magnitude, is given by:

$$x_n^{(s)}=\delta+\frac{p}{\delta}+\frac{q-p^2}{\delta^3}+\frac{r-4pq+2p^3}{\delta^5}+\cdots \qquad (2)$$

where

$$\delta=\frac{s\pi}{k-1}, \quad p=\frac{m+3}{8k}, \quad m=4n^2,$$

$$q=\frac{4(m^2+46m-63)(k^3-1)}{3(8k)^3(k-1)},$$

$$r=\frac{32(m^3+185m^2-2053m+1899)(k^5-1)}{5(8k)(k-1)}.$$

It is perhaps not necessary to point out that since this series involves asymptotic forms for the Bessel functions the series is better for large x. Of course k is also involved, and as $k\to 1$, $\delta\to\infty$ and $x_n^{(s)}\to\delta$ or, in other words, the expression for $x_n^{(s)}$ is given more nearly by the first term of the series the larger x is. While it is mentioned in several places that relation (2) is not as valid for small s as it is for large s, the writer has not seen any statement to the effect that the first root of (1) or

$$\frac{J_n'(x)}{N_n'(x)}-\frac{J_n'(kx)}{N_n'(kx)}=0 \quad k>1 \qquad (3)$$

is not given at all by (2) except when $n=0$. It is part of the purpose of this discussion to state that the M'Mahon expression gives the $(s+1)$st root $(s\neq 0)$ when the value "s" is used in (2). Actually this last statement is not quite true; the M'Mahon expression omits not only the first root for a given "n," but an entire sequence of roots beyond the first root because the M'Mahon formula does not apply until x has reached a value greater than the first zero of $N_n'(x)$, and many higher roots are thereby left out.

Only those roots of (1) for the case of $n=0$ appear to have been published, and because

[1] Annals of Mathematics 9, 23 (1894–95), or see *Bessel Functions*, by Gray Matthews and MacRobert.

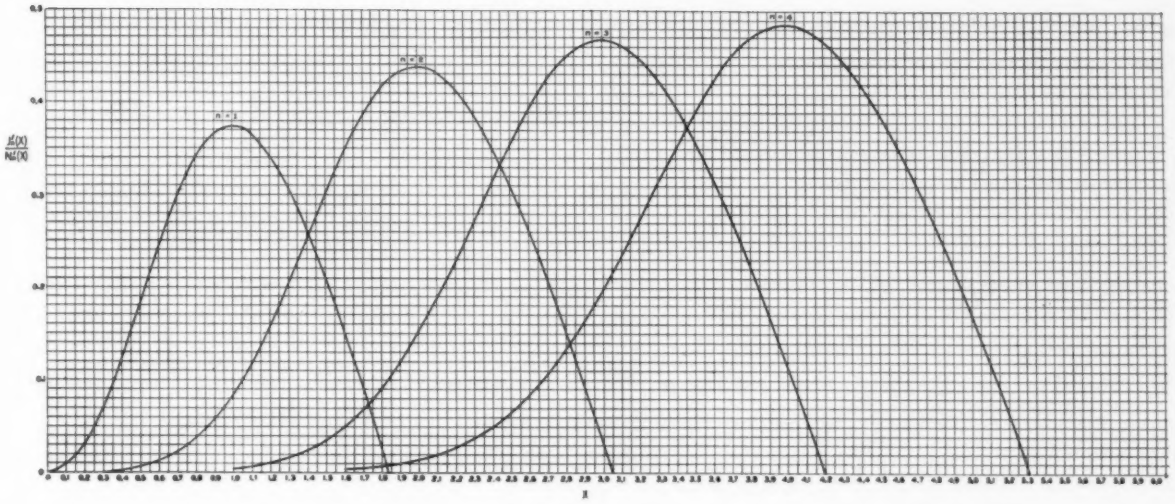

FIG. 1.

analytical methods for obtaining these roots are inconvenient to use, the following numerical method has been used by the writer to obtain the first roots of (1) for $n=1$, 2, 3, and 4.

For each value of n, plots of $[J_n'(x)]/[N_n'(x)]$ are made as a function of x. (See Fig. 1.) The function, for all n except $n=0$, increases from zero at $x=0$ to a relative maximum at $x=n$;[2] then it decreases to zero and goes to $-\infty$ on the lower side of the discontinuity. On the other side of discontinuity $[J_n'(x)]/[N_n'(x)]$ has large positive values which decrease to zero as x increases and again to large negative values where a second discontinuity occurs and so on. The first roots occur in the first positive region before $N_n'(x)$ reaches its first zero; hence it is this region only that need be used. From (3)

$$\frac{J_n'(x)}{N_n'(x)}=\frac{J_n'(kx)}{N_n'(kx)} \qquad k>1.$$

When for a given n in Fig. 1 any value of x

[2] Proved at end of article.

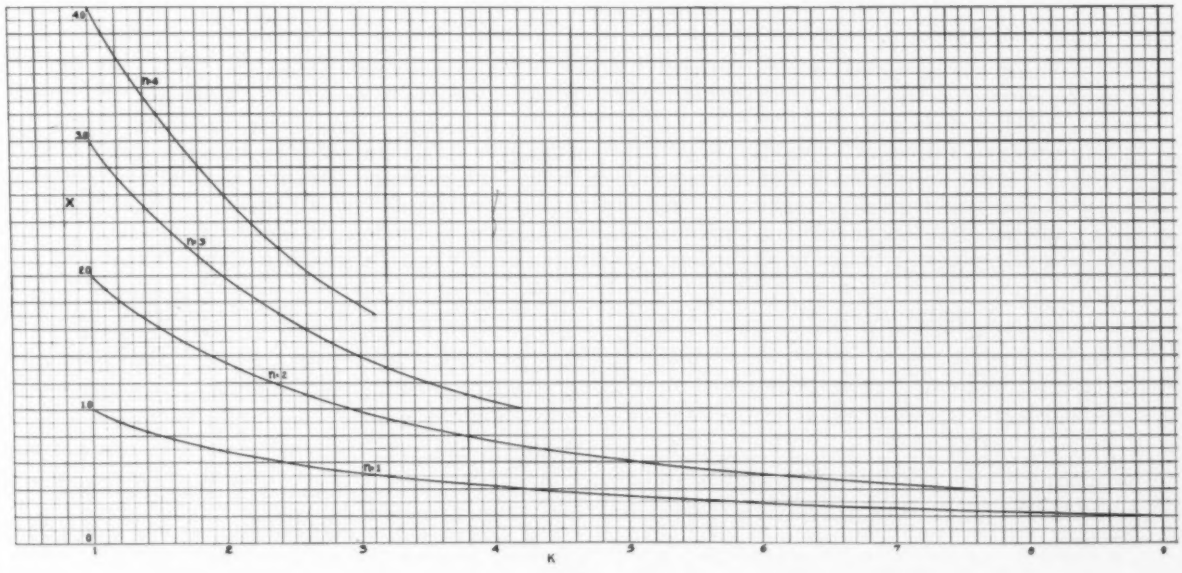

FIG. 2.

below the relative maximum (in the first positive region) is chosen, the same value of the ordinate occurs at both x and kx.

Values of k and of the corresponding first root x are found from Fig. 1 in the manner indicated, and Fig. 2 shows plots of $x \sim k$ for $n=1$, 2, 3, and 4.

The following is a proof that one and only one relative maxima of the functions $[J_n'(x)]/[N_n'(x)]$ exists and occurs at $x=n$ except when $n=0$, in which case no relative maxima occur for finite x:

$$\frac{J_n'(x)}{N_n'(x)}=\frac{J_{n-1}(x)-J_{n+1}(x)}{N_{n-1}(x)-N_{n+1}(x)},$$

$$\frac{d}{dx}\left(\frac{J_n'(x)}{N_n'(x)}\right)=(-1)\frac{J_n'(x)N_n''(x)}{(N_n'(x))^2}+\frac{J_n''(x)}{N_n'(x)}$$

$$=\left(\frac{n(n-1)}{x^2}-1\right)\{J_n(x)N_n'(x)-J_n'(x)N_n(x)\}$$

$$+1/x\{J_{n+1}(x)N_n'(x)-J_n'(x)N_{n+1}(x)\}; \quad (4)$$

then with $(d/dx)[J_n'(x)]/[N_n'(x)]=0$ the roots are sought.

Using the following recurrence formulae, the relation can be simplified.

$$J_n(x)N_n'(x)-J_n'(x)N_n(x)=\frac{2}{\pi x},$$

$$J_n'(x)=\tfrac{1}{2}[J_{n-1}(x)-J_{n+1}(x)],$$

$$N_n'(x)=\tfrac{1}{2}[N_{n-1}(x)-N_{n+1}(x)],$$

$$J_{n+1}(x)N_n(x)-J_n(x)N_{n+1}(x)=\frac{2}{\pi x},$$

so that

$$\frac{d}{dx}\frac{J_n'(x)}{N_n'(x)}=\frac{2}{\pi x^3}(n^2-x^2)=0 \quad \text{or} \quad n=\pm x,$$

and when

$$n=0, \quad \frac{d}{dx}\frac{J_n'(x)}{N_n'(x)}=-\frac{2}{\pi x},$$

which, clearly, is without a zero for finite x.

I am indebted to Dr. H. B. DeVore* for the numerical method used, and to Dr. D. O. North* who noticed that the first roots are not given by the M'Mahon expression. Dr. L. S. Nergaard* helped to simplify some of the relations used, and Professor L. P. Smith of Cornell University discussed all of the features of the article with me.

* RCA Laboratories, Princeton, New Jersey.

Electrical Circuit Analysis of Torsional Oscillations

LOUIS A. PIPES
Graduate School of Engineering, Harvard University, Cambridge, Massachusetts

(Received April 18, 1943)

The equivalence between the torsional oscillations of a general dynamical system and those of a certain electrical circuit is considered. This equivalence makes it possible to compute the behavior of the dynamical system by making use of some well-known results of electrical circuit theory. It also makes it possible to determine the critical speeds and the response of the mechanical system by simple electrical measurements of the equivalent system. The forced oscillations of a damped multi-disk system and those of continuous shafts are studied. The results may be applied by a mere change in notation to the analysis of the longitudinal oscillations of linear spring and mass systems as well as to that of the longitudinal oscillations of prismatic bars.

INTRODUCTION

IN recent years, the analysis of dynamical systems undergoing torsional oscillations has been the subject of considerable study. Various mathematical techniques have been applied to the problem.[1-3] The analysis of these systems is a fundamental one in the study of vibrations in electrical machinery, Diesel engines, internal combustion engines, and propeller shafts. The actual system under consideration is idealized to that of considering the oscillations of several disks on a shaft.[4-6] Most of the investigations

[1] L. A. Pipes, J. App. Phys. **13**, 434–444 (1942).
[2] M. A. Biot, J. Ae. Sci. **8**, 107–112 (1940).
[3] M. A. Biot, J. App. Phys. **11**, 530–537 (1940).
[4] J. P. Den Hartog, *Mechanical Vibrations* (McGraw-Hill, 1940), Chapter 5.
[5] S. Timoshenko, *Vibration Problems in Engineering* (D. Van Nostrand, 1937), Chapter 5.
[6] F. M. Lewis, Trans. Soc. Nav. Arch. Marine Eng. **33**, 109 (1925).

have been concerned with determining the natural or resonant frequencies of the system, without much consideration to the forced oscillations. Damping is usually neglected. It is the purpose of this discussion to demonstrate the advantages of considering the problem from the point of view of its electrical analogue. By doing this, not only is it possible to use many well-known results of electrical circuit theory to advantage, but the electrical analogue suggests methods of studying complex problems experimentally. Since the science of electrical measurements is very well developed, this should give an impetus to the experimental analysis of systems which are thought to be too complex to be studied analytically. The results may be applied to the study of the longitudinal oscillations of mass and spring systems, the longitudinal oscillations of bars, the transverse oscillations of loaded strings, and the transverse oscillations of continuous strings.

I. STATEMENT OF THE PROBLEM

The problem under consideration is the study of the free and forced oscillations of the dynamical system shown in Fig. 1. This system consists of a set of disks of moments of inertia, J_r, connected together by shafting of torsional flexibility, k_r. Damping of the viscous friction type is assumed to act on the various disks. There are two types of coefficient of damping. The damping coefficients, g_r, produce a retarding torque proportional to the angular velocity of the various disks, while the damping coefficients, b_r, produce a retarding torque proportional to the relative angular velocities of adjacent disks. This assumed type of damping is an idealization of the more complex type that actually exists but the results obtained based on this simplifying assumption are probably not too far in error and will give at least a qualitative view of the effects of damping. In most practical systems, the damping is small and in the usual analysis it is neglected.

II. THE EQUATIONS OF MOTION AND THE EQUIVALENT ELECTRICAL CIRCUIT

Let $(\theta_1 \cdots \theta_n)$ be the angles of rotation of the various disks of Fig. 1 during vibration. Then if the left end of the shaft is acted on by a couple $T_0 \cos(\omega t)$, the equations of motion of the system are,

$$\begin{aligned}
&J_1\ddot{\theta}_1+g_1\dot{\theta}_1+(\theta_1-\theta_2)/k_1+b_1(\dot{\theta}_1-\dot{\theta}_2) \\
&\qquad\qquad = T_0\cos(\omega t). \\
&J_s\ddot{\theta}_s+g_s\dot{\theta}_s+(\theta_s-\theta_{s-1})/k_{s-1}+(\theta_s-\theta_{s+1})/k_s \\
&\qquad +b_{s-1}(\dot{\theta}_s-\dot{\theta}_{s-1})+b_s(\dot{\theta}_s-\dot{\theta}_{s+1})=0. \\
&J_n\ddot{\theta}_n+g_n\dot{\theta}_n+(\theta_n-\theta_{n-1})/k_{n-1} \\
&\qquad\qquad +b_{n-1}(\dot{\theta}_n-\dot{\theta}_{n-1})=0.
\end{aligned} \tag{1}$$

Consider the electrical circuit shown in Fig. 2.

This is an n-mesh electrical circuit. The i_s quantities are the various mesh currents of the network. R_s and r_s are resistances, L_s are inductances and c_s are capacitances. If an electromotive force $E_0 \sin(\omega t)$ is inserted in the first mesh of the system, the differential equations governing the current distribution are,

$$\begin{aligned}
&L_1\frac{d^2i_1}{dt^2}+R_1\frac{di_1}{dt}+\frac{(i_1-i_2)}{c_1}+r_1\left(\frac{di_1}{dt}-\frac{di_2}{dt}\right) \\
&\qquad\qquad =\omega E_0\cos(\omega t). \\
&L_s\frac{d^2i_s}{dt^2}+R_s\frac{di_s}{dt}+\frac{(i_s-i_{s-1})}{c_{s-1}}+\frac{(i_s+i_{s+1})}{c_s} \\
&\qquad +r_{s-1}\left(\frac{di_s}{dt}-\frac{di_{s-1}}{dt}\right)+r_s\left(\frac{di_s}{dt}-\frac{di_{s+1}}{dt}\right)=0. \\
&L_n\frac{d^2i_n}{dt^2}+R_n\frac{di_n}{dt}+\frac{(i_n-i_{n-1})}{c_{n-1}} \\
&\qquad\qquad +r_{n-1}\left(\frac{di_n}{dt}-\frac{di_{n-1}}{dt}\right)=0.
\end{aligned} \tag{2}$$

If we compare the set of Eqs. (1) with the set (2), we see that they are identical provided we introduce the following correspondence between the mechanical and electrical quantities,

$$\begin{aligned}
&J_s\rightarrow L_s, \quad g_s\rightarrow R_s, \\
&\theta_s\rightarrow i_s, \quad b_s\rightarrow r_s, \\
&k_s\rightarrow c_s, \quad T_0\rightarrow\omega E_0.
\end{aligned} \tag{3}$$

It is thus apparent that the introduction of an electromotive force $E_0 \sin(\omega t)$ in the electrical system produces currents i_s that have the same magnitude as the angular displacement of the mechanical system produced by a torque $T_0 \cos(\omega t)$ provided we make the above cor-

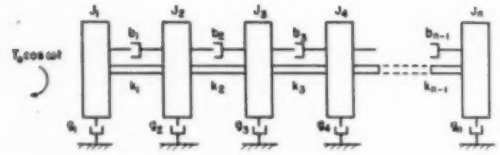

Fig. 1

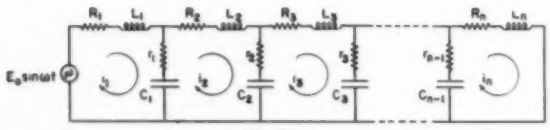

Fig. 2

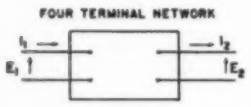

Fig. 3

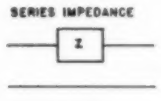

Fig. 4

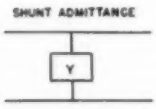

Fig. 5

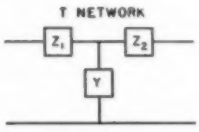

Fig. 6

FIGS. 1–6.

respondence between the electrical and mechanical quantities.

The above correspondence between the angular displacement and the current is not the usual one but it offers distinct advantages. For example, it is only necessary to measure the current in the various condensers to obtain the angle of twist of the shaft, and the current in the various inductances to obtain the corresponding position of each disk.

III. THE COMPLEX CURRENTS

In accordance with the usual steady-state alternating current theory, we write

$$E_0 \sin(\omega t) = Im(E_0 e^{j\omega t}), \tag{4}$$

$$i_s(t) = Im(I_s e^{j\omega t}) \tag{5}$$

where $j=\sqrt{-1}$ and Im denotes "the imaginary part of." Introducing these transformations, the set of Eqs. (2) are transformed into the following set.

$$\begin{aligned} Z_1 I_1 + z_1(I_1 - I_2) &= E_0, \\ Z_s I_s + z_{s-1}(I_s - I_{s-1}) + z_s(I_s - I_{s+1}) &= 0, \\ Z_n I_n + z_{n-1}(I_n - I_{n-1}) &= 0, \end{aligned} \tag{6}$$

where

$$Z_s = R_s + j\omega L_s, \tag{7}$$

$$z_s = r_s + \frac{1}{j\omega c_s} = \frac{1}{Y_s}. \tag{8}$$

These are the complex impedances of the various sections of the electrical circuit of Fig. 2. The set of Eqs. (6) may be solved for the various complex currents I_s and the actual instantaneous currents may then be obtained by the use of Eq. (5). In practice, however, it is much simpler to use the theory of four-terminal networks as outlined in the next section.

IV. THE FUNDAMENTALS OF FOUR TERMINAL NETWORK THEORY

The determination of the natural frequencies of the free oscillations of the dynamical system and also the response to forced oscillations is greatly simplified by the application of four-terminal network theory to the equivalent electrical circuit.

It may be shown[7-8] that the complex currents and potentials of a 4-terminal system joined by the interconnection of linear, passive bilateral, circuit elements as shown in Fig. 3 satisfies the following equations,

$$E_1 = AE_2 + BI_2, \quad I_2 = CE_2 + DI_2. \tag{9}$$

The sense in which the currents and potentials are taken is shown in Fig. 3. The quantities A, B, C, and D are complex quantities that satisfy the relation.

$$AD - BC = 1. \tag{10}$$

It is convenient to write the Eqs. (9) as a single matrix equation in the following manner.

$$\begin{Bmatrix} E_1 \\ I_1 \end{Bmatrix} = \begin{bmatrix} A & B \\ C & D \end{bmatrix} \begin{Bmatrix} E_2 \\ I_2 \end{Bmatrix}. \tag{11}$$

We then call the square matrix,

$$[u] = \begin{bmatrix} A & B \\ C & D \end{bmatrix} \tag{12}$$

the associated matrix of the four-terminal network. We note that because of (10), the determinant of the matrix $[u]$ is equal to unity.

---

[7] L. A. Pipes, Phil. Mag. **30**, 370–395 (1940).
[8] E. A. Guillemin, *Communication Networks* (J. Wiley, 1935), Chapter 4.

By a consideration of the Eq. (11), it is easily seen that the associated matrices of the four-terminal networks of Fig. 4 and Fig. 5 are,

$$[u]=\begin{bmatrix}1 & Z\\ 0 & 1\end{bmatrix}, \tag{13}$$

and

$$[u]=\begin{bmatrix}1 & 0\\ Y & 1\end{bmatrix}. \tag{14}$$

By the interconnection of these fundamental four-terminal networks in series, we can construct the general ladder circuit of Fig. 2, by the process of multiplying the associated matrices of the individual component parts of the system together. For example, the associated matrix of the T-network of Fig. 6 is obtained in the following manner:

$$[u]=\begin{bmatrix}1 & Z_1\\ 0 & 1\end{bmatrix}\cdot\begin{bmatrix}1 & 0\\ Y & 1\end{bmatrix}\cdot\begin{bmatrix}1 & Z_2\\ 0 & 1\end{bmatrix}$$
$$=\begin{bmatrix}(1+Z_1Y) & (Z_1+Z_1Z_2Y+Z_2)\\ Y_1 & (1+Z_2Y)\end{bmatrix}. \tag{15}$$

The elements of the matrix (u) of Eq. (15) are the over-all four-terminal constants of the T network of Fig. 6. In the same manner, the four-terminal constants of more complex four-terminal networks may be obtained by a chain of matrix multiplication.

V. DETERMINATION OF THE FREQUENCY EQUATION

If the dynamical system is not too complex its natural frequencies may be determined by obtaining the frequency equation of the system and solving it. The manner in which the frequency equation may be obtained will be illustrated by the following examples.

Let us suppose that the dynamical system is the one given in Fig. 7.

This system consists of three disks of moments of inertia J_1, J_2, and J_3 interconnected by two shafts of torsional flexibilities k_1 and k_2. The two ends of the shaft are free and friction is neglected. The equivalent electrical circuit of this system is given in Fig. 8.

Since there is no external torque applied to the mechanical system, the equivalent electrical system is short-circuited at both ends and we have the condition

$$E_1=E_2=0. \tag{16}$$

Inserting this into (11), we have

$$\begin{Bmatrix}0\\ I_1\end{Bmatrix}=\begin{bmatrix}A & B\\ C & D\end{bmatrix}\begin{Bmatrix}0\\ I_2\end{Bmatrix} \tag{17}$$

or since I_1 and I_2 are not zero, we must have

$$B=0. \tag{18}$$

The frequency equation is thus obtained by the calculation of the over-all four-terminal constant B of the network of Fig. 8 and equating it to zero. Combining the individual network elements, we have:

$$\begin{bmatrix}A & B\\ C & D\end{bmatrix}=\begin{bmatrix}I & Z_1\\ 0 & 1\end{bmatrix}\cdot\begin{bmatrix}1 & 0\\ Y_1 & 1\end{bmatrix}\cdot\begin{bmatrix}1 & Z_2\\ 0 & 1\end{bmatrix}$$
$$\cdot\begin{bmatrix}1 & 0\\ Y_2 & 1\end{bmatrix}\cdot\begin{bmatrix}1 & Z_3\\ 0 & 1\end{bmatrix}. \tag{19}$$

Performing the matrix multiplication, we obtain,

$$B=Z_1Z_2Z_3Y_1Y_2+Y_1(Z_1Z_3+Z_1Z_2)$$
$$+Y_2(Z_2Z_3+Z_1Z_3)+Z_1+Z_2+Z_3=0. \tag{20}$$

Using the Eqs. (7) and (8), we obtain, on cancelling out a factor of $j\omega$, the following frequency equation

$$\omega^4L_1L_2L_3c_1c_2-\omega^2(L_1L_2c_1+L_1L_3c_1$$
$$+L_2L_3c_2+L_1L_3c_2)+(L_1+L_2+L_3)=0. \tag{21}$$

This is the frequency equation that determines the natural frequencies of the electric circuit of

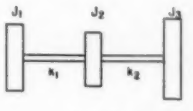

Fig. 7

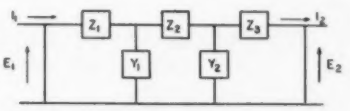

Fig. 8

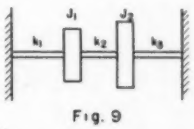

Fig. 9

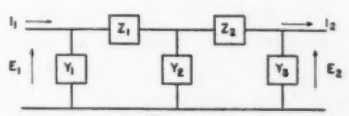

Fig. 10

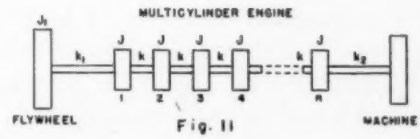

Fig. 11

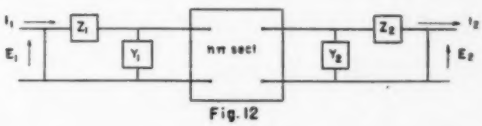

Fig. 12

FIGS. 7–12.

Fig. 8, and its mechanical analogue of Fig. 7. To obtain the equation in terms of mechanical quantities, it is only necessary to replace the inductances L_s by the moments of inertia J_s and the capacities c_s by the torsional flexibility coefficients, k_s.

As another example, let it be required to find the frequency equation of the system of Fig. 9.

This system consists of two disks J_1 and J_2 connected together through a shaft of torsional flexibility k_2 and to fixed supports by shafts of torsional flexibilities k_1 and k_3, respectively.

The equivalent electrical circuit is shown in Fig. 10.

Since the dynamical system is fixed at both ends, the electrical circuit is open-circuited at both ends. We thus have $I_1=I_2=0$. Equation (11) in this case, becomes

$$\begin{Bmatrix} E_1 \\ 0 \end{Bmatrix} = \begin{bmatrix} A & B \\ C & D \end{bmatrix} \begin{Bmatrix} E_2 \\ 0 \end{Bmatrix}. \tag{22}$$

Hence the frequency equation in this case is given by,

$$C=Z_1Z_2Y_1Y_2Y_3+Z_1(Y_1Y_2+Y_1Y_3) +Z_2(Y_1Y_3+Y_2Y_3)+Y_1+Y_2+Y_3=0. \tag{23}$$

Substituting the values of the impedances and admittances as given by (7) and (8) into (23), we obtain:

$$\omega^4L_1L_2c_1c_2c_3-\omega^2[L_1(c_1c_2+c_1c_3) +L_2(c_1c_3+c_2c_3)]+(c_1+c_2+c_3)=0. \tag{24}$$

VI. NATURAL FREQUENCIES OF MULTICYLINDER ENGINES

A. Analytical Method

Let us consider the system of Fig. 11.

Figure 11 represents the distribution of the moments of inertia of the rotating parts of a multicylinder engine. n identical disks of moments of inertia J_1 are connected to each other by shafts of torsional flexibility k and to two disks J_1 and J_2 by shafts of torsional flexibility k_1 and k_2, respectively. This is the arrangement in the case of a multicylinder engine and flywheel attached to a machine. The equivalent electrical circuit of Fig. 11 is given in Fig. 12. Where

$$y_1=(Y_1-Y/2), \quad Y=j\omega c, \quad Y_1=j\omega K_1, \quad y_1=j\omega c_1, \tag{25}$$

$$y_2=(Y_2-Y/2), \quad Y_2=j\omega K_2, \quad y_2=j\omega c_2, \tag{26}$$

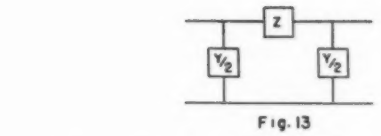

Fig. 13

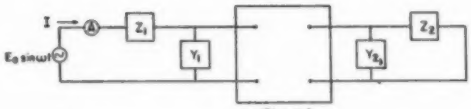

Fig. 14

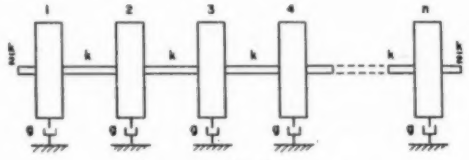

Fig. 15

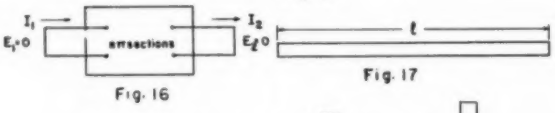

Fig. 16 Fig. 17

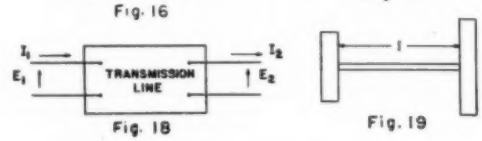

Fig. 18 Fig. 19

FIGS. 13–19.

the circuit inside the box is a four-terminal network composed of n sections of the π type as shown in Fig. 13.

The associated matrix of a section of the π type as shown in Fig. 13 is

$$\begin{bmatrix} A & B \\ C & D \end{bmatrix} = \begin{bmatrix} (1+ZY/2) & Z \\ [Y+(ZY^2/4)] & (1+ZY/2) \end{bmatrix}. \tag{27}$$

It may be shown[7] that the associated matrix of the four-terminal network within the box is given by

$$\begin{bmatrix} A & B \\ C & D \end{bmatrix}^n = \begin{bmatrix} \cosh(an) & Z_0\sinh(an) \\ \sinh(an)/Z & \cosh(an) \end{bmatrix} \tag{28}$$

where n is the number of π sections contained within the box and,

$$\cosh(a)=\left(1+\frac{ZY}{2}\right)=\left(1-\frac{\omega^2Lc}{2}\right), \tag{29}$$

$$Z_0=\frac{\sinh(a)}{[Y+(ZY^2/4)]}. \tag{30}$$

If we let

$$a=(jb), \quad j=\sqrt{-1} \tag{31}$$

and substitute into (29) and (30), we obtain

$$\omega=\frac{2}{(Lc)^{\frac{1}{2}}}\sin\left(\frac{b}{2}\right) \tag{32}$$

and

$$Z_0=\frac{\sin(b)}{\omega c\cos^2(b/2)}. \tag{33}$$

The frequency equation of the circuit of Fig. 12 may be obtained by realizing that the two ends are short-circuited and hence $E_1=E_2=0$. The associated matrix of the entire circuit of Fig. 12, is

$$\begin{bmatrix}A_0 & B_0\\ C_0 & D_0\end{bmatrix}=\begin{bmatrix}(1+Z_1y_1) & Z_1\\ y_1 & 1\end{bmatrix}\cdot\begin{bmatrix}\cosh(an) & Z_0\sinh(an)\\ \sinh(an)/Z_0 & \cosh(an)\end{bmatrix}\cdot\begin{bmatrix}1 & Z_2\\ y_2 & (1+Z_2y_2)\end{bmatrix}. \tag{34}$$

The condition that the two ends be short-circuited and that there be oscillations is given by

$$B_0=0. \tag{35}$$

Carrying out the matrix multiplication in (34) and using (35) we obtain after some reductions,

$$\tan(bn)=\frac{\omega^3L_1L_2(c_1+c_2)-\omega(L_1+L_2)}{Z_0[\omega^4L_1L_2c_1c_2-\omega^2(L_1c_1+L_2c_2)+1]-\dfrac{\omega^2L_1L_2}{Z_0}}. \tag{36}$$

Equation (36) may be written with the aid of (32) and (33) as a transcendental equation in b whose solution yields the various natural frequencies as given in (32). In the general case, the solution of (36) may only be effected graphically.

Some special cases that may be solved exactly will be considered.

Special Case 1.

First let us consider the case in which the n-cylinder engine of Fig. 11 is not connected to either the flywheel or the machine. In this case we have,

$$k_1=k_2=\infty. \tag{37}$$

In the analogous electrical circuit we must place

$$K_1=K_2=\infty. \tag{38}$$

By Eqs. (25) and (26) this leads to the conditions

$$c_1=c_2=\infty. \tag{39}$$

Inserting this condition into (36) yields the following equation

$$\tan(bn)\frac{\sin(b)}{\cos^2(b/2)}=0. \tag{40}$$

Hence

$$b=(r\pi/n)\quad r=0, 1, 2, \cdots(n-1). \tag{41}$$

From (32) we obtain the n natural angular frequencies

$$\omega_r=\frac{2}{(Lc)^{\frac{1}{2}}}\sin\left(\frac{r\pi}{2n}\right)\quad r=0, 1, 2, \cdots(n-1). \tag{42}$$

Special Case 2.

Another special case that may be solved exactly is that in which the multicylinder engine of Fig. 11 is not connected to anything on the left but is connected to a machine of infinite moment of inertia on the right by means of a shaft whose torsional flexibility is k. In this case from Eqs. (25) and (26) we have

$$c_1=\infty, \tag{43}$$

$$c_2=c/2, \tag{44}$$

$$L_2=\infty. \tag{45}$$

Inserting these values into (36), we obtain

$$\tan(bn)=\frac{2}{Z_0\omega c}=\frac{2\cos^2(b/2)}{\sin(b)}. \tag{46}$$

By the use of trigonometric identities this may be put in the following form

$$\cos\left[\left(\frac{2n+1}{2}\right)\cdot b\right]\frac{\sin(b)}{\sin(b/2)}=0. \tag{47}$$

Hence

$$b=\left(\frac{2r-1}{2n+1}\right)\pi\quad r=1, 2, 3, \cdots n. \tag{48}$$

By (32) the various angular frequencies are given by

$$\omega_r=\frac{2}{(Lc)^{\frac{1}{2}}}\sin\left[\frac{(2r-1)\pi}{2(2n+1)}\right]\quad r=1, 2, \cdots n. \tag{49}$$

Special Case 3.

Another important special case is that in which the flywheel and the machine may be regarded as having infinite moments of inertia and that

$$k_1=k_2=k. \tag{50}$$

This leads to the conditions

$$L_1=L_2=\infty, \tag{51}$$

$$c_1=c_2=c/2. \tag{52}$$

Substituting these values into (36), we obtain after some reductions, the equation

$$\frac{\sin\,(n+1)b}{\sin\,(b)}=0. \tag{53}$$

Hence

$$b=\frac{r\pi}{(n+1)} \quad r-1,\ 2,\ 3,\ \cdots n. \tag{54}$$

From (32), the angular frequencies of this system are given by,

$$\omega_r=\frac{2}{(Lc)^{\frac{1}{2}}}\cdot\sin\left[\frac{r\pi}{2(n+1)}\right] \quad r=1,\ 2,\ 3,\ \cdots n. \tag{55}$$

B. Experimental Method

In the general case of the analysis of the multicylinder engine, it is necessary to solve the general equation (36). This may be effected graphically but it is a laborious process. The natural frequencies may be determined experimentally by inserting a variable alternating potential source and an ammeter in the equivalent circuit of Fig. 12 in the manner shown in Fig. 14.

The ammeter, A, is inserted between the alternating current source and the circuit. Now as the frequency of the alternating current source is changed continuously, the ammeter reading will pass through a succession of maximum values. Each maximum value indicates a resonance condition. The angular frequency, ω, of the alternating source at this condition will be that of one of the natural angular frequencies of the system.

By constructing the circuit of Fig. 14 so that each inductance and capacitance is variable, then it will be able to represent a whole group of engines. Furthermore, if a particular design happens to have a resonant frequency at or near a normal running speed, then by varying the various inductances and capacitances, it is possible to determine the optimum changes to be made to remove this condition.

VII. EFFECT OF DAMPING

The effect of any friction which produces a retarding torque proportional to the angular velocity of the system may be represented in the equivalent electrical circuit by a resistance. As an example of the method let us consider the free oscillations of the multicylinder engine of Fig. 15.

This system consists of n equal disks of moments of inertia J coupled to each other by equal sections of shaft of torsional flexibility k. Each disk will be assumed to be retarded by a frictional force of the viscous type whose coefficient of friction is g.

The equivalent circuit of the dynamical system of Fig. 15 is given in Fig. 16.

This circuit consists of n, π sections as shown in Fig. 13 short-circuited at both ends. In this case we have,

$$Z=R+j\omega L, \qquad j=\sqrt{-1} \tag{56}$$

$$Y=j\omega c. \tag{57}$$

The associated matrix of the circuit of Fig. 16 is given by (28). The condition of free oscillations gives

$$Z_0\sinh\,(an)=0. \tag{58}$$

Hence

$$a=\frac{r\pi j}{n} \quad r=0,\ 1,\ 2,\ \cdots(n-1). \tag{59}$$

To obtain the frequency equation, we substitute these values of a into (29) and obtain

$$\cos\left(\frac{r\pi}{n}\right)=\left(1+\frac{ZY}{2}\right)=1+\tfrac{1}{2}(j\omega cR-\omega^2Lc) \tag{60}$$

or

$$\begin{aligned}\omega_r&=\frac{jR}{2L}\pm\frac{1}{2}\left[\frac{16}{Lc}\sin^2\left(\frac{r\pi}{2n}\right)-\frac{R^2}{L^2}\right]^{\frac{1}{2}}\\&=j\alpha\pm\beta_r \quad r=0,\ 1,\ 2,\ \cdots(n-1).\end{aligned} \tag{61}$$

This shows that oscillations of the type

$$i_1=\epsilon^{-\alpha t}\sum_{r=0}^{r=(n-1)}M_r\cos\,(\beta_r t)+N_r\sin\,(\beta_r t), \tag{62}$$

where, M_r and N_r are arbitrary constants are

possible. The decrement factor, α, shows that the oscillations decay with time exponentially. If all the values of ω_r as given by (61) are pure imaginary quantities, then no oscillations are possible. This is the case of

$$R>4\left(\frac{L}{c}\right)^{\frac{1}{2}}\sin\left[\frac{(n-1)\pi}{2n}\right]. \tag{63}$$

In this case, all the modes of oscillation are critically damped.

The effect of viscous friction may be studied experimentally by inserting proper resistances in series with the various inductances and capacitances of the equivalent circuit. It is then only necessary to measure the currents through the various members to determine the various angular displacements in the mechanical systems.

VIII. NATURAL FREQUENCIES OF CONTINUOUS SHAFTS

In the case of long shafts, the distributed mass of the shafts may not be neglected. In this section we shall consider how the natural frequencies of systems containing long shafts may be determined.

Let us consider the electrical circuit equivalent to the long uniform shaft of Fig. 17.

If l is the length of this shaft and J is its distributed moment of inertia per unit length and k its torsional flexibility per unit length, then its electrical analogue is given by the transmission line shown in Fig. 18.

This figure represents a transmission line of length l, having an inductance L, and a capacitance c per unit length. The relation between the potentials and currents at the two ends of this line are given by,[7]

$$\begin{Bmatrix} E_1 \\ I_1 \end{Bmatrix}=\begin{bmatrix} \cosh(\theta) & Z_0\sinh(\theta) \\ \sinh(\theta)/Z_0 & \cosh(\theta) \end{bmatrix}\begin{Bmatrix} E_2 \\ I_2 \end{Bmatrix} \tag{64}$$

where

$$Z_0=(L/c)^{\frac{1}{2}}, \tag{65}$$

$$\theta=j\omega l(Lc)^{\frac{1}{2}}. \qquad j=\sqrt{-1} \tag{66}$$

The associated matrix of the transmission line is given by the square matrix of Eq. (64). As an example of the use of this matrix to determine the oscillations of shafts under various terminal conditions, consider a shaft free at both ends. Its electrical equivalent is a transmission line short-circuited at both ends. From (64) we have

$$Z_0\sinh(\theta)=0. \tag{67}$$

Hence

$$\theta=r\pi j, \quad r=0, 1, 2, \cdots \quad j=\sqrt{-1}. \tag{68}$$

From (66) we obtain

$$\omega_r=\frac{r\pi}{l(Lc)^{\frac{1}{2}}} \quad r=0, 1, 2, \cdots \tag{69}$$

for the natural angular frequencies. Another case is the determination of the natural frequencies when the shaft is fixed at the right end. In this case, we consider a transmission line open-circuited at the right end and short-circuited at the left end. In this case, we have from (64)

$$\cosh(\theta)=0 \tag{70}$$

or

$$\theta=\left(\frac{2r-1}{2}\right)\pi j \quad r=1, 2, 3, \cdots. \tag{71}$$

Hence by (66) we have

$$\omega_r=\frac{1}{l(Lc)^{\frac{1}{2}}}\left(\frac{2r-1}{2}\right)\pi \quad r=1, 2, 3, \cdots. \tag{72}$$

As another example, let it be required to determine the natural frequencies of the system of Fig. 19.

This figure represents a system consisting of two disks of moments of inertia J_1 and J_2 connected by a uniform shaft of length l. The equivalent circuit is given in Fig. 20.

The associated matrix of the circuit of Fig. 20 is given by

$$\begin{bmatrix} A & B \\ C & D \end{bmatrix}=\begin{bmatrix} I & Z_1 \\ 0 & 1 \end{bmatrix}\cdot\begin{bmatrix} \cosh\theta \\ \sinh\theta/Z_0 \end{bmatrix}\cdot\begin{bmatrix} Z_0\sinh\theta \\ \cosh\theta \end{bmatrix}\cdot\begin{bmatrix} 1 & Z_2 \\ 0 & 1 \end{bmatrix}. \tag{73}$$

If we make use of the fact that the circuit is short-circuited at both ends and set B equal to zero, we obtain

$$\sinh\theta\left[Z_0+\frac{Z_1Z_2}{Z_0}\right]+\cosh\theta[Z_1+Z_2]=0. \tag{74}$$

Letting

$$\theta = j\omega l(Lc)^{\frac{1}{2}} = j\phi \tag{75}$$

and

$$Z_1 = j\omega L_1, \tag{76}$$

$$Z_2 = j\omega L_2, \tag{77}$$

we obtain after some reductions

$$\tan\phi = \frac{\phi(m+n)}{(mn\phi^2-1)}. \tag{78}$$

where

$$m = L_1/L_0, \quad n = L_2/L_0 \tag{79}$$

and $L_0 = lL$ is the entire inductance of the transmission line. Equation (78) is a transcendental equation in ϕ and may be solved graphically. The natural angular frequencies are given by

$$\omega = \frac{\phi}{l(Lc)^{\frac{1}{2}}}. \tag{80}$$

The use of the associated matrix (64) makes it possible to obtain the frequency equations of composite systems in a simple manner.

IX. GEARED SYSTEMS

If the system under consideration contains gears and pinions, the electrical circuit equivalent of this system is an ideal transformer. Consider the gear system of Fig. 21. Let n_1 be the number of teeth of the upper gear and n_2 be the number of teeth of the lower gear. Let j_1 be the moment of inertia of the upper gear and j_2 be the moment of inertia of the lower gear. Let k_1 and k_2 be the torsional flexibilities of the connecting shaft.

The equivalent electrical circuit is given in Fig. 22.

If N_1 and N_2 are the number of turns on the transformer windings as shown in Fig. 22, let

$$n_2/n_1 = N_2/N_1 = a. \tag{81}$$

The over-all associated matrix of the system is given by

$$\begin{bmatrix} A & B \\ C & D \end{bmatrix} = \begin{bmatrix} 1 & j\omega L_1 \\ j\omega c_1 & (1-\omega^2 L_1 c_1) \end{bmatrix} \cdot \begin{bmatrix} -1/a & 0 \\ 0 & -a \end{bmatrix} \cdot \begin{bmatrix} (1-\omega^2 L_2 c_2) & j\omega L_2 \\ j\omega c_2 & 1 \end{bmatrix}. \tag{82}$$

This associated matrix is very useful in obtaining the frequency equations of geared systems. If the moments of inertia of the gears may be neglected, then (82) has a simple form. As an example, let it be required to obtain the frequency equation of the system shown in Fig. 23.

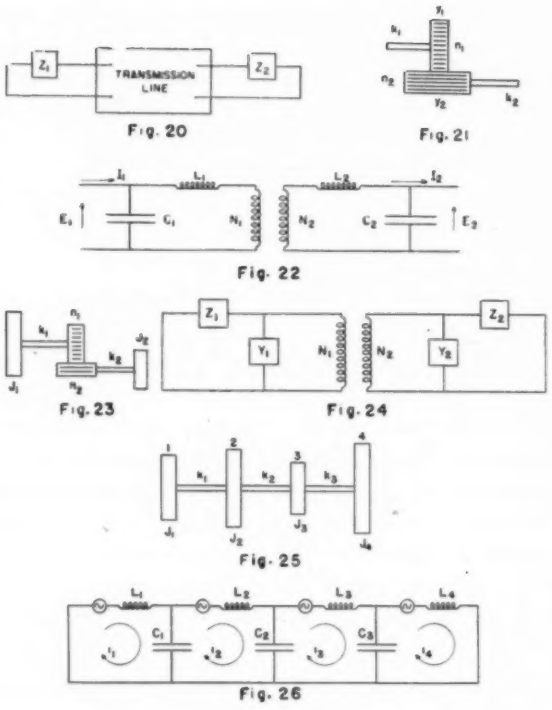

FIGS. 20–26.

Let the moments of inertia of the gears be neglected. The equivalent electrical circuit is given in Fig. 24.

The associated matrix of the system is given by

$$\begin{bmatrix} A & B \\ C & D \end{bmatrix} = \begin{bmatrix} (1+Z_1Y_1) & Z_1 \\ Y_1 & 1 \end{bmatrix} \cdot \begin{bmatrix} -1/a & 0 \\ 0 & -a \end{bmatrix} \cdot \begin{bmatrix} 1 & Z_2 \\ Y_2 & (1+Z_2Y_2) \end{bmatrix}. \tag{83}$$

Carrying out the matrix multiplication and setting $B=0$, the following frequency equation is obtained,

$$\omega^2(L_1L_2c_1 + a^2L_1L_2c_2) - (a^2L_1 + L_2) = 0 \tag{84}$$

where a is defined by (81).

X. FORCED OSCILLATIONS

A. Analytical Method

The determination of the forced oscillations of a disk and shaft system may be effected con-

veniently by the consideration of the equivalent electrical circuit.

The method will be illustrated by the analysis of a special case. Consider the system of Fig. 25.

Let $T_r \cos(\omega t)$ be the external torque applied to the rth disk. By the general theory of Section II, the electrical equivalent of this system is given in Fig. 26.

The rth mesh has impressed upon it an electromotive force of the form $E_r \sin(\omega t)$ where by (3)

$$T_r = \omega E_r \tag{85}$$

numerically.

In accordance with Section III we let

$$E_r \sin(\omega t) = Im(E_r \epsilon^{j\omega t}) \tag{86}$$

and

$$i_r(t) = Im(I_r \epsilon^{j\omega t}) \tag{87}$$

where Im denotes "the imaginary part of" and use the usual methods of alternating circuit theory to determine the complex mesh currents I_r. To determine the complex currents, I_r, it is convenient to draw the circuit of Fig. 26 in the form given in 27.

Apply Kirchhoff's second law to the successive meshes of Fig. 27, we obtain the following matrix equation[9]

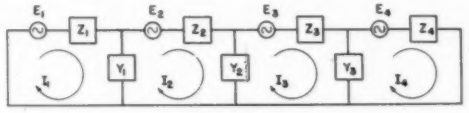

Fig. 27

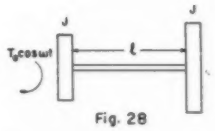

Fig. 28

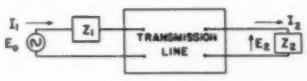

Fig. 29

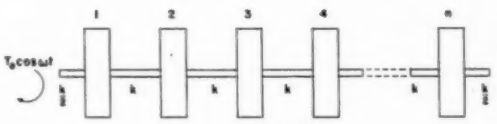

Fig. 30

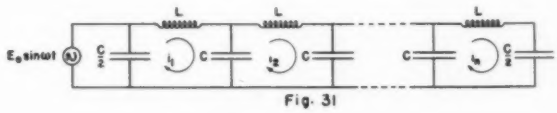

Fig. 31

FIGS. 27–31.

$$\begin{bmatrix} Z_{11} & Z_{12} & 0 & 0 \\ Z_{21} & Z_{22} & Z_{23} & 0 \\ 0 & Z_{32} & Z_{33} & Z_{34} \\ 0 & 0 & Z_{43} & Z_{44} \end{bmatrix} \cdot \begin{bmatrix} I_1 \\ I_2 \\ I_3 \\ I_4 \end{bmatrix} = \begin{bmatrix} E_1 \\ E_2 \\ E_3 \\ E_4 \end{bmatrix} \tag{88}$$

or

$$[Z] \cdot \{I\} = \{E\} \tag{89}$$

where

$$\begin{aligned} Z_{11} &= \left(j\omega L_1 + \frac{1}{j\omega c_1} \right), \\ Z_{22} &= \left(j\omega L_2 + \frac{1}{j\omega c_1} + \frac{1}{j\omega c_2} \right), \\ Z_{33} &= \left(j\omega L_3 + \frac{1}{j\omega c_2} + \frac{1}{j\omega c_3} \right), \\ Z_{44} &= \left(j\omega L_4 + \frac{1}{j\omega c_3} \right), \\ Z_{12} &= Z_{21} = \frac{-1}{j\omega c_1}, \\ Z_{23} &= Z_{32} = \frac{-1}{j\omega c_2}, \\ Z_{34} &= Z_{43} = \frac{-1}{j\omega c_3}. \end{aligned} \tag{90}$$

In order to solve the set of equations expressed by the matrix equation (88), it is necessary to compute the inverse of the square matrix $[Z]$. If we let

$$[Y] = [Z]^{-1} \tag{91}$$

the solution of (88) for the complex currents, I_r may be expressed in the form

$$\{I\} = [Y] \cdot \{E\}. \tag{92}$$

The symmetry of the matrices $[Z]$ and $[Y]$ greatly reduces the labor of computing the elements of the matrix $[Y]$. Equation (92) determines the complex currents I_r and the instantaneous currents are given in phase and magnitude by (87).

B. Experimental Method

The response of the system of Fig. 25 to the applied external torques may be studied experimentally by inserting an alternating source of potential in each mesh of the circuit of Fig. 26

[9] L. A. Pipes, Elect. Eng. **56**, 1177–1190 (1937).

of the proper amplitude and measuring the currents in the various parts of the system. It is not necessary to use more than one alternating potential source. If we first apply the source of potential to the first mesh and measure all the currents, then to the second mesh and again measure all the currents and continue the process until the source has been placed in each mesh then the resultant currents which would flow if there were simultaneous potential sources in all the meshes are, by Eq. (92), the vector sum of all the measured currents in the various parts of the system.

The effect of damping may be taken into account by adding proper resistance elements in the circuit of Fig. 26.

XI. FORCED OSCILLATIONS OF A UNIFORM SHAFT

A problem that occurs frequently in the study of torsional oscillations is that of determining the forced oscillations of a system in which an engine is connected to a machine by means of a long uniform shaft. Such a system is shown in Fig. 28.

An oscillatory torque is applied to the disk at the left end. Let J and k be the distributed moment of inertia and torsional flexibility of the shaft of length l connecting the disks whose moments of inertia are J_1 and J_2, respectively. The equivalent electrical circuit of Fig. 28 is given in Fig. 29.

By using Eq. (64), we obtain

$$\begin{bmatrix} E_1 \\ I_1 \end{bmatrix} = \begin{bmatrix} 1 & Z_1 \\ 0 & 1 \end{bmatrix} \cdot \begin{bmatrix} \cosh\theta & Z_0 \sinh\theta \\ \sinh\theta/Z_0 & \cosh\theta \end{bmatrix} \cdot \begin{bmatrix} E_2 \\ I_2 \end{bmatrix}. \tag{93}$$

Since the circuit of Fig. 29 is terminated on the right by an impedance Z_2 we have

$$E_2 = I_2 Z_2. \tag{94}$$

Carrying out the matrix multiplication in (93) and using the relation (94), we obtain

$$Z = \frac{E_1}{I_1} = \frac{\cosh\theta(Z_1+Z_2) + \sinh\theta[Z_0 + (Z_1Z_2/Z_0)]}{(\cosh\theta + \sinh\theta Z_2/Z_0)}. \tag{95}$$

This is the impedance of the circuit of Fig. 29 looking from the right. If $Z=0$ we obtain Eq. (74) of Section VIII. This is the condition of resonance. If $Z \neq 0$, then we obtain

$$I_1 = E_1/Z. \tag{96}$$

This gives the motion of the first disk. The motion of the second disk is obtained by solving Eq. (93) for I_2 using the relation (96).

We thus obtain

$$I_2 = I_1 \cosh\theta + \frac{\sinh\theta}{Z_0}\{I_1Z_1 - E_1\}. \tag{97}$$

This gives the motion of the second disk when that of the first one has been determined by (96).

XII. TORSIONAL FILTERS

Consider the system of Fig. 30. This system consists of n disks of equal moments of inertia, J, connected by shafts of equal torsional flexibility, k.

The equivalent electrical circuit is given in Fig. 31.

This is a low pass filter of n sections. It passes currents of frequencies lying in the range[8]

$$0 < \omega < \frac{2}{(Lc)^{\frac{1}{2}}}. \tag{98}$$

It is thus apparent that the torsional system of Fig. 30 may be utilized as a torsional filter to prevent oscillations of certain frequencies to pass from an engine to the rest of an oscillating system that may be brought into resonance by one of the unwanted frequencies.

XIII. ANALYSIS OF OTHER DYNAMICAL SYSTEMS

The above discussion has been limited to the use of the electrical analogue in the study of torsional oscillations of disk and shaft systems. The same ladder network which has been used to study torsional oscillations may be used to study the free and forced oscillations of the following systems:

1. Transverse oscillations of continuous and loaded strings.
2. Longitudinal oscillations of spring and mass systems.
3. Longitudinal oscillations of prismatic bars.

It is only necessary to recognize the equivalent quantities and proceed as in the case of torsional oscillations.

Résumés of Recent Research

Cylindrical Cavity Resonators Containing Several Dielectric Media

A cavity resonator containing several dielectric media may oscillate in a triply-infinite set of natural modes which are simple functions of the dimensions of the resonator, and of the lengths and the electrical constants of the dielectrics. The resonators which are considered by D. Middleton in a recent paper[1] are cylindrical and perfectly conducting, of fixed length, containing two air chambers separated by a dielectric disk, and may resonate in any one of a variety of allowable modes, whose frequencies change as the disk is moved about within the tube. Such a variation in frequency is shown in Fig. 1. Resonators of this type are tunable over a considerable range, up to 500 mc/sec., or more, depending on the dimensions and dielectric constant of the disk, as well as on the geometry of the tube. These resonators at once suggest themselves as tunable tank-circuit elements. A modification of the above also discussed is the hollow pipe partially filled at one end by a dielectric slab. Cavity resonators in this form may act as filters, for the particular mode excited, with a fixed lower cut-off frequency, and an upper cut-off frequency which depends on the thickness of the dielectric used. Intermediate frequencies and resonant

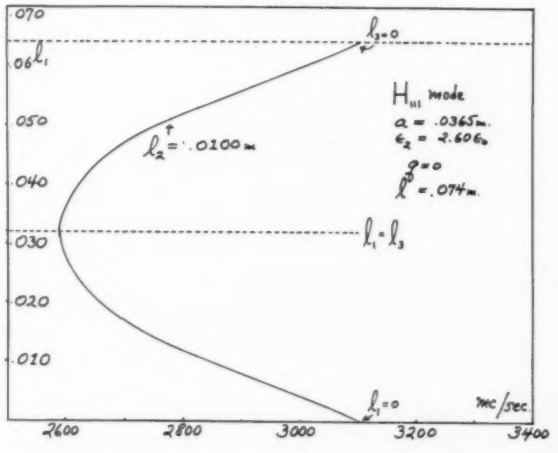

FIG. 1. Resonant air length $l_1^{(2)}$ as a function of frequency, $l_2 = 1.0$ cm, in a resonator of constant total length $l = 0.074$ m, for one-half wave-length of the H_{111} mode.

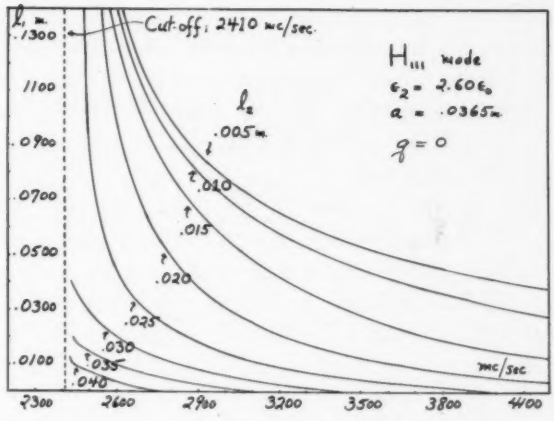

FIG. 2. Resonant air length $l_1^{(2)}$ as a function of frequency for different thicknesses of dielectric l_2, for a half-wave-length in the tube, H_{111} mode.

lengths, corresponding to a range of dielectric thicknesses, have been calculated for several numerical cases, and are shown in Fig. 2, for the H_{111} mode.

A tube containing two different dielectric media, for example, a section of the particular sample under test at one end, the rest of the interior filled with air, suggests a simple absolute method of measuring dielectric constants at microwave frequencies. This method is used to obtain data for a polystyrene sample. The advantages of the method over previous ones are that a minimum of experimental data is necessary, and that the calculations are somewhat simplified; a possible disadvantage is a lack of sensitivity, if the H modes are excited, and any error which may be introduced because of the asymmetry of the apparatus.

Formulae relating the various resonant lengths and natural frequencies in the two- and three-dielectric cases are also developed, as well as expressions for the fields and charge and current distributions.

[1] D. Middleton, Phys. Rev. **63**, 343 (1943).

An Empirical Approach to Lens Design

Equations available to the lens designer do not in general give anything but an approximation to the desired design of a lens, the approximation being the closer the more completely the analytical work is carried out. However, the complexity of the equations grows so rapidly with the in-

clusion of higher aberrations that even for only a fair approach to the desired design the computing job becomes most laborious, and even then the design in most cases has to be further perfected by differential correction or by trigonometric ray tracing or both.

In a recent article by W. M. Stempel,* an empirical method of approaching the design lens has been suggested. Tables and curves derived from extensive ray tracings, covering the entire useful range for the Huygens eyepiece as a starter in this empirical type of approach to the lens design problem, have been given. From these curves (or from tables, though with a small amount of simple computing, if higher precision is desired) one can write down in a few minutes the complete prescription for a Huygens eyepiece for any use and for any part of the useful range, and with the assurance that the eyepiece will be perfectly satisfactory in regard to all aberrations generally considered in such eyepieces. A particular eyepiece is fully analyzed as an illustration of the usefulness of the method. The same aberrations are also calculated by H. Dennes Taylor's method as a check on the trustworthiness of the latter. Both methods are checked against the true aberrations obtained from ray tracings. The article contains in addition some useful, rapid, slide-rule formulae for correcting eyepieces slightly defective in some particular respect.

* W. M. Stempel, J. Opt. Soc. Am. **33**, 278 (1943).

New Instrument Booklets

Allied Releases 1943 Buying Guide, published by the Allied Radio Corporation, Chicago, covers the field of radio and electronics, with special emphasis on industrial, research, and production requirements. Included are complete detailed listings of transformers, resistors, condensers, rheostats, relays, switches, rectifiers, electronic tubes, tools, wire and cable, batteries, sockets, generators, power supplies, converters, and all other types of equipment in this field. A large section is devoted to sound equipment and accessories. In the technical book section recent worthwhile publications are listed. Factual descriptions of all items and detailed illustrations simplify selection of materials. May be obtained without charge from Allied Radio Corporation, 833 West Jackson Boulevard, Chicago, Illinois.

Bakelite Review, April, 1943, Vol. 15, No. 1, strikingly illustrates their featured article on plastic bayonets and other equipment made from such materials. Other articles with illsutrations are "Heatronic molding" and "Application of vinyl resins and plastics to textiles." This booklet is a quarterly publication of the Bakelite Corporation and the Plastics Division of Carbide and Carbon Chemicals Corporation, 30 East 42 Street, New York, New York (24 pages).

Bulletin 43 shows a complete line of radial and pivot type bearings from $\frac{1}{8}$ to $\frac{5}{16}$ inch outside diameter in both steel and non-magnetic beryllium. Dimensions and load

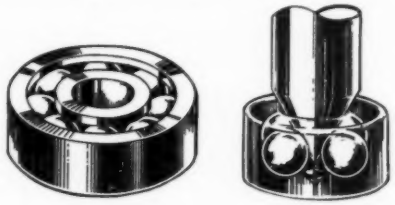

ratings are given at various speeds for each size and type of bearing, as well as illustrations of actual size. Available on request to engineers and designers. Published by Miniature Precision Bearings, Keene, New Hampshire (4 pages).

Chemical Digest, Vol. 9, No. 1, Spring, 1943, stresses the increasing prominence of the soy bean and peanut, due to the exigencies of war. Publication of Foster D. Snell, Inc., 305 Washington Street, Brooklyn, New York (4 pages).

Mitchell Fluorescent Fixtures—Catalog No. 400—announces the new, all-purpose line of fluorescent fixtures for war industry. Illustrations and descriptions of the various models are presented. Mounting accessories are also shown. Throughout the catalog are graphs, tables, and charts to help solve lighting problems and to simplify selection of proper fixtures. Request copies from Mitchell Distributors or from Mitchell Manufacturing Company, 2525 N. Clybourn Avenue, Chicago, Illinois.

Ohmite News, April, 1943, contains a résumé of the career of Nikola Tesla, inventor of the Tesla transformer. Instruments illustrated in this booklet are "Corrib" resistors, for motor starting circuits and similar intermittent duty (and continuous duty) applications, stock and special rheostats, tap switches, and chokes. Ohmite Manufacturing Company, 4835–41 Flournoy Street, Chicago, Illinois is the publisher (2 pages).

Westinghouse Research, No. 14, April, 1943, is published every other month by Westinghouse Research Laboratories, East Pittsburgh, Pennsylvania. The principal article describes how mirrors measure steel plates. A complete schedule of the 15-minute weekly radio program given by Westinghouse and called "Adventures in Research" is listed by stations (4 pages).

Wheelco Comments, February-March, 1943, Vol. 2, No. 5, relates facts pertaining to control instruments providing uniformity in aluminum castings. Published by Wheelco Instruments Company, Wheelco Building, Harrison and Peoria Streets, Chicago, Illinois and available on request (4 pages).

New Books

Science Remakes Our World

By James Stokley. Pp. 298+xii, Illustrated, 15×23 cm. Ives Washburn, New York, 1942. Price $3.50.

Most of us learn about our world vicariously: We listen to the radio to learn what is happening in Australia or Europe; we read books of travel to enjoy the places we have not been ourselves; we read history in an effort to understand other times than our own, or to understand our own times better. So too, in the field of scientific progress, we must learn what is happening by the reports brought to us by competent observers upon whom falls the important responsibility of telling clearly what is happening and, to a certain extent, of interpreting what new discoveries mean to the public. Even to the man of science or the researcher concentrating in a single field, many of the developments in allied fields are only vaguely understood; and to the layman, vast areas of scientific exploration would be completely closed unless they were thus reported in straightforward language, accurate but not technical. This is just what Mr. Stokley has succeeded in doing admirably. As I read this account of recent developments in numerous fields, I was compelled over and over again to compare Stokley's book with that excellent volume, *Atoms in Action*, by G. R. Harrison; the comparison is quite favorable. No higher praise should therefore be required for physicists who are acquainted with the latter book. But Mr. Stokley has done for *both* chemistry and physics what Dr. Harrison did primarily for physics; his range is considerably larger than that of *Atoms in Action*, for he spends the first third of his book on matters primarily chemical, on subjects which Harrison scarcely touches at all. He has packed into one small volume a great many matters of genuine interest to layman and scientist alike.

To state all the fronts of science touched by Mr. Stokley would require a list of its twenty chapter headings and numerous sub-topics, and that would make less interesting reading than the book itself; but a few selected topics may serve to show the range covered: chemical sythesis, the vast developments of petroleum, explosives, plastics, synthetic rubber, sulfa drugs, vitamins, metals and alloys, a fascinating chapter on "Mining the sea" in which the story of bromine extraction for ethyl gasoline and the story of magnesium are told, etc. The latter part of the volume deals with things physical, and one is constantly aware of the fact that the author has obtained his information from individuals who know. The very extent of the ground covered is impressive, and the long list of acknowledgments shows that the author was not content to write without first-hand information. The book is intensely *factual* and it is singularly devoid of the "blurbs" that so frequently clutter writing of this kind, wherein the author expatiates upon the glories of a field without telling anything significant about it. It is up to date, including many discoveries made within recent months; it is easy reading and although it is not graced with any remarkable literary style, it is clear and straightforward, which in itself is perhaps the best "style" that such a book can have. The author occasionally takes a look at future prospects, but he is usually restrained and doesn't go off into rapturous excesses. When one reads about vitamins, for example, one feels that what is said is dependable and that there has been a genuine effort to extract valid truth from wild claims in a field that has attracted so much popular interest in recent years.

Science Remakes Our World is another report of modern scientific progress, aimed to point out the great gains that have come from pure research and from men's efforts to meet their problems intelligently. It is recommended as a readable account by an author who has taken pains to get at the facts and to write them down clearly.

Richard M. Sutton,
Haverford College

The "Particles" of Modern Physics

By J. D. Stranathan. Pp. 571+xvi, Figs. 211, 15½×23 cm. The Blakiston Company, Philadelphia, 1942. Price $4.00.

This book is a notable addition to the general survey books available in the field of modern physics. It will be of value not only to the students for whom it was intended, but also to a wide group of scientific people who have not had the opportunity to follow in detail the many advances in the field of "particle" physics. As the title indicates, the book represents a fresh approach to the general field of modern physics. A good indication of its scope can be obtained from the chapter titles: Gaseous ions, The electron, The electrical discharge, Cathode rays, Positive rays, Photons, X-rays, α, β, and γ rays, The positron, The neutron, Particles?—or waves? Each of these chapters includes a tremendous amount of material presented in a neat and orderly fashion. The author is to be congratulated for the effort spent in collecting and organizing so much material. Each chapter is a complete study, containing an historical sketch of the subject at hand, an account of the fundamental experimental researches relating thereto, and finally, the results of recent researches. The chapters are rendered even more valuable by an unusually large number of references both to the original papers and to recognized summary and review articles. These alone will make this work of great value to many. However, the inclusion of so much factual information, many and varied references, and at times the lack of critical analysis of the material by the author, make the book difficult reading for the undergraduate. The author's method of approach also leads to certain difficulties. The material is compartmentalized more than is desirable, and the complete treatment of the topics often requires methods and theory with which the beginning student has had no experience and therefore will not understand and appreciate. On the other hand, this very method may become a challenge to the more mature student, and Dr. Stranathan, by the inclusion of many references at strategic places, guides him to abundant source material.

The author's choice of subject matter is good. The reviewer feels, however, that several topics might very well

have been included or developed in more detail. The electron plays a prominent role in the book and though its charge and mass are treated at length, its other properties, spin and magnetic moment, at times of great importance, are mentioned only in a brief, qualitative manner. A brief discussion of blackbody radiation might be included and the introduction of Planck's constant should be given a more prominent place. A free use of energy level diagrams would clarify the discussions in many places. A brief treatment of quantum mechanics and the inclusion of some features of that theory would also be a help to the student. He cannot treat the interaction of the "particles" without its aid. A chapter devoted to atomic structures might serve to tie together the many concepts presented and leave the reader with a better impression of the unity of modern physics.

The volume is well printed, attractively bound, and contains numerous diagrams, tables, and photographs. The majority of these are well chosen and give the book a graphic character which is to be commended.

C. D. HAUSE

Applied Nuclear Physics

BY ERNEST POLLARD AND WILLIAM L. DAVIDSON, JR., Pp. 249+vii, Figs. 65, 15×23 cm. John Wiley and Sons, Inc., New York, and Chapman and Hall, Ltd., London, 1942. Price $3.00.

For many years nuclear physicists have wished for a book which they could recommend to beginners in nuclear physics and also to biologists, physicians, chemists, metallurgists, and others with whom they were collaborating on problems utilizing radioactive or stable tracer isotopes. The need was for a pleasantly written, essentially non-mathematical, orientation course covering the fundamental ideas in nuclear physics, the properties of stable and radioactive nuclei, and the methods and results of applying these to practical problems. Pollard and Davidson meet these requirements. They maintain an informal conversational style and constantly take the reader into confidence pointing to many of the unsolved problems in nuclear physics and freely admitting the heartaches as well as the triumphs of the experimental nuclear physicist.

As the authors say "This book does not aim at being a complete reference source; it is intended to make available many known facts in nuclear physics to the people who are advancing the subject of applied nuclear physics, and to make others appreciate their work."

The contents include a description of the basic properties of nuclei and nuclear radiations, the methods of accelerating atomic particles, and the mechanism of transmutation and radioactivity. Various methods of detecting radioactivity, and a qualitative description of a few selected results from the application of radioactive isotopes are given. There is a separate chapter on the stable isotopes and their application in analytical and tracer problems. The book concludes with a brief discussion of nuclear fission and nuclear forces. Tables of some of the properties of known nuclei, and their radiations, are given in the appendices. It is unfortunate that some isotopes discussed in the text are not included in these tables.

The uninitiated may be misled by a number of basic errors of fact, such as occur in the discussion of rest mass and energy, the radioactive decay of isomers, the asymmetry of beta-ray spectra, and elsewhere. Such errors will probably be eliminated in later revisions, but for supervised orientation reading they will not be serious. The book is the first to appear which could form a suitable basis for the widely needed undergraduate course in nuclear physics.

ROBLEY D. EVANS
Massachusetts Institute of Technology

What Is Mathematics?

BY RICHARD COURANT AND HERBERT ROBBINS. Pp. 521+xix, Figs. 287, 16×23½ cm. Oxford University Press, New York, 1941. Price $5.00.

The recent demand for large numbers of technically trained persons has produced a group of books that profess to give a working knowledge of the useful parts of mathematics with a minimum of effort on the part of the student. The book by Professor Courant and Dr. Robbins does not belong to this class. Instead of treating the technique of mathematics, it attempts to give a real understanding of many of the ideas, objectives, and methods, and gives almost no attention to the development of skill in the use of these methods. Nevertheless, each chapter is accompanied by a set of exercises that enable a student to determine if he has really understood the text.

Starting with a discussion of integers, it presents some of the ideas and points of view of the theory of numbers and then progresses gradually to a discussion of rational and irrational numbers, of complex numbers, and of algebraic and transcendental numbers. In the course of this treatment, some of the basic methods of mathematical proof are illustrated with aptly selected examples.

In the treatment of geometry, little attention is given to the type of work usually treated in high school courses, but considerable attention is given to the significance of geometrical constructions and the famous problems of squaring the circle, doubling a cube, and trisecting an angle. Projective geometry and non-Euclidean geometries are given enough attention so that a careful reader can form some idea of the nature of the subject matter in these fields without getting the idea that he has mastered them.

As is proper, analysis comes in for a good share of attention. The ideas of functions, limits, and continuity are carefully described and illustrated, and the methods of the calculus are shown to have a foundation that can be precisely stated. This part would be of great value to one making applications of mathematics, who may frequently wonder just how far the formal methods may be carried.

This book would be an excellent text for required courses in mathematics that are supposed to be cultural in their content. It contains an excellent selection of material for students who have no desire to develop mathematical skills but who may be willing to look briefly into this field of intellectual activity. It would certainly not please the

casual reader, because real mental effort is required to comprehend it; neither would it have any appeal to one who hopes in a short time to acquire sufficient skill to make engineering or scientific calculations. But for the inquiring student who wishes to know what real mathematics is about, or for the trained engineer or physicist who has some interest in the justification of the procedures he uses, it should prove a source of great pleasure and satisfaction.

Throughout the whole book the authors protest against a purely formalistic conception of mathematics. They emphasize both the intuition necessary for its creation and the careful criticism and examination necessary for its justification. Their point of view is indicated by a statement about mathematics that, "If the crystallized deductive form is the goal, intuition and construction are at least the driving forces."

W. V. HOUSTON

Heat Transfer by Infrared Radiation in the Atmosphere

BY WALTER M. ELSASSER, Pp. 107, Figs. 34, 18½×25 cm. Harvard University Blue Hill Meteorological Observatory, Milton, Massachusetts, 1942. Price $1.25.

Much of the preparation of this monograph was carried out at the California Institute of Technology. Financial support was provided in part by a U. S. grant under the Bankhead Jones Act.

The subject matter is discussed under three main headings. "Part I deals with the general theory of radiative heat transfer in the atmosphere, without regard to the particular structure of the far infrared spectrum. Part II analyzes this spectrum and shows the connection between its structural elements, which are the primary data of spectroscopy, and the integral effects observed as radiative flow of heat. Part III deals with the direct measurement of radiative heat flow in the atmosphere, and with empirical relationships derived from such measurements." In Part I, (1) the initial discussion centers about the laws of Kirchhoff and Planck. Later in logical sequence there is considered (2) the transfer of monochromatic radiation by absorption and emission by a slab of material only partially opaque, (3) the corresponding transfer of non-monochromatic radiation, (4) the general transfer problem in an atmosphere of arbitrary constitution and varying temperature, and (5) the radiation chart from which it is possible to compute rather quickly the rate of emission of radiant energy by a column of atmosphere of any lateral extent and any probable variation of temperature and humidity. This chart, constructed for the lower atmosphere, depends upon empirical relations which have been integrated graphically. Water vapor and carbon dioxide are assumed to be the main radiative transfer substances. Ozone which is recognized as another such substance is disregarded here because its effects are largely limited to the stratosphere. Oxygen and nitrogen, though they possess great optical thickness, are believed to contribute but little. Due to the absorptance of CO_2, being very intense throughout the region where it absorbs at all, the contribution to the radiative transfer by the atmosphere in the CO_2-band regions is simple to take into account. For these regions the atmosphere is assumed opaque and black. Computations involving the contributions of the water vapor bands, however, are more complicated, in part, because its absorption coefficient is a function of pressure.

In Part II of the monograph, details of the construction of the radiation chart are given. In Part III instruments, methods, and results of nocturnal radiation measurements are discussed. Difficulties are experienced in sky radiation measurements because of convection currents. No instrument seems to be free from such sources of errors. However, as perhaps the best approach to an instrument with such errors reduced to a minimum, the author cites the Aldrich radiation instrument known as the melikeron, which has a honeycomb construction. For the results of measurements, the monograph should be consulted. A few interesting results for the non-specialist in this field may be quoted. "In a record of sky radiation made at Pasadena (unpublished) the author found that whenever the air was stable enough to prevent day-time convection, the radiation from the sky at sufficient distance from the sun was very little different from that at night."

"With clear skies the incoming radiation is practically always between 50 percent and 85 percent of the blackbody flux corresponding to the temperature of the air near the ground and is most commonly between 65 and 75 percent of this flux." Though not so stated by the author, the reviewer interprets the latter figures to mean that, under the same conditions, the heat loss from the ground to the upper air amounts to from 25 to 35 percent of the corresponding blackbody flux. Illustrating the effects of clouds the author states, "The figures mentioned refer to sky radiation observation with perfectly clear sky, any cloud present greatly reduces the heat loss of the ground and with a solid overcast the outgoing flux is only of the order of 5–10 percent of the blackbody flux."

The monograph which is thoroughly sound would seem to be of great value to the worker in meteorology. Personally the reviewer would have appreciated a table in which symbols and their meanings were collected and on occasion more precise statements in words of what those symbols stand for.

A. G. WORTHING

Introduction to the Theory of Relativity

BY PETER GABRIEL BERGMANN. Pp. 287+xvi, Figs. 9, 16×23½ cm. Prentice-Hall, Inc., New York, 1942. Price $4.50.

This book undoubtedly satisfies a definite need although it is difficult to say whether it will satisfy a mathematician or a physicist more. It appeals rather to the physicist and philosopher in a mathematician and to the philosopher and mathematician in a physicist. Its purpose is to represent the logical development which led to Relativity Theory; to show how its principles can be formulated through the search for the simplest and most natural assumptions which avoid the logical difficulties and contradictions of the clas-

sical theories. This logical (but not axiomatic) approach is carried consistently through the whole book. The exposition is clear, simple, and interesting.

The book is divided into three parts. The first contains the Special Relativity Theory. Here not only the approach, but also the material is somewhat different from that which one usually finds in books on relativity. Modern applications of the ideas of relativity theory, like cosmic rays, Compton effect, de Broglie waves, are included in this part. The second part contains an excellent exposition of General Relativity Theory. It leads the reader (in its final chapter) to such difficult problems as the deduction of the equations of motion from field equations. The third and smallest part is devoted to the Unitary Field Theory. It goes so far as to explain the problems on which Einstein and the author of this book collaborated.

The book is excellent and undoubtedly much more than an introduction, as the title would indicate. The specialist will find this book refreshing and interesting in its originality. A great part of it might not be too difficult for a graduate student. Lecturers in relativity theory will find this book most valuable and helpful.

L. INFELD
Toronto, Ontario

Mathematical Tables

The mathematical tables thus far made available through the National Bureau of Standards are listed below. They were prepared by the *Project for the Computation of Mathematical Tables* conducted by the Federal Works Agency, Works Project Administration for the City of New York, under the sponsorship of the National Bureau of Standards, and are of especial interest to physicists, engineers, chemists, biologists, mathematicians, computers, and others engaged in scientific and technical work.

Copies of the tables can be purchased at the prices indicated. Payment is required in advance and remittance should accompany order. When remitting, please make check or money order payable to National Bureau of Standards.

Copies of these publications have been sent to various Government depositories throughout the country, such as public libraries in large cities, and colleges and universities, where they can be consulted.

A list of the various tables it is planned to publish is included on the closing pages of each publication. A similar list will be sent free on request.

Those who desire to receive announcements concerning new mathematical tables as they become available should write to the Information Section, National Bureau of Standards, Washington, D. C., asking that their names be added to the mailing list maintained for this purpose.

MT1. Table of the First Ten Powers of the Integers from 1 to 1000. Pp. viii+80, heavy paper cover (1939). Price 50 cents.

MT2. Tables of the Exponential Function e^x. Pp. xv+535, bound in buckram (1939). Price $2.00.

The ranges and intervals of the argument and the number of decimal places in the entries are given below:

Range of x	Interval of x	No. of decimals given
−2.5000 to 1.0000	0.0001	18
1.0000 to 2.5000	0.0001	15
2.500 to 5.000	0.001	15
5.00 to 10.00	0.01	12

MT3. Tables of Circular and Hyperbolic Sines and Cosines for Radian Arguments. Pp. xvii+405, bound in buckram (1939). Price $2.00.

Contains 9 decimal place values of $\sin x$, $\cos x$, $\sinh x$, and $\cosh x$ for x (in radians) ranging from 0 to 2 at intervals of 0.0001.

MT4. Tables of Sines and Cosines for Radian Arguments. Pp. xxix+275, bound in buckram (1940). Price $2.00.

Contains 8 decimal place values of sines and cosines for radian arguments ranging from 0 to 25 at intervals of 0.001.

MT5. Tables of Sine, Cosine, and Exponential Integrals. Volume I. Pp. xxvi+444, bound in buckram (1940). Price $2.00.

Values of these functions to 9 places to decimals from 0 to 2 at intervals of 0.0001.

MT6. Tables of Sine, Cosine, and Exponential Integrals. Volume II. Pp. xxxvii+225, bound in buckram (1940). Price $2.00.

Values of these functions to 9, 10, or 11 significant figures from 0 to 10 at intervals of 0.001, with auxiliary tables.

MT7. Table of Natural Logarithms. Volume I. Pp. xviii+501, bound in buckram (1941). Price $2.00.

Logarithms of the integers from 1 to 50,000 to 16 places of decimals. (See also MT9, MT10, and MT12.)

MT8. Tables of Probability Functions. Volume I. Pp. xxviii+302, bound in buckram (1941). Price $2.00.

$$H'(x)=\frac{2}{\sqrt{\pi}}\exp(-x^2) \quad \text{and} \quad H(x)=\frac{2}{\sqrt{\pi}}\int_0^x \exp-(\alpha^2 d\alpha).$$

Values of these functions to 15 places of decimals from 0 to 1 at intervals of 0.0001 and from 1 to 5.6 at intervals of 0.001.

MT9. Table of Natural Logarithms. Volume II. Pp. xviii+501, bound in buckram (1941). Price $2.00.

Logarithms of the integers from 50,000 to 100,000 to 16 places of decimals. (See also MT7, MT10, and MT12.)

MT10. Table of Natural Logarithms. Volume III. Pp. xviii+501, bound in buckram (1941). Price $2.00.

Logarithms of the decimal numbers from 0.0001 to 5.0000 to 16 places of decimals. (See also MT7, MT9, and MT12.)

MT11. Tables of the Moments of Inertia and Section Moduli of Ordinary Angles, Channels, and Bulb Angles With Certain Plate Combinations. Pp. xiii+197 bound in green cloth (1941). Price $2.00.

MT12. Table of Natural Logarithms. Volume IV. Pp. xxii+506, bound in buckram (1941). Price $2.00.

Logarithms of the decimal numbers from 5.0000 to 10.0000 to 16 places of decimals. (See also MT7, MT9, and MT10.)

MT13. Table of Sine and Cosine Integrals for Arguments from 10 to 100. Pp. xxxii+185, bound in buckram (1942). Price $2.00.

(A sequel to MT6, Volume II of Tables of Sine, Cosine,

and Exponential Integrals.) Contains ten-place values of the functions $\mathrm{Si}(x)$ and $\mathrm{Ci}(x)$ at intervals of 0.01. Second central differences are tabulated for all entries. Three auxiliary tables are appended.

MT14. Tables of Probability Functions. Volume II. Pp. xxi+344, bound in buckram (1942). Price $2.00.

$$\frac{1}{\sqrt{2\pi}}\exp(-x^2/2) \quad \text{and} \quad \frac{1}{\sqrt{2\pi}}\int_{-x}^{x}\exp(-\alpha^2/2)d\alpha.$$

Values of these functions from 0 to 1 at intervals of 0.0001 and from 1 to 7.800 at intervals of 0.001 to 15 decimal places; and from 7.800 to 8.285 at various intervals to 15 decimal places.

MT15. The Hypergeometric and Legendre Functions with Applications to Integral Equations of Potential Theory. Pp. 319, bound in heavy paper covers. Price $2.00

Compiled for workers in applied mathematics, its scope is intermediate between tables of numerical values of these functions and a treatise on their pure theory. The linear and quadratic transformations and analytic continuations of the ordinary hypergeometric function are derived and written out at length with special space devoted to the general associated Legendre functions, and to a smaller extent Heun's generalization of the hypergeometric function. Applications to potential theory (91 pages) where the potential is given on surfaces of revolution include most of the elementary separable coordinate systems. Use is made of the potential equation in a form invariant to inversions, and from the point of view of integral equations with Legendre's function, $Q_{m-\frac{1}{2}}$, of the second kind as nucleus. Some generalizations of Fourier's integral are obtained in which the development function satisfies a second-order differential equation of rather general form. These are utilized in obtaining the formal solution of various potential problems. A set of normal functions is constructed satisfying the Lamé-Wangerin equation in "annular" coordinates which include toroidal coordinates and oblate spheroidal as limiting cases. The publication was reproduced by photo-offset process from original handwritten manuscript.

MT16. Table of Arc Tan *X*. Pp. xxv+169, bound in buckram (1942). Price $2.00.

The principal value of the inverse tangent may be defined by the integral

$$\text{Arc tan } x = \int_0^x \frac{du}{1+\mu^2}.$$

Since Arc tan $(-x) = -$Arc tan x, it is sufficient to tabulate the values of the integral for positive values of x. Some tables of the function in sexagesimal measure are available; but there seems to be no comprehensive table of the integral in radians. To meet this need, the function is tabulated in this volume to twelve decimal places over the following range of the independent variable x:

Range of x	Interval between successive arguments
0 to 7	0.001
7 to 50	0.01
50 to 300	0.1
300 to 2,000	1
2,000 to 10,000	10

The intervals between successive arguments have been so chosen, that interpolation to twelve decimals may be made with the aid of the second central differences which are tabulated alongside of the entries.

M-17. Miscellaneous Physical Tables.

Planck's radiation functions and electronic functions. A review of this book appears below.

Miscellaneous Physical Tables—Planck's Radiation Functions and Electronic Functions

Prepared by the Federal Works Agency Work Projects Administration for the City of New York, Dr. Arnold Lowan, Technical Director, conducted under the sponsorship of the National Bureau of Standards. Pp. 58+vi, Tables 5, 20½×28 cm. Price $1.50.

Table I lists, to the extent of five significant figures, four blackbody radiation functions; namely, $R_{0-\lambda}/R_{0-\infty}$, $R_\lambda/R_{\lambda\,\max}$, $N_{0-\lambda}/N_{0-\infty}$ and $N_\lambda/N_{\lambda\,\max}$. R_λ is called spectral radiancy and is defined by the ordinary Planck equation, $R_\lambda = c_1\lambda^{-5}[\exp(c_2/\lambda T)-1]^{-1}$. N_λ is similarly defined by the equation, $N_\lambda = 2\pi c\lambda^{-4}[\exp(c_2/\lambda T)-1]^{-1}$ and differs in concept from R_λ only in that it evaluates radiation in terms of numbers of photons or quanta rather than in terms of energy units. $R_{0-\lambda}$ and $N_{0-\lambda}$, are the portions of the total rates of emission of energy and of photons for the region of wave-lengths between 0 and λ. All values are in terms of λT as the independent variable. The range is 0.050 cm K° $<\lambda T<$ 2.00 cm K°. First differences and second central differences are given for interpolation purposes.

Table II similarly shows tabulated values of $R_{0-\lambda}$, R_λ, $N_{0-\lambda}$ and N_λ as functions of λ for a temperature of 1000°K. Table III shows $N=f(\lambda)$ for 7 temperatures ranging from 1000°K to 6000°K and for the range $0.25\mu<\lambda<10.00\mu$. Table IV is a one-page table giving means for the quick determination of changes in the functions noted above with change of value for c_2.

Table V concerns electronic functions. For values of $\beta(=v/c)$ as the independent variable, there are recorded values of $G[=1/(1-\beta^2)^{\frac{1}{2}}]$, βG, V, the kinetic energy of an electron corresponding to the given β, and H, the constant product of magnetic field strength and radius of curvature of path that results when an electron with a speed βc moves in a constant magnetic field in a direction perpendicular to the direction of that field. Values for V are expressed in electron kilovolts for H in gauss cm. For low values of β, the β-interval is 0.005. However, for much of the 27-page table the interval is 0.001, after which it is decreased from time to time to an interval of 1×10^{-10}. All values for the function are given to at least six significant figures, some range up to 12.

It is obvious that wherever extended computations involve spectral distributions of radiant energy or electronic functions, these tables will have fields of application. Many computations will be greatly shortened or rendered more accurate and more reliable because of them. As such this volume will be highly appreciated.

A. G. WORTHING

Here and There

Need for Scientific Personnel in Navy

Warfare of today demands the best of scientific knowledge for effective use of the technical weapons with which we fight. Mathematics, physics, and related subjects hold the scientific key to beating the enemy on this important front.

The Navy needs men to plan, organize, administer, and teach these scientific subjects. Candidates for these teaching billets must have the qualities of leadership to attract and hold the interest of Navy men who volunteer for these courses. An ability to speak fluent Spanish and French is desirable, but not essential.

Applicants who are commissioned must be physically fit for duty overseas, as many of these courses will be given at advance bases and at outlying stations; also at naval training stations in the United States. With a degree and good scholastic record in this field, any individual fitted for this billet should apply at the Naval Office of Officer Procurement located in the nearest major city.

★

The War Manpower Situation in Physics

It is now possible to say definitely that, on the average, for every physicist engaged in college teaching in January of this year there must be at least one and one-half teachers of physics recruited from other sources. This ratio is based on official information regarding presently available teachers of physics and the number of teachers needed adequately to take care of the urgent demands that will be made by the Army and Navy training programs, as well as what will remain of normal programs. In view of this situation, no institution has a right to recruit teachers of physics from any college which is at all likely to have a training unit or to have a sufficiently large enrollment of women, younger men, and physically disqualified men to justify the continuance of the department. If, after the training programs are under way, any institution has a ratio of genuine to "ersatz" teachers of physics higher than one to one and one-half, it will find itself open to severe criticism if any of the experienced teachers have been recruited from institutions needing them.—Homer L. Dodge, *Science*, March 12, 1943, Vol. 97, No. 2515, pp. 243–244.

★

Science Wing of Palo Alto Museum

The Palo Alto Museum, California opened its new Science Wing to the public on Easter Sunday, April 25, according to *Museum News*. At the dedication ceremony the building was presented to the City of Palo Alto by the president of the museum, Mrs. Don Hibner. Mayor Byron Blois accepted for the city. Robert C. Miller, director of the California Academy of Sciences was the guest speaker at a preview and reception for members and guests on April 24.—*Science*, April 23, 1943, p. 375.

Wartime Conference of Science Librarians

Meeting as part of the second Wartime Conference of the Special Libraries Association, at the Hotel Pennsylvania, New York, on June 22–24, the Science-Technology Group of the Association representing engineering, chemical, rubber, utilities, and aeronautical libraries, both institutional and belonging to various firms, held an annual conference. Guest speakers on the program were several representative scientists. Other topics discussed were shortcut methods for finding the information which these libraries are now so heavily called upon to produce. Miss Elsie P. Garvin, Eastman Kodak Company, Rochester, New York, is Chairman of the Science-Technology Group. Ernest F. Spitzer, Consolidated Oil Corporation, New York, is Vice Chairman; Katherine Deneen, Corning Glass Works, Corning, New York, is Secretary.

★

Army-Navy Production Award

On April 3, 1943 the War Department officially awarded to the Harrison Works of the RCA, for the second time, the Army-Navy Production Award for meritorious service. This award is manifested by the addition of a white star to the Army-Navy "E" pennant received in September, 1942.

★

Summer Courses at Polytechnic Institute

The Polytechnic Institute of Brooklyn announces the following summer courses to be given by the Graduate Electrical Engineering Department under the Engineering, Science, and Management War Training program:

Introduction to Microwave Theory
Introductory Experiments in Microwaves
Theory of Cathode-Ray Circuits
Experiments in Cathode-Ray Circuits
Experience in Ultra-High Frequency Generators and Receivers
Measurements at Ultra-High Frequencies
Advanced Theory of Ultra-Short Electromagnetic Waves

★

Westinghouse Scholarship Winners

Ten top-ranking seniors in high schools and preparatory schools spanning the nation recently were announced as winners of George Westinghouse scholarships at the Carnegie Institute of Technology's College of Engineering. The winners were: Allen I. Bennett, Jr., Pittsburgh, Pennsylvania; August E. Binder, Seattle, Washington; Robert A. Charpie, Rocky River, Ohio; Wilbur S. Cook, Wadsworth, Ohio; Richard M. Drisko, Oklahoma City, Oklahoma; Thomas J. Farrahy, Jr., Yonkers, New York; Charles Hansen, Westfield, New Jersey; Donald R. Harris, Jr., Johnstown, Pennsylvania; John D. Krummell, LaGrange Park, Illinois; Edward Von Halle, New York, New York.

Opportunities for College Women in Federal Government Service

Like the armed forces the civilian services of government offer important fields of work for women college graduates today. In these civilian services as well as in the armed forces, women can frequently release men for more direct combat duty. Although most appointments to government positions today are for the duration of the war and six months thereafter, government and the public service constitute a growing and a challenging field for college women in peace as well as in war.

The immediate need is for women to replace men in numerous government positions and to fill the increased number of positions which the war has created in the government service. An order of the War Manpower Commission announced in the papers on February 3, 1943 will wipe out the deferred status of many federal employees between 18 and 38 and probably increase the need for women. The proportion of all government positions filled by women had been growing even before the war—from 15 percent in 1933 to an estimated 24 percent in 1942. The number is still growing.

These various government positions are so widely scattered throughout the country that a large number are not located in Washington, D. C. At the end of June, 1942, only an estimated 24 percent of all women employed in the federal government were employed in Washington.

The present needs are for persons already trained in the physical and natural sciences, such as mathematics, physics, chemistry, geology, geography, metallurgy, engineering, medicine, and certain specialized areas of these fields. The special fields for which needs are urgent are as follows:

Physical Sciences

Physics There are not nearly enough physicists in the whole country to meet the government needs at this time, especially in the fields of ballistics, electronics, radio, electricity, sound, optics, and photoelasticity. As this is a radio war, every course in physics should include the study of the fundamentals of radio, that is the most important part of electronics as well as of physics in relation to war needs.

Chemistry There is a general demand for industrial chemists and in Washington, D. C. there is particular request for those who have special training or experience in the fields of essential oils, rubber, explosives, industrial hygiene, and plastics. All chemical or chemical engineering experts are employed and demands for personnel in these fields cannot be supplied. It is probable that the chemical situation will become more acute in 1943 and 1944 because of the development of work on synthetic rubber and because of the loss of men chemists to the armed forces.

Technology Technology means necessary production, engineering and scientific research work essential to the successful operation of an industrial plant where the operation of the plant is based on a thorough-going knowledge of an applied science in one of its branches. There is considerable need for people to plan direction and interpret research or investigation in such branches of technology as explosives, fuels, plastics, minerals, rubber, and textiles. The demand for rubber technologists far exceeds the supply.

Metallurgy There is an acute need for people trained to conduct investigative developmental, or productive work in the various branches of metallurgy; to assist in the design, construction installation, and operation of metallurgical equipment; or to perform metallurgical work in the fabrication of metals.

Meteorology There are not enough trained meteorologists in the country to meet the needs of the Weather Bureau and the Army and Navy for instructors and forecasters. Persons are desired primarily who have training in synoptic and dynamic meteorology.

Geography There is need for people to compile map data and to construct maps used in vital war work; to prepare reports on the geography (physical, economical, social, and political) of foreign areas critically concerned in war or post-war plans; to administer modern and historical map collections.

The Federal Government has junior positions which may be entered by means of either "assembled" examinations, selection through written tests of the U. S. Civil Service Commission, or "unassembled" examinations, selection as a result only of submission of credentials indicating training and experience, if any. Chief among the ways in which young women just out of college may enter the government service is through the Junior Professional Assistant examination, or through one of the junior examinations in the physical sciences. College students who plan to enter the government service on the professional level, should register with the National Roster of Scientific and Specialized Personnel of the War Manpower Commission. The Roster does no placement itself, but working with the Civil Service Commission and the U. S. Employment Service recommends names of available people for specialized positions.—"Higher Education and National Defense" published by American Council on Education, 744 Jackson Place, Washington, D. C.

★

News of Societies

The Pittsburgh Chapter of the American Society of Heating and Ventilating Engineers were hosts for the Semi-Annual Meeting 1943 held at the William Penn Hotel, June 7 and 8.

Adam MacKenzie, Vice President in charge of Manufacturing, Carboloy Company, Inc., was recently elected Chairman of the Detroit Section, American Institute of Mining and Metallurgical Engineers.

National Wartime Conference

A National Wartime Conference of the professions, arts, sciences, and white-collar fields was held in the Hotel Commodore on May 8 and 9 under the sponsorship of eighteen national organizations and two hundred individuals who are leaders in these four groups. Chairman of the conference was Dr. Kirtley F. Mather, Professor of Geology at Harvard University and President of the American Association of Scientific Workers. The purpose of the conference was stated as an endeavor to find ways by which fuller use can be made of the available skill and talent which still lies untapped throughout the country. Dr. Leonard A. Carmichael, President of Tufts College and Director of the National Roster of Scientific and Specialized Personnel, spoke on the present and potential contribution of trained personnel to the war effort, and Dean Wayne Morse, public member of the National War Labor Board, spoke on economic stabilization and the problems of salaried professionals. Six panel discussions were held on May 9, including one on science and technology.—*Science*, April 23, 1943, p. 375.

★

Honors and Awards

Professor Peter Kapitza, Soviet physicist, has received the award of the Order of Lenin, it was announced recently, and many workers at the Institute of Physical Problems that he heads have been decorated. Dr. Kapitza has been honored in this country and Britain for his work in thermal research.

Sir Henry Hallett Dale, President of the Royal Society, has been awarded the Harben Gold Medal of the Royal Institute of Public Health and Hygiene, London.

The National Academy of Science has awarded the annually presented Henry Draper Gold Medal to Professor Ira Sprague Bowen of the California Institute of Technology. The citation is: "in recognition of his contributions to astronomical physics; more especially his researches on the spectra and chemical composition of the gaseous nebulae."

The Council of the Physical Society in London has awarded the Duddell Medal for 1942 to Dr. C. R. Burch, formerly of the Research Department of the Metropolitan-Vickers Electrical Company. Dr. Burch is continuing his work in the Physics Laboratories of the Imperial College and the University of Bristol. The award has been made primarily in recognition of Dr. Burch's contributions to the advancement of vacuum technique.

★

Staff Changes

James R. Killian, Jr., has been made Executive Vice President of the Massachusetts Institute of Technology and assumes his new post on July 1. Mr. Killian has been executive assistant to the president since January, 1939.

Lewis W. Waters, Vice President in charge of research and development for General Foods Corporation, New York City, has been appointed Vice President in charge of scientific relations, a newly established position.

Henry Dressel has recently been appointed Supervisor of Electronic Components Engineering by the Stackpole Carbon Company with whom he has been associated for several years as a member of the engineering staff. Prior to that he was with the Oak Manufacturing Company in Chicago.

★

Necrology

Dr. Herbert E. Hawkes, Professor of Mathematics and Dean of Columbia University, died on May 4 at the age of seventy.

Dr. Ellwood B. Spear, Manager and Director of Research of the Vultex Chemical Company for the past fifteen years, and previously a member of the faculty at the Massachusetts Institute of Technology, died on May 1 at the age of sixty-eight.

Calendar of Meetings

July
10 American Physical Society, Stanford University, California

September
12–13 American Mathematical Society, New Brunswick, New Jersey

October
7–9 Optical Society of America, Pittsburgh, Pennsylvania
29–30 Society of Rheology, New York, New York

November
26–27 American Physical Society, Chicago, Illinois

December
27–Jan 1 American Association for the Advancement of Science, Cleveland, Ohio

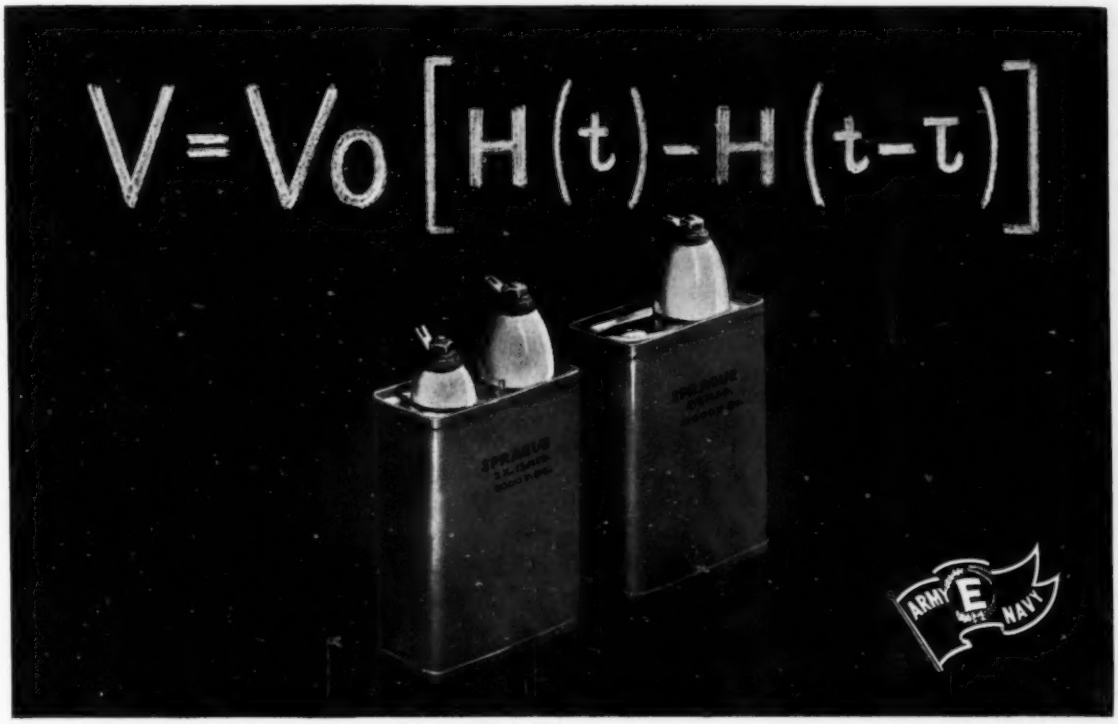

...AND Vo IS ANYTHING UPWARDS OF 1 Kv.!

If you're dealing with voltages of a type indicated by the above formula—well, we don't have to tell you that the job of finding suitable components is a tough one, especially if these V's are working into low Z's.

Obviously then, we don't pretend that transient voltages of this order haven't been a contributing factor to premature gray hairs for Sprague engineers charged with developing condensers and Koolohm Resistors to meet these difficult specifications. They have—and some problems remain to be solved. We're working on them now!

On the other hand, more often than not, eminently suitable components have been forthcoming. A typical illustration is the Sprague Type PX-25 "VITAMIN Q" Paper Capacitor that reads "off scale" on megohm bridges at more than 200,000 megohms.

Let us know just what your problems are, and how the capacitors are to be used. We'll make our recommendations accordingly—telling you frankly and honestly just what you can expect.

SPRAGUE
SPECIALTIES COMPANY
NORTH ADAMS, MASS.

SUB-CONTRACTORS, ATTENTION!

Sprague Specialties Company will be glad to hear from reliable firms having screw machine and metal stamping facilities available for sub-contract work on high-priority orders; also from concerns equipped to make up jigs and fixtures, and having female help available.

F. W. McNAMARA, *Purchasing Agent*
Telephone: NORTH ADAMS (MASS.) 804

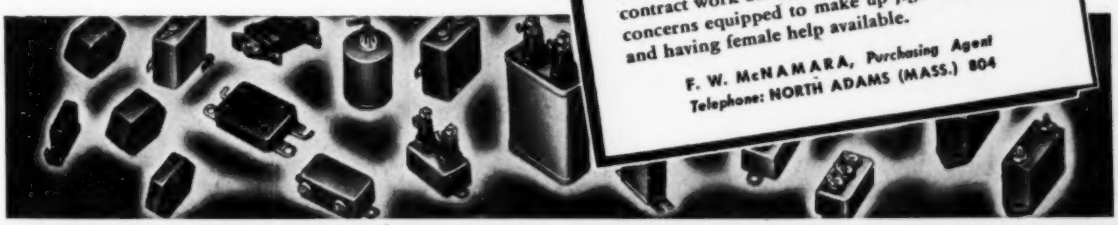

MANUFACTURERS OF A COMPLETE LINE OF RADIO and INDUSTRIAL CAPACITORS and KOOLOHM RESISTORS

Recent Applications of Physics

Rifle Sighting Gauge A new equipment developed by the General Electric Company and officially known as an "Optical Rifle Sighting Gage" is enabling the United States armed forces to sight Garand semi-automatic rifles with mirrors. The equipment will save up to 13 rounds of ammunition formerly used in sighting each gun, and will permit a girl to do the job in less than two minutes per rifle, about half the time it took two men by the old method. Less room than the average domestic kitchen is required for this equipment, whereas sighting by firing requires a 100-yard rifle range.

When sighted by the optical gauge, all the rifle "fires" is a light ray at a mirrored target approximately six feet in front of it. The ray is caught by another mirror on the gauge equipment at the operator's eye level, and thrown onto a ground glass screen in the image of a cross. Superimposing this image upon another cross on the ground glass correctly positions the rifle, and the gun is then sighted by adjusting its rear sight so that its shadow, magnified 25 times on the screen of a projector directly above it, is in the same relative position as the shadow of the front sight, similarly magnified on another projector above it.

N. F. Barnes and K. R. Geiser of General Electric's general engineering laboratory originated the optical sighting gauge. Their equipment was designed by William Fears, also of the General Electric Laboratory. Although built specifically for the Garand rifle, it can be adapted to sight other types of rifles.

What the gauge actually does is to transfer the sight setting from a "master" rifle, correctly sighted by firing, to rifles subsequently sighted in the equipment. The gauge is set for accurate use by placing the master rifle in it, and adjusting the equipment to conform to the bore direction and sight positions of the master rifle. When other rifles placed in the gauge are aligned with the target optical system, and their sights moved to the proper relation as designated by the sight projectors, they are given the line-of-sight to line-of-bore relationship established by the master rifle.

Electric "Brain" A paper and aluminum "brain" that memorizes surges of electric current and records them for the benefit of research engineers has been built by William E. Pakala, a research engineer at the Westinghouse Electric and Manufacturing Company. It was designed to help scientists study the Ignitron, an electronic device that converts alternating electric current into the direct current required by aluminum and magnesium plants. Teamed with an oscillograph, which jots down on photographic film a record of the electricity passing through a switch, motor, or electronic tube, the arrangement tells engineers exactly what happens inside the Ignitron. With this information, it is now possible to design new and better equipment to insure a steady flow of vitally needed direct current. The Ignitron converts alternating electric current to direct current that flows in one direction only—just as a valve in a water line lets the water flow in only one direction.

Occasionally an Ignitron will arc back and there is no way to forecast when this will occur. Previously, engineers studied such electrical phenomena with the oscillograph. The oscillograph alone was unsatisfactory, according to Mr. Pakala, because no one knew when the arc back was coming and it was impractical to expose hundreds or perhaps thousands of feet of film while waiting for it. From a standstill, the oscillograph can not go into action fast enough to get a picture of the arc back which lasts only one-sixtieth of a second.

Mr. Pakala got the idea of putting a machine between the Ignitron and the oscillograph that would remember what happened inside the Ignitron. This would give the oscillograph a chance to begin operating and then the memory machine would recite the message so it could be picked up and photographed. To do this, an ordinary electric motor, not much bigger than the one on a washing machine, was converted by stripping the copper wires from the revolving part of the motor and replacing them with layers of aluminum foil and paper. These electric reservoirs can store an electric charge, then release it when they are tapped. Each capacitor was connected to one of the copper bars on the motor's commutator and the whole memory machine was hitched to a real electric motor that made the brain whirl at a steady speed.

New Workshop Clean as Hospital A new electronics workshop, hospital-like in cleanliness, with gleaming white machinery and a brilliant ultra-modern lighting system, has been put into operation at the Westinghouse Lamp Division to produce electronic equipment for the armed forces. Protected from the tiniest particles of dust and moisture, delicate electronic tubes, such as those for high power radio transmission, are assembled by the several hundred men and women employed in the new laboratory. Absolute cleanliness is all-important in the production of an efficient electronic tube, according to George W. Keown, manager of electronics manufacturing. Clean white cotton gloves are issued daily to workers on certain operations, so that no moisture from a workman's hands can touch the delicate tube parts.

In the assembly of vacuum tubes freedom from moisture or dust is of extreme importance. Moisture on a tube part collects grease. Then when the tube is heated, the grease vaporizes leaving particles of dirt which may interfere with the efficient operation of the tube. Floors, walls, ceilings, and work benches are kept a spotless white. Dirt or dust can be more easily detected under modern fluorescent lighting.

The electronics workshop is divided into two departments. In the Mounting Department, the operating mechanisms of electronic tubes are assembled. As many as 225 different operations are performed, ranging from spot

PLATES AND FILMS
for Spectrum Analysis

THE Eastman Kodak Company makes a number of plates and films which are suited to the various requirements of spectrum analysis. One of the most recent of these products is *Eastman Spectrum Analysis Film, No. 2.* It has good speed, moderate contrast, and medium resolving power and granularity. Its contrast and wave length characteristics are very uniform throughout the spectral region λ2400A–λ4400A.

Particulars concerning this and other films and plates for spectrum analysis will be forwarded promptly upon request.

EASTMAN KODAK COMPANY

Research Laboratories **Rochester, N. Y.**

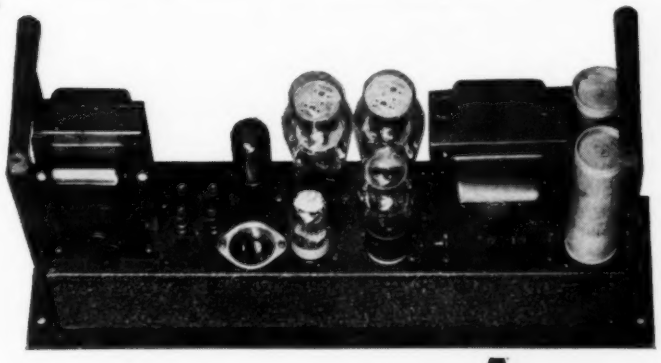

STABILIZED

POWER

SUPPLY

A PRECISION INSTRUMENT

FOR LABORATORY D. C. SOURCE

HARVEY *Radio Laboratories, Inc.*

445 CONCORD AVENUE · CAMBRIDGE · MASS.

welding to meticulous hand assembly of filaments finer than a human hair. In the Sealing Department, the finished mounts are sealed into glass bulbs or envelopes by means of the latest automatic equipment.

The new laboratory is housed in three large rooms with no windows through which dust or excess humidity might enter. The entire laboratory is cleaned once each day. The walls are washed continuously; when the electric washing apparatus has completed the circuit, it begins all over again.

Morse Code Album A modern system of instruction in the International Morse Code has been incorporated in a six-record album which Victor has released recently. Prepared by John N. Cose, Director of Instruction at the RCA Institutes, the album and accompanying booklet are designed to acquaint students with the actual sound of the Morse code letters as they would be sent over the air to provide them with specially prepared practice transmissions which should develop the students' ability to copy regular code messages. A novel feature of the Morse code album is the incorporation of instructions on the records themselves, with the handbook as a check on all practice messages transmitted.

The first eight lessons are devoted to alphabet instruction and special practice in letters introduced. The album then moves on to a study of coded five-letter groups, longer plain English words, sentence structure, "hard to memorize" English transmission, and a practice session of five-letter cipher groups using all the letters of the alphabet in unfamiliar combinations.

Innovations in Instruments

Sodium Vapor Inspection Light

The visual advantages of sodium vapor illumination arise from distinct characteristics of the light. First, its truly monochromatic nature permits needle-sharp focus; secondly, its soft yellow color is a color to which the eye happens to be more sensitive than to other colors. As a result, eye strain is lessened, vision is improved, and less intense illumination is required. For instance, 100 footcandles of sodium vapor illumination give vision equal to 500 footcandles of illumination from the entire spectrum, while, at the same time, producing less objectionable glare than does the higher intensity.

When used for critical inspection, sodium vapor light discloses minute objects, cracks, or markings that are invisible under ordinary light. Similar advantages are obtained in microscopic inspection.

A monochromatic light also is valuable as a means of creating interference bands in the checking of surfaces by means of optical gauges, which make it possible to measure the sphericity of lenses and the flatness, parallelism, length, and thickness of gauge blocks to within one-millionth of an inch.

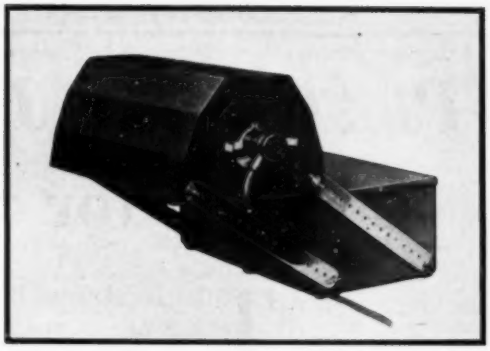

Other uses of monochromatic light include: identification of the *Z* axis by the concentric ring pattern and observation of twinning in quartz crystals; analysis of organic compounds where readings of rotation of polarized light are used; and microphotography.

The new monochromatic light announced by George W. Gates and Company requires no filters, since it makes use of the truly monochromatic spectrum produced by a sodium vapor arc rather than of a many-colored heterochromatic light source, such as mercury vapor or polychromatic source, as incandescent light, fluorescent light, or carbon arc.

These units are made in several different types, depending upon the application for which they are intended. The illustration shows a Universal Bench Model, the reflector of which can be swung into various positions in order to direct illumination as desired—upward or downward—over a wide field or a narrow field. Other information or literature may be obtained from George W. Gates and Company, Franklin Square, Long Island, New York.

★

Yoder Roll-Grinding Machine

A new roll-grinding machine has been recently announced by the Yoder Company. The new design has as its objectives time saving, lower cost, and ease of handling. Elimination of adjustments, usually included on a "grinder," that are not necessary to this particular group of operations is another feature of the machine. High points of this model are: 16″ diameter capacity, 20″ length between centers, manually synchronized table and cross feeds, two-speed table feed, nine-speed work head drive, without belt or gear change, precision-built high speed spindle, dust protection, centralized controls.

★

Flight Recorder

Brown flight recorder is a new instrument, developed especially to compile test data on the Douglas B-19, world's largest military plane, and is capable of automatically printing on paper, during the test flight, the temperatures of all 72 cylinders of the four motors, changing temperatures of the carburetor, exhaust, and of the oil in the fuel lines, and the pressures on wing struts, bulkheads, and tail surfaces.